University of Alberta

Modulation of Dendritic Excitability

by

Trevor James Hamilton

A thesis submitted to the Faculty of Graduate Studies and Research
in partial fulfillment of the requirements for the degree of

Doctor of Philosoply

Centre for Neuroscience

Fall, 2009
Edmonton, Alberta

Examining committee

Dr. William F. Colmers
Supervisor
Department of Pharmacology

Dr. Klaus Ballanyi – University of Alberta
Supervisory committee member
Department of Physiology

Dr. Peter Smith – University of Alberta
Supervisory committee member
Department of Pharmacology

Dr. Clayton Dickson – University of Alberta
Examining committee member
Department of Psychology

Dr. Yu Tian Wang - University of British Columbia
External examiner
Brain Research Center and Department of Medicine

To my mother and father, Barbara and Walter,
brother Scott, and lovely wife Angela.

ABSTRACT

The computational ability of principal neurons and interneurons in the brain and their ability to work together in concert are thought to underlie higher order cognitive processes such as learning, memory, and attention. Dendrites play a very important role in neuronal information processing because they receive and integrate incoming input and can undergo experience-dependent changes that will alter the future output of the neuron.

Here, I have used whole-cell patch clamp recordings and fluorescent Ca^{2+}-imaging to examine the modulation of dendritic excitability in principal neurons of the rat and human hippocampus and neocortex. First, I determined that dendrites of dentate granule cells of the hippocampus are tuned to high frequencies of both afferent input and backpropagating action potentials. Under these conditions they are also capable of generating regenerative dendritic activity that can propagate to the soma, which is prone to modulation. In particular, Neuropeptide Y (NPY) Y1 receptors can decrease frequency-dependent dendritic Ca^{2+} influx. Dopamine D1 receptors (D1Rs) have an opposite effect; they potentiate frequency-dependent dendritic excitability. These two neuromodulators also have an opposing effect on plasticity, with dopamine acting to induce, and NPY acting to inhibit long-term potentiation (LTP). Parallel observations of D1-induced LTP and an NPY-mediated decrease in dendritic excitability in rodents were complemented by findings in human dentate granule cells.

Second, I examined the role of NPY receptors on dendrites of layer 5 pyramidal neurons. In these neurons I found that NPY acts post-synaptically on distal dendrites via the Y1 receptor to inhibit frequency-dependent Ca^{2+}-currents, similar to the findings in dentate granule cells. NPY also decreased regenerative Ca^{2+} currents caused by the appropriate pairing of pre- and post-synaptic input.

Together, these observations demonstrate that the role of NPY in the hippocampus and neocortex is not solely as an anti-epileptic agent. NPY release, likely to occur during high

frequency oscillatory activity, can act locally to limit dendritic excitability, which can have a profound effect on plasticity. In the dentate gyrus, NPY can inhibit a D1R induced increased dendritic excitability and resultant changes in synaptic strength. These findings will further the understanding of dendritic information processing in the hippocampus and neocortex.

ACKNOWLEDGEMENTS

To my supervisor, Dr. William Colmers, I would like to express my utmost appreciation. Thank you for your consistent enthusiasm and support of my work and abilities. The opportunities that you have given me have been incredible, from working with human brain tissue, to learning how to perform dendritic recordings with your collaborator in Switzerland. You have a wholehearted dedication to science and the pursuit of knowledge, which is something I truly admire.

To my supervisory committee, Drs. Peter Smith and Klaus Ballanyi, thank you for your consistent support, encouragement, and valuable criticism. Thank you for providing so many significant insights and suggestions.

To my examining committee, Drs. Yu Tian Wang and Clayton Dickson, thank you for taking the time to read my thesis and provide valuable comments and observations. To Dr. David Collins, thank you for being the chair of my final examination.

To Matthew Larkum, thank you for welcoming me to your laboratory and taking time from your busy schedule to teach me how to record from dendrites.

To Carol Ann Johnson, thank you for guiding me through many of the steps necessary to finish this thesis. I always enjoyed coming to visit and discussing administrative details, among other things.

To fellow members of the Colmers lab: Dr. Bouchaib El Bahh, thank you taking the time to teach me how to perform dissections and extracellular recordings; Dr. Nina Pronchuk, thank you for your help with immunohistochemistry and being one of the most kind and patient people I have ever met; Dr. Melissa Chee, thank you for your constant support and very worthwhile discussions. I will truly miss working with you; Chantelle Giesbrecht, thank you for your open ear and willingness to laugh no matter what time of the day.

To fellow neuroscience graduate students who have shared many enjoyable moments on and off campus. In particular, Jan Kowalczewski and Robin Clugston, thank you for being along side me during this endeavor and keeping things optimistic and the glass more than half full.

To post-doctoral friends and colleagues: Drs. Gavin Searle and Nicola Webster, for spreading your knowledge of electrophysiology, and making sure I point the right way down the mountain; Dr. Kevin Murphy, even though you are across the pond, thank you for all of your helpful comments, NPY related or otherwise.

To my friends who have supported me on and off campus: Rod and Michelle, Walter and Wallace, Martin and Moira, Dak and Jenny, neighbour Dave, thank you for all of your successes, academic and personal that has allowed us to celebrate many great things; To Evan and Teri, for helping me stay grounded at high or low elevations; to Gregory de Pascale, my good friend and McGill alumnus, thank you for helping push the boundary of excess.

To my extended family Tadeusz Kazmierczak, Tim and Ivona Shchurek, Tymon Kazmierczak and Stephanie Aumais, thank you all of your help over the course of this project.

Finally, to my loving family who have provided steady and dependable support. Mom, Dad, Scott, and Angela, I could have never accomplished this without you.

TABLE OF CONTENTS

Chapter 1

General Introduction

Chapter 2

Dopamine and Neuropeptide Y Modulate Dendritic Excitability and Synaptic Plasticity in Dendrites of Rat and Human Dentate Granule Cells

Chapter 3

Neuropeptide Y Inhibits Frequency-Dependent Ca^{2+} Electrogenesis in Layer 5 Pyramidal Neurons

LIST OF FIGURES

LIST OF TABLES

LIST OF ABBREVIATIONS

4-AP	4-aminopyridine
aCSF	Artificial cerebrospinal fluid
ADP	Afterdepolarization
AM	Acetoxymethyl ester
AMPA	Alpha-amino-3-hydroxy-5-methyl-4-isoxazolepropionic acid
AP	Action potential
APV	DL-2-Amino-5-phosphopentanoic acid
ATP	Adenosine triphosphate
bAP	Backpropagating action potential
BAPTA	1,2-bis(2-aminophenoxy)ethane-N,N,N,N-tetraacetic acid
BK	Ca^{2+}-activated K^{+}-channel, BK-subfamily
CA1	Cornu Ammonis 1
CA2	Cornu Ammonis 2
Ca^{2+}-Na^{+}-APs	Calcium-sodium action potentials, Ca^{2+} spikes
$[Ca^{2+}]_i$	Intracellular Ca^{2+} concentration
CA3	Cornu Ammonis 3
CaM	Ca^{2+}-calmodulin
CaMKII	Calcium-calmodulin dependent protein kinase II
cAMP	Cyclic adenosine 3, 5-monophosphate
CCD	cooled charge-coupled device
CF	Critical frequency
CLSM	Confocal laser scanning microscopy
CgTx	ω-conotoxin-GVIA
C_m	Membrane capacitance
CNS	Central nervous system
D1R	Dopamine D1-receptor
DGC	Dentate granule cell
EGTA	Ethylene glycol-bis(β-aminoethyl ether) N,N,N,N-tetraacetic acid
EPSP	Excitatory postsynaptic potential

fEPSP	Field EPSP
FS	Fast spiking
GABA	γ-aminobutyric acid
GCL	Granule cell layer
G_{IRK}	G-protein coupled inwardly rectifiying potassium channel
GPCR	G-protein coupled receptor
GTP	Guanosine triphosphate
HCN	Hyperpolarization activated cation channels
HEPES	4-(2-hydroxyethyl)-1-piperazineethanesulfonic acid
IA	Inhibitory avoidance
IB	Intrinsically bursting
I_h	Hyperpolarization activated cation channels
IK	Ca^{2+}-activated K^+-channel, IK-subfamily
IR	Input resistance
IR-DIC	Infrared differential interference contrast
K_{Ca}	Calcium-activated potassium channel
K_d	Dissociation constant
KPBS	Potassium phosphate buffer solution
L2/3	Layer 2/3
L5	Layer 5
LEC	Lateral entorhinal cortex
LTD	Long-term depression
LTP	Long-term potentiation
MAPK	Mitogen-activated protein kinase
MEC	Medial entorhinal cortex
mEPSP	Miniature exctitatory post-synaptic current
MF	Mossy fibers
MPP	Medial perforant pathway
Na^+-APs	Sodium action potentials
Nif	Nifedipine
NMDA	N-methyl-D-aspartate
NPY	Neuropeptide Y
OGB-1	Oregon green 488 BAPTA-1
P	Proline

PKA	Protein kinase A
PKC	Protein kinase C
PNS	Peripheral nervous system
PP	Pancreatic polypeptide
PTX	Picrotoxin
PYY	Peptide YY
R_i	Axial resistance
R_m	Membrane resistance
RMP	Resting membrane potential
ROI	Region of interest
RS	Regular spiking
SA	Streptavidin
SEM	Standard error of means
sEPSC	Spontaneous excitatory post-synaptic current
sEPSP	Simulated excitatory post-synaptic potential
SGZ	Subgranular zone
SK	Ca^{2+}-activated K^+-channel, IK-subfamily
STDP	Spike-timing dependent plasticity
Syn Blk	Synaptic blockade
TBP	Theta burst pairing
TTX	Tetrodotoxin
VDCCs	Voltage-dependent Ca^{2+} channels
VIP	Vasoactive intestinal peptide
V_m	Membrane potential
VTA	Ventral tegmental area
Y	Tyrosine
Y1R	NPY1 receptors

CHAPTER 1

General Introduction

The Hippocampal Formation

The hippocampal formation is located in the medial temporal lobe of the mammalian brain and considered a part of the limbic system along with the amygdala, hypothalamus, cingulate gyrus, fornix, mammillary body, nucleus accumbens, orbitofrontal cortex, parahippocampal gyrus, and the thalamus. The hippocampal formation was named for its resemblance to a seahorse ("hippocampus") in 1597 by the Italian anatomist, Arantius (Lewis, 1923), and consists of the dentate gyrus and the hippocampus proper, which include areas cornu Ammonis ("Ammon's Horn") 1, 2, and 3 (CA1, CA2, and CA3; Fig. 1.1). There is controversy whether the entorhinal cortex (EC) and subicular complex are also included in the 'hippocampal formation' because of their dense connectivity with the dentate gyrus and CA regions. Therefore, for simplicity and clarity, the 'hippocampal formation' will refer to the dentate gyrus and Ammon's Horn, and the 'retrohippocampal region' will refer to the entorhinal cortex and subicular complex for the remainder of this thesis. The function of the hippocampal formation has been under intense study since the 1950's when patient H.M. had a large section of his temporal lobes removed to treat intractable epilepsy, and thereafter was unable to form new memories (Scoville and Milner, 1957). Subsequently, it was confirmed that the hippocampal formation is crucial for the encoding of new declarative memories (Zola-Morgan et al., 1986; Eichenbaum and Cohen, 1988). These processes are heavily modulated by cortical inputs, which primarily arrive from the EC. However, there remains much to be learned about how the hippocampal formation can interact with the cortex to regulate memory formation (Ranganath et al., 2005).

Ramon y Cajal and Lorente de Nó were instrumental in describing the intrinsic and extrinsic pathways of the hippocampal formation with the use of the Golgi technique. Since then, anterograde and retrograde tracers as well as electrophysiological methods have been used to further examine hippocampal connectivity. Early physiological studies

Figure 1.1. The Hippocampus in the Rat Brain.

The hippocampus is a "C" shaped structure that runs from septal nuclei rostrally (S) to the temporal cortex (T). The slice of hippocampus is in the transverse (TRANS) plane and is perpendicular to the septo-temporal axis. The trisynaptic pathway is illustrated in the transverse slice. The trisynaptic circuit is as follows: Perforant pathway (PP) from the EC to the Dentate Gyrus (DG). Mossy fiber pathway (mf) from the DG to CA3. Schaffer collaterals (sc) from CA3 to CA1. S - subiculum. Adapted from Witter et al. 2000.

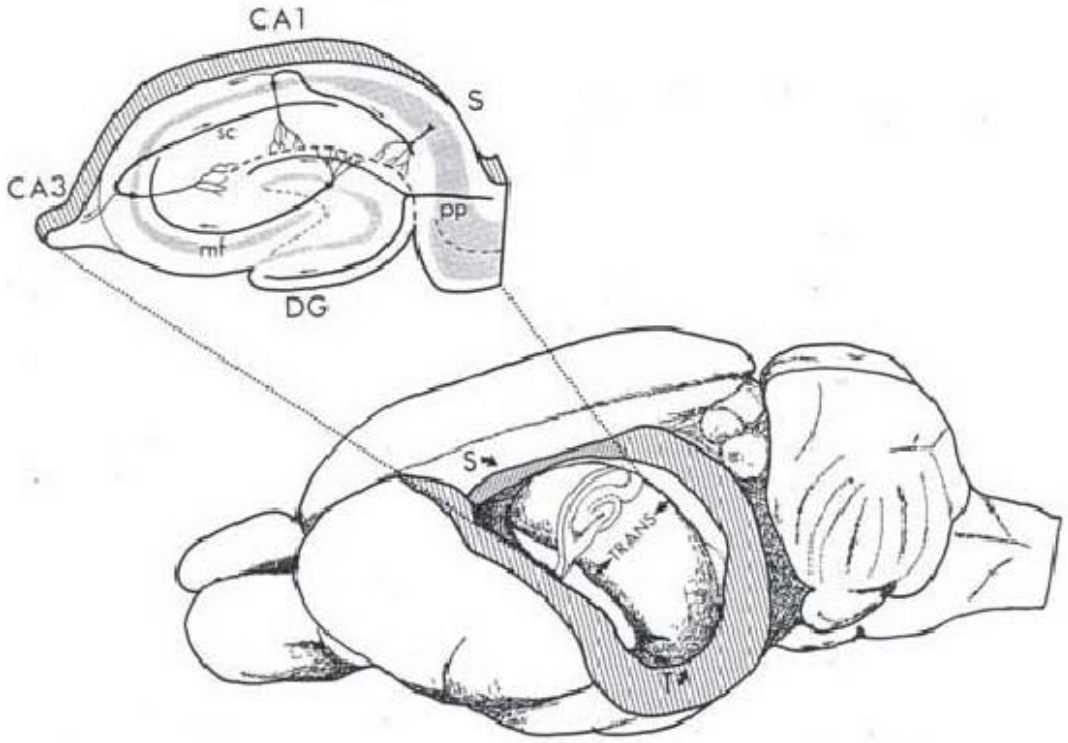
CA1
S
sc
CA3
pp
mf
DG
S
TRANS

of the rabbit hippocampal formation led to the hypothesis that this structure is anatomically organized in small slices known as lamellae. The lamellar hypothesis posits that the transfer of information through the excitatory trisynaptic pathway (perforant path - PP, to mossy fibers - MF, to Schaffer collaterals - SC, and alvear fibers of CA1) occurs within each lamella, in the same transverse plane (Fig. 1.1; Andersen et al., 1971). This organizational scheme is analogous to the mutually exclusive ocular dominance columns of the visual cortex (Amaral and Witter, 1989). Based on this model, neural activity would flow through the trisynaptic pathway in the plane of a transverse slice, enabling simultaneous and separate parallel computation in different slices of the EC-hippocampal loop (Andersen et al., 1971). Many of the structural connections of the hippocampal formation, including the trisynaptic pathway, occur in the transverse plane, which makes this orientation the most widely used method for preparation of hippocampal slices. The injection of anterograde tracers into EC layers II and III clearly indicate a significant, overlapping divergence of input to the molecular layer of the dentate gyrus (Amaral and Witter, 1989). Consistent with the lamellar hypothesis is the mossy fiber projection that almost exclusively travels in the transverse plane in a linear manner. The only non-laminar portion is from area CA3 to CA1 where the fibers turn caudally for approximately 2 mm (Swanson et al., 1978). Although the trisynaptic pathway is fundamental to hippocampal signal processing, there are many additional efferent and afferent connections. Also projecting from the dentate is the non-laminar associational pathway where axons exit the hilus to travel parallel with the longitudinal axis, and can project up to 2250 μm away from their point of emergence (Amaral and Witter, 1989). Thus, the lamellar hypothesis is a gross generalization that oversimplifies the connectivity of the hippocampal formation. The extrinsic and intrinsic connections of the hippocampal formation are in fact complex and in many cases divergent.

The Entorhinal Cortex

The entorhinal cortex is a major interface between the higher order cortical areas and the hippocampal formation and is a key component of the trisynaptic circuit (Witter, 2002). It is thought to organize multimodal sensory input from the neocortex and hippocampal formation. Commonly considered a part of the parahippocampal region, the EC receives input from the perirhinal and postrhinal cortices, and projects to the dentate gyrus, CA1-CA3, and the subiculum. Area CA1 and the subiculum also send connections back to the EC to complete the EC-hippocampal loop. The EC can be subdivided into a medial area (MEC) containing cells that process spatial information and a lateral area (LEC) containing cells that process non-spatial, olfactory and somatosensory information (Canto et al., 2008). In non-primates and monkeys the presence of a projection from the presubiculum to the MEC, and not LEC, has also been used to functionally subdivide the EC (Canto et al., 2008). The organization of these areas remains consistent across the longitudinal axis of the EC, but does vary somewhat in the transverse and radial axes (Witter et al., 2000). The EC contains six layers that are similar to the neocortex, with the following characteristics; (closest to the pia) layer 1 – a sparse cell layer containing non- or moderately-spiny multipolar cells and axons from other layers. Horizontal cells are located on the border of layers 1 and 2 that run in a transverse direction are and also considered part of layer 1; layer 2 – a narrow layer containing relatively large stellate and modified pyramidal cells; layer 3 – a broad medium sized pyramidal cell layer with a sporadic arrangement; layer 4 – a narrow layer referred to as 'lamina dissecans' containing no cell bodies; layer 5 – a definitive pyramidal cell layer containing horizontal cells and cell bodies of large pyramidal cells; layer 6 – a broad cell layer with a multilaminate appearance (Witter and Amaral, 1991; Canto et al., 2008).

Perforant Pathway

The perforant path originates in layers 2 and 3 of the EC and projects via the angular bundle and subiculum to the dentate gyrus, CA3, and CA1. Layer 2 LEC projection neurons terminate in the outer third of the molecular layer of the dentate gyrus and outer third of stratum laculosum moleculare of CA3 (Fig. 1.2; Steward and Scoville, 1976) and likely conveys highly processed motivational and intrinsic information (Witter et al., 2000). Layer 2 MEC projection neurons terminate in the middle third of the molecular layer of the dentate gyrus and middle third of stratum laculosum moleculare of CA3 (Fig. 1.2; Steward and Scoville, 1976) and likely convey sensory related information (Witter et al., 2000). Furthermore, destruction of the MPP results in impaired place learning (Ferbinteanu et al., 1999). Both MEC and LEC terminating fibers project from layer 2 and layer 3 and travel through the subiculum, then across the hippocampal fissure and into the molecular layer where they make excitatory connections with dendritic spines (Witter and Amaral, 1991). The subdivision of the lateral and medial perforant pathway is also observed pharmacologically. In the dentate molecular layer there is a considerably increased effect of NMDA antagonists, baclofen, and carbachol on MEC stimulation, whereas L-AP4 has a greater effect on LEC stimulation (Hanse and Gustafsson, 1992).

Similar to layer 2 neurons, projections from LEC and MEC layer 3 innervate the hippocampal formation; however these axons enter area CA1, and are termed the temporoammonic pathway. These fibers terminate on to inhibitory basket cells and chandelier cells of stratum laculosum moleculare (Dvorak-Carbone and Schuman, 1999). Specifically, MEC neurons terminate in proximal CA1 and distal subiculum, whereas, LEC neurons terminate in distal CA1 and proximal subiculum (Steward and Scoville 1976, Witter, 1986, Amaral, 1993). These fibers that project from layer 3 travel laterally from the EC through the subiculum before innervation (Witter and Amaral, 1991). Thus, the perforant pathway is topographically organized and maintains an entorhinal lateral-to-

Figure 1.2. The Connectivity of the Hippocampal Formation.

The major pathways of the hippocampus form a principally uni-directional network. Input from the entorhinal cortex (EC) travels to the dentate gyrus (DG) via the perforant pathway (PP). The medial perforant pathway (MPP) travels to the medial aspect of the molecular layer of the DG, whereas the lateral perforant pathway (LPP) travels to outer molecular layer. DG granule cells project to area CA3 via the mossy fiber pathway (MF). CA3 pyramidal neurons send axons to CA1 via the Schaffer Collateral pathway (SC), and also to the contralateral hippocampus through the associational commissural pathway (AC). Pyramidal neurons in CA1 also receive input from the PP, and send axons to the subiculum (Sb). From the subiculum axons travel back to the EC. Image from: http://www.bris.ac.uk/Depts/Synaptic/info/pathway/hippocampal.htm.

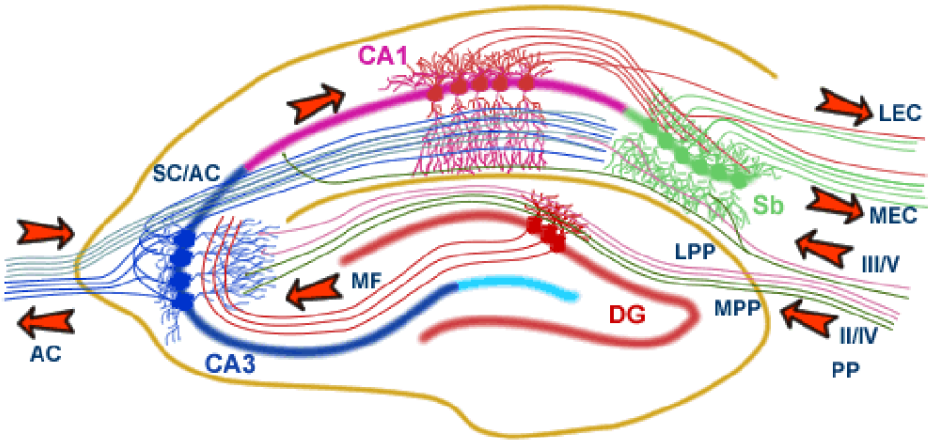
CA1
LEC
SC/AC
Sb
MEC
LPP
III/V
MF
DG
MPP
II/IV
AC
CA3
PP

medial gradient that projects on to the septal-to-temporal (longitudinal) hippocampal axis. Since the EC also receives information in a compartmentalized manner, this implies that there is segregation and processing of information that differs between input from layers 2 and 3 and along the longitudinal axis of the hippocampal formation.

Perforant pathway projections from excitatory glutamatergic synapses play a critical role in the generation of theta (4-12 Hz) and gamma (30-100 Hz) oscillations, which occur during waking and paradoxical sleep (Chrobak and Buzsaki, 1996). Theta oscillations have been shown to be the predominant rhythm in the hippocampal formation (Green and Arduini, 1954; Vanderwolf, 1969). They have been observed in the rat during movement, sniffing, exploration of the environment and during REM sleep (Vanderwolf, 1969) and are thought to modulate synaptic plasticity (Larson et al. 1993; Buzsaki, 2002). During theta wave activity there are 'nested,' temporally-organized population volleys of gamma frequency (40-100 Hz; Chrobak and Buzsaki, 1996) due to sporadic firing of Layer 2 and 3 EC neurons that can evoke synchronized activation of the dentate gyrus, CA1, CA3, and subicular cortex. Gamma oscillations may also be generated in the dentate gyrus; however, they most likely occur from a complex interplay of synaptic and nonsynaptic network mechanisms (Towers et al., 2002). These gamma volleys nested in theta waves are thought to contribute to synaptic plasticity, memory formation, and play a role in emergent functions such as perception, attention, and consciousness (Csicsvari et al., 2003).

Layer 4-6 projection

The perforant pathway projection to the outer two thirds of the dentate gyrus molecular layer, and lack EC input to the inner third, led to the term "entorhinal zone" being used to describe the outer two thirds of the molecular layer (Blackstad, 1956; Zimmer, 1971; Swanson et al., 1978). However, more recent work has identified a

projection from layers 4-6 of the EC that terminates in the inner third of the molecular layer on proximal dendrites and somata of granule cells, and dendritic shafts of GABAergic neurons (Deller et al., 1996). These fibers terminate on GABAergic neurons in the inner molecular zone and also in the hilus, which likely represents feed-forward inhibition from the EC. However, this projection also synapses onto GABA-negative dendrites in the hilus and dendrites and soma of DGCs (Deller et al., 1996) indicative of an excitatory feed-forward role.

Dentate gyrus

A cross-section of the dentate gyrus reveals a C- or V- shaped tri-laminar structure. In the middle is a compact layer containing only the densely-packed somata of the principal neurons of the dentate, DGCs. Across mammalian species, approximately 90 % of neurons in the dentate are DGCs (Seress, 2007). On the outer side is the molecular layer that contains dendrites of the DGCs and sparse interneurons, and on the inner is the hilus, or polymorph layer, that contains axons of DGCs, a variety of GABAergic interneurons, and mossy cells (Freund and Buzsaki, 1996; Amaral et al., 2007). Input to the DG comes primarily from the perforant pathway that synapses onto the dendrites of granule cells in the outer two-thirds of the molecular layer (Fig. 1.3). The inner third of the molecular layer of the DG is termed the "hippocampal zone" because it is where associational and commissural fibers from the dentate hilus terminate. The DG also receives input from the septum, and the noradrenergic and serotinergic inputs from the locus coeruleus and the raphe nucleus, respectively (Leranth and Hajszan, 2007). Extrinsic input to the DG also includes dopaminergic afferents from the ventral tegmental area (VTA) that synapse on to the middle third of the molecular layer (Gasbarri et al., 1994). Intrinsic GABAergic and NPYergic interneurons can also modulate input to the DGCs (Freund and Buzsaki, 1996). The somata of DGCs are located in a densely packed

Figure 1.3. Dentate Gyrus Anatomy.

(A) A dentate granule cell was filled with biocytin and the image is fused with a cresyl violet stained image of the same section. The dendritic tree branches from the densely packed granule cell layer (g) out into the molecular layer (m). The molecular layer can be further subdivided into an outer (distal from the granule cell layer), middle, and inner portion (adjacent the granule cell layer). In the hilus (h) white arrows show local mossy fibre collaterals and the black arrow shows the mossy fibre that synapses in CA3. Modified from Acsady et al., 1998). (B) An image of the densely packed granule cell layer. This layer can also be divided into outer (adjacent to the molecular layer), middle, and inner (adjacent to the hilus) thirds. On the upper right is a patch pipette. Image by T. Hamilton.

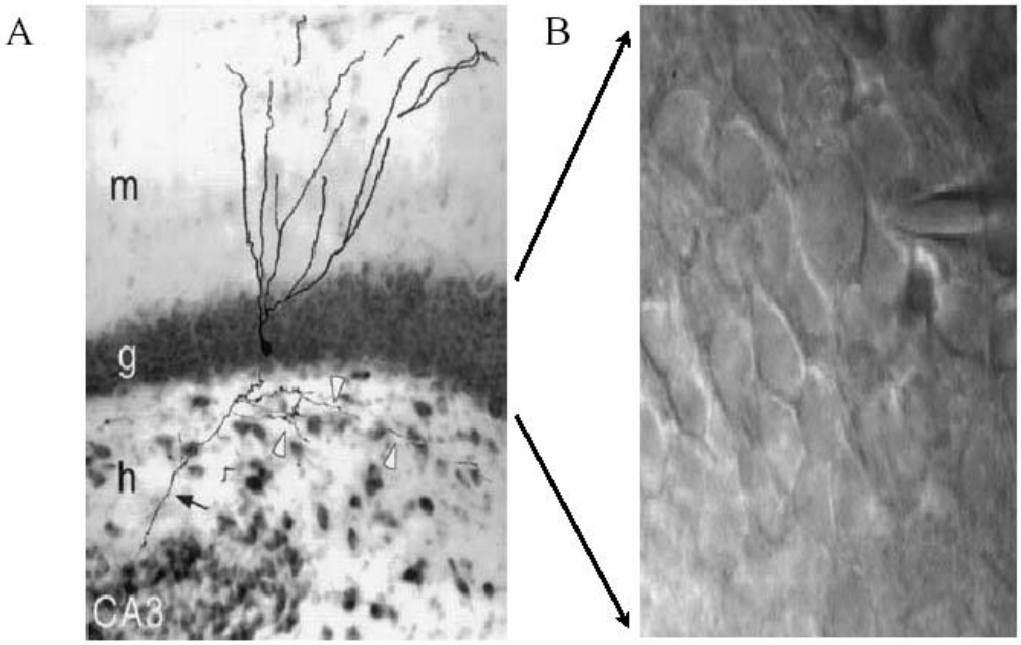
A
B
m
g
h
CA3

layer called stratum granulosum, or the 'granule cell layer' (GCL), that can be subdivided into three sections; outer (closest to the molecular layer), middle, and inner (closest to the hilus; Fig. 1.3). There are approximately 15 million DGCs in the human hippocampal formation and 1 million in the rat (Amaral et al., 2007). Apical dendrites of DGCs are in a cone-shaped arrangement with distal tips reaching as far as the hippocampal fissure. Golgi staining has shown that the cell bodies of neurons within the outer third of the GCL have substantially more dendritic material, different length and number of branches, and wider dendritic fields (Green and Juraska, 1985). This gradient in size is because DGCs are constantly being born in the subgranular zone (SGZ, medial to the inner GCL) and migrate towards the outer GCL as they age (Gould et al., 1999).

In the last decade, it has become clear that neural precursor cells in the SGZ of the dentate gyrus supply new granule cells on an ongoing basis up to at least 70 years of age in humans (Parent, 2007). In the SGZ, neuronal precursors proliferate and continually migrate into the GCL where they mature and become functional granule cells. The specific factors that influence neurogenesis in the DG are, therefore, of significant interest because their impact will modify the memory formation process. Exercise, growth factors, environmental enrichment, aging, hormones such as estrogen and prolactin, glutamatergic neurotransmission, adrenal hormones, long-term potentiation (LTP), lesions, seizure activity, and the presence of NPY are all associated with a regulation of dentate neurogenesis (Parent, 2007). Furthermore, immature DGCs have increased excitability because of higher input resistance and increased Ca^{2+} channel distribution that can lead to enhanced LTP (Schmidt-Hieber, et al., 2004). This property of immature neurons of the dentate is hypothesized to play a role in the encoding of time in a memory trace (Aimone et al., 2006) however this has yet to be explored.

In the transverse plane, the DG is also subdivided into infrapyramidal and suprapyramidal blades (also called inner and outer, or medial and lateral, respectively).

DGCs in these regions have differences in dendritic structure (Claiborne et al., 1990). The branching of dendrites is also such that most DGCs have the widest extent of their dendritic tree parallel to the transverse plane of the hippocampal formation (Claiborne et al., 1990), which is an additional rationale for the use of the transverse slice orientation. Surrounded by the GCL is the dentate hilus that contains neurons that both receive and transmit information to DGCs.

Dentate Hilus

The dentate hilus, or polymorph layer, is located between the supra- and infrapyramidal blades of the dentate gyrus. The dentate hilus contains both excitatory and inhibitory neurons that have dendrites in the molecular layer to receive perforant pathway input. In fact, most hilar neurons have a lower threshold for activation than granule cells (Scharfman, 1991). Many hilar neurons can also project to distant ipsilateral sites in the molecular layer, as well as the contralateral hippocampal formation via hilar cell projections (Laurberg and Sorensen, 1981). When first discovered, large spiny hilar neurons termed 'mossy cells' by Amaral (1978) were believed to be a continuation of the adjacent pyramidal cells of CA3 (Lorente de Nó, 1934). Both CA3 pyramidal neurons and mossy cells have high input resistances, long time constants, spontaneous excitatory postsynaptic potentials, and large complex dendritic spines (Scharfman, 1993). However, compared to CA3 pyramidal neurons, mossy cells have larger somata, a different dendritic branching pattern that is more confined to the hilus, more highly specialized dendritic spines called 'thorny excrescences,' and axonal projections to the dentate molecular layer rather than CA1 (in the case of CA3 pyramidal neurons), and are therefore not considered a continuation of the CA3 pyramidal cell layer (Buckmaster et al., 1993). Intracellular studies have indicated that mossy cells are excitatory neurons with monosynaptic connections onto DGCs and interneurons that are

located adjacent to the mossy cell's soma (Scharfman, 1995). Physiologically, mossy cells have the potential to be powerful integrators of multiple input patterns because they are activated by the perforant pathway (Scharfman, 1991), CA3 pyramidal neurons (Scharfman, 1994), subcortical inputs (Loy et al., 1980), and granule cells (Scharfman, 1995). There is a positive feedback loop between granule cells and mossy cells, and at present, the physiological function of this loop is unknown.

The Mossy Fiber Pathway

The second synapse in the 'trisynaptic pathway' is the termination of DGC axons onto hilar and CA3 neurons (Fig. 1.3). This mossy fiber pathway has axons that contain large varicosities and filamentous extensions that have the visual appearance of moss. However, it was due to the anatomical similarity in appearance to mossy fibers in the cerebellum that influenced Cajal to term them 'mossy fibers.' In the human there are approximately 15 million granule cell axons that contribute to the pathway (Simic et al., 1997), whereas in the rat there are approximately 1 million (Boss et al., 1985). The MF pathway synapses on to mossy cells and many types of interneurons in the hilus, and on to pyramidal neurons and interneurons in area CA3 (Gutierrez, 2003). Chelatable zinc and peptides such as enkephalin, dynorphin, cholecystokinin, neuropeptide Y (NPY), neurokinin B, are also released from the MF pathway (Henze et al., 2000).

The diverse distribution of synapses along the axons of DGCs is a distinctive aspect of the MF pathway. Unmyelinated mossy fiber axons first synapse on to excitatory and inhibitory polymorphic neurons of the hilus via fine collaterals less than 0.2 μM thick (Henze et al., 2000). After the axons travel through CA3 via the stratum lucidum, the remainder of the synapses occur on proximal and apical dendrites of CA3 pyramidal neurons, dendrites of local circuit excitatory neurons, and CA3 interneurons (Henze et al., 2000). The average length of mossy fibers in the rat is around 3200 μM,

with a span of approximately 800 μm in the hilus (CA3c), 1050 μm in CA3b, and 1400 μm in CA3a (Acsady et al., 1998). Each mossy fiber contacts approximately 140-150 cells in the hilus, with an average of 10 of these on mossy cells and the remainder on inhibitory interneurons (Frotscher, 1985; Acsady et al., 1998; Henze et al., 2000), and 11-18 on CA3 pyramidal neurons (Claiborne et al., 1986; Acsady et al., 1998). Clearly, the MF pathway is extremely dissimilar in connectivity with the majority of synapses being on inhibitory GABAergic interneurons rather than excitatory glutamatergic hilar mossy cells and CA3 pyramidal neurons (Acsady et al., 1998). Therefore, the traditional trisynaptic theory that depicts an excitatory role for the MF pathway is only partially correct, as a major component of the pathway results in driving inhibitory cells.

An examination of the morphology of MF synapses provides further insight into the excitatory and inhibitory features of the pathway. Dentate granule cells are unique in that their axons have more than one terminal type. Mossy fibers provide three morphologically specialized terminals that provide input to hilar and CA3 neurons; the large mossy terminals responsible for the pathway's name, filopodial extensions of the mossy terminals and small *en passant* synapses (Ramon y Cajal, 1911, in Amaral, 1979; Claibourne et al., 1986).

Area CA3

Hippocampal area CA3 has the potential to condense and modify incoming information from the mossy fiber pathway that primarily synapses onto proximal apical dendrites, and perforant pathway that primarily synapses onto distal apical dendrites of pyramidal neurons (Li et al., 1994). The processing ability of CA3 comes from what is termed a 'rich autoassociative network' made possible by its recurrent connections (Chrobak et al., 2000). This network circuitry is thought to organize neocortical information to decrease overlap between different distinct inputs (McNaughton and

Morris, 1987). The output of area CA3 includes a vast system of pyramidal cell collaterals that contact other CA3 fibers in the CA3 field, termed the "longitudinal association bundle" by Lorente de Nó. Pyramidal cell collaterals also travel to area CA1 termed the "Schaffer collaterals," as briefly discussed above. The Schaffer collateral pathway extends from the axons of CA3 pyramidal neurons and projects to stratum radiatum and stratum oriens of CA1, and contacts neurons in a different septo-temporal level (Hjorth-Simonsen, 1973; Amaral and Witter, 1989). In the rat, a single CA3 pyramidal cell contacts between 30 000 to 60 000 other neurons via extensive arborizations that terminate in area CA3 and CA1, the subiculum, the hilus, the dentate molecular layer, and into the contralateral hippocampal formation (Li et al., 1994).

Entorhinal Cortex-Hippocampal Synchrony

The excitatory connections described above,in combination with inhibitory interneurons throughout the EC and hippocampal formation ultimately allow for the generation of rhythmicity. It has been demonstrated that gamma oscillations (40-100 Hz) are generated in layer 2 and 3 of the entorhinal cortex during exploratory behaviour and these oscillations are entrained into theta and nested gamma oscillations in the dentate gyrus and CA1 (Bragin et al., 1995; Csicsvari et al., 1999). During non-theta states that occur during consummatory behaviour or slow wave sleep, the hippocampal formation produces output to layer 5 and 6 of the EC in the form of 140-200 Hz ripples and hippocampal sharp waves (Buzsaki et al., 1992; Chrobak and Buzsaki 1994, 1996). Current theory posits that oscillations in the hippocampal-entorhinal network are fundamental in the detection of novelty in external stimuli, computing the difference in top-down and bottom-up input, and reconstructing neocortical information (Chrobak et al., 2000).

Function of the Dentate Gyrus

Since the bilateral removal of a large portion of the temporal lobes from patient H.M. there has been a consensus among scientists that the hippocampal formation is crucial for the storage of long-term episodic memories. However, the mechanisms by which this occurs remain uncertain. The role of the hippocampal formation has become clearer with the discovery and study of 'place cells' in rodents. The first evidence of place cells was in CA1 and CA3 when O'Keefe and Dostrovsky (1971) found that certain hippocampal neurons became more active when an animal was in a particular place in a spatial environment. As an animal moves through the 'field' of a place cell, it will fire high-frequency bursts of action potentials (APs; Ranck, 1973). Place cells in the dentate gyrus have smaller and more plentiful fields, and are discontiguous (Jung and McNaughton, 1993). However, according to some scientists the notion that cell assemblies in the hippocampal formation only represent an animal's spatial location is too simplistic an explanation. Because hippocampal neurons respond to many external cues, such as odor (Eichenbaum et al., 1998), they have been proposed to represent various aspects of the context of the external world and not just spatial location (Smith and Mizumori, 2006).

A basic property of the hippocampal formation during learning behaviours is to form representations through organized neuronal firing, with different patterns representing different situations or sets of circumstances that can be termed 'contexts' (Smith and Mizumori, 2006). As an animal learns a specific context, this memory is organized as a specific set of highly plastic and distinct connections in the recurrent CA3 network following input from the dentate gyrus and EC, which is considered 'pattern separation.' As cortical information travels to the dentate gyrus, it diverges into an extensive system of sparsely firing DGCs that then make sparse connections to area CA3 via the mossy fiber pathway. This network is suited to separate, or distinguish between,

the vast patterns of representations from the cortex. This sparse coding system uses only a small population of available neurons to form a representation and is beneficial in many ways. Specifically, it maximizes storage capacity, decreases overlap between representations, minimizes synaptic modifications required to form the representation (Jung and McNaughton, 1993), and allows representations to be formed rapidly. Contextual memories can be further separated into the spatial and temporal domains. The dentate gyrus is necessary for spatial, not temporal, pattern separation and area CA1 is necessary for temporal, not spatial, pattern separation (Gilbert et al., 2001).

Based upon data across species, hippocampal connectivity has been conserved throughout mammalian evolution such that information flows not only in a transverse, or laminar fashion, but also along the longitudinal or septo-temporal axis, both ipsilaterally and contralaterally. This indicates that the opposite of parallel, lamellar processing, is occurring, with different hippocampal levels contacting one another and integrating specific components of information. However, it is also evident that there are gradients of topographically-organized areas that process different types of input such as layer 2 LEC and layer 2 MEC neurons conveying motivational and intrinsic information, and sensory related information, respectively. It seems that the hippocampal formation and entorhinal cortex are structures that contain specialized pathways, feedback and feedforward loops, a multitude of neuronal subtypes, neurotransmitters and neuropeptides, and both contribute to the processing and encoding of declarative memories in different, yet complimentary ways. This likely occurs via oscillatory activity through the EC-hippocampal formation loop that is itself heavily modulated by intrinsic and extrinsic influences. Furthermore, increased cortico-hippocampal interaction is associated with successful memory formation (Ranganath et al., 2005) indicating the necessity to examine both extrinsic neocortical interaction and intrinsic

properties of the EC-hippocampal loop to determine the role of the hippocampal formation in contextual memory encoding.

The Neocortex

The neocortex is the most recent brain area in mammalian evolution and is involved in complex tasks such as perception, cognition, memory, and volitional motor control. The mammalian neocortex can perform these operations because of its intensive connectivity and neuronal specificity throughout its six layers, or lamina. The majority of input to the neocortex comes from glutamatergic thalamic relay neurons that carry sensory information from the periphery and densely innervate the neocortex (Huguenard et al., 1995). Neuronal computation and processing of this input occurs throughout the network of approximately 10 billion neurons in humans. Approximately 75 % of neocortical neurons are excitatory, glutamatergic (spiny), and the remainder are inhibitory GABAergic (nonspiny or 'smooth') neurons (Jones et al., 1993). Cortical neurons contain a diversity of voltage- and receptor-dependent ion channels that shape their input-output characteristics, and ultimately, dictate their firing patterns. Cortical neurons can be differentiated according to their firing characteristics and morphology.

Since the advent of the Golgi technique (Golgi, 1886) cortical neurons have been classified according to their location, size, shape and neurites. Excitatory neurons, are fundamentally subdivided into either "pyramidal," or "non-pyramidal" (i.e., stellate and granule cells). Pyramidal neurons are the most plentiful neuronal class in the cortex with somata typically located in layers 2, 3, 5, and 6 (Mountcastle, 1998) and are the only type that project out of the cortex. Their axons can travel great distances, branch extensively, and innervate other cortical regions and subcortical structures (Mountcastle, 1998). Pyramidal neurons are set apart from stellate and granule cells by having a large apical dendrite emanating from the soma. Aside from this, these cell types have spiny

dendrites, respond to glutamate, and receive synapses throughout their dendritic arbors and on their somata and axon initial segments (Bannister, 2005). In the human neocortex, a pyramidal cell can emit and receive 40 000 synapses. Therefore, an understanding of the physiological role of the pyramidal neuron is crucial to discern the various functions of the neocortex.

Layer 5 Pyramidal Neurons

Layer 5 (L5) pyramidal neurons are compartmentalized structures with three distinct regions: the soma and basal dendrites, proximal apical dendrite including the oblique dendrites, and the distal apical dendrites (Fig. 1.4; Larkum et al., 2001). The basal dendrites are relatively short, emanate from the soma, reside in the same layer as the soma, and are directly innervated by thalamic axons or local collaterals (Spruston, 2008). Oblique dendrites branch from the trunk of the proximal apical dendrite from the soma to the distal branch point and receive input from layers 2, 3, and 4 (Larkman, 1991). As the apical dendrite leaves the soma it ascends superficially and can reach up to 2.5 mm in the human cortex (Marin-Padilla, 1967). Layer 5 apical dendrites tend to bundle together vertically with dendrites of layer 2/3 (L2/3) pyramidal neurons into dendritic clusters (Peters and Kara, 1987). These clusters typically receive similar synaptic input and are organized in a manner that is appropriate for synchrony (Douglas and Martin, 2004). Distally, the apical dendrite can also split, or 'bifurcate,' typically once or twice at a branch point resulting in two or more distal apical dendrites (Fig. 1.4). These end in a 'tuft' in layers 1 and 2, meaning that at the most superficial aspect the dendrite branches profusely, greatly increasing its surface area. The tufted region receives the majority of its excitatory input from distal cortical areas (Douglas and Martin, 2007) that are part of the "feedback" network crucial to associative learning and attention (Sjöström and

Figure 1.4. Regions of Layer 5 Pyramidal Neurons.

Neurobiotin filled rat L5 pyramidal neurons with three morphologically distinct compartments: Basal dendrites that emanate from the soma, oblique dendrites from the proximal apical dendrite, and a distal dendritic tuft region. In the distal apical dendritic region pyramidal neurons can branch once (right cell), or twice (left cell) before the tuft. Scale Bar (200 μm). Image by T. Hamilton.

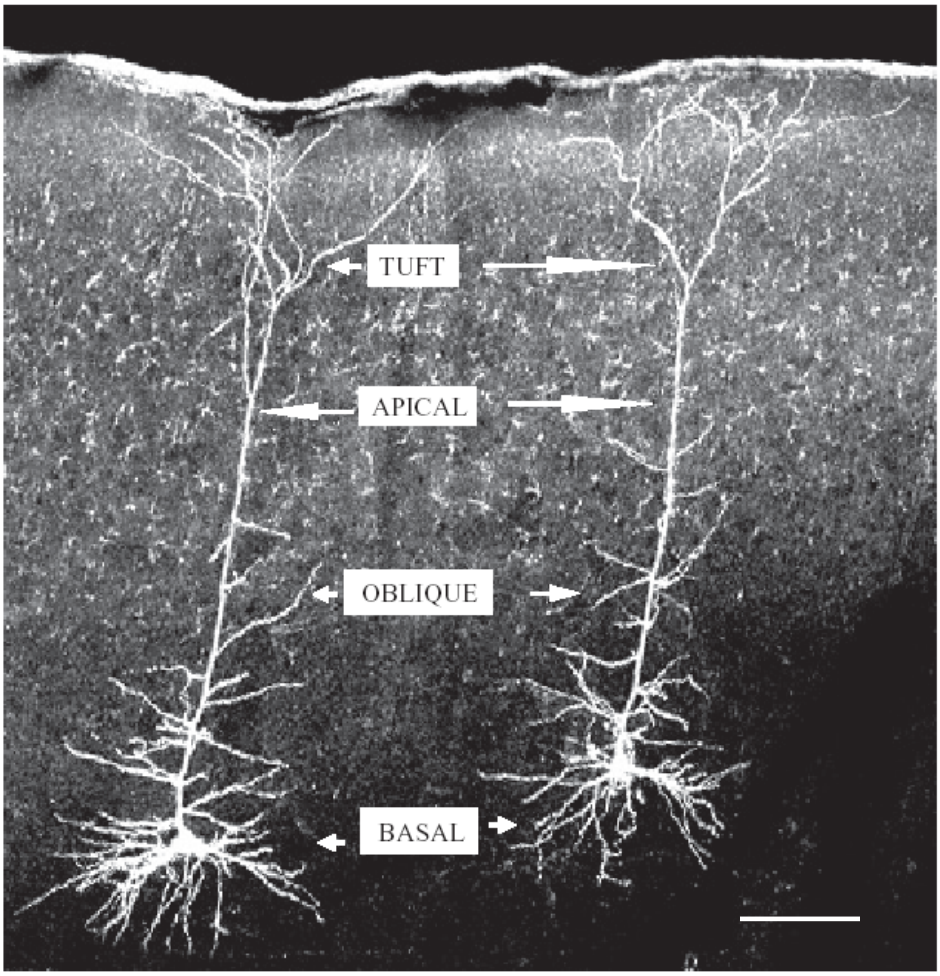
TUFT
APICAL
OBLIQUE
BASAL

Hausser, 2006; Gilbert and Sigman, 2007). However, there is also large innervation of layer 1 from thalamic association, limbic, motor, and nonlemniscal sensory nuclei (Rubio-Garrido et al., 2009).

Although distal synaptic inputs are located up to 1 mm from the soma and would appear to have, at best, modest influences on the output of L5 neurons, a large body of recent work suggests that dendritic properties can aid in faithfully transmitting information along these vast structures. The distribution of some active conductances in the dendrites of pyramidal neurons is not uniform and can have a great influence on synaptic integration (Johnston et al., 1996). Although cell-attached and whole-cell recordings from apical dendrites have shown that the density of Na^+ channels along apical dendrites is fairly uniform (Huguenard et al., 1989), there have been opposite findings for some voltage-dependent Ca^{2+} and K^+ channels. A non-uniform distribution of voltage-dependent Ca^{2+} channels (VDCCs) has been observed in CA1 pyramidal neurons with a higher density of L-type near the soma, and T-, and R-type in the distal dendrites (Magee and Johnston, 1995; Johnston et al., 1996). Apical dendrites of L5 pyramidal neurons have been shown to contain Cd^{2+}- and Ni^{2+}-sensitive VDCCs (Yuste et al., 1994; Schiller et al., 1997; Larkum et al., 1999b), yet there have been no investigations of the relative density of VDCCs along these dendrites. Because of physiological evidence that Ca^{2+} spikes are generated in distal tufts (Schiller et al., 1997; Larkum et al., 1999ab) it can be hypothesized that there is a greater density of at least one subtype of VDCCs in this region, similar to CA1 pyramdial neurons. A-type K^+ channels are distributed in a linear manner in L5 pyramidal neuron dendrites (Korngreen and Sakmann, 2000) unlike in CA1 pyramidal neurons where their density increases with distance from the soma (Hoffman et al., 1997). However, hyperpolarization activated cation channels (HCN or I_h) are found with increasing density with distance from the

soma in L5 pyramidal neurons (Lorincz et al., 2002), which decreases coupling between the soma and distal tuft (Berger et al., 2001).

The integration of the thousands of synaptic inputs on dendrites of pyramidal neurons will shape output depending on the strength, polarity (excitatory or inhibitory), and location of input. The ability to perform simultaneous intracellular whole-cell recordings along distal sections of the L5 apical dendrite has greatly furthered the understanding of somato-dendritic connectivity and the influence of synaptic input in dendritic compartments. Action potentials resulting from activation of voltage-dependent Na^+ channels (Na^+-APs) at the axon initial segment propagate both down the axon and backward or antidromically, up the dendritic tree (Kim and Connors, 1993; Stuart and Sakmann, 1994). The distal apical dendrite can also generate APs that depend partly on activation of VDCCs, but also require participation of Na^+ channels (Ca^{2+}-Na^+-APs; Schiller et al., 1997; Helmchen et al., 1999). These distal dendritic APs can propogate to the soma where they can depolarize the cell and even cause bursts of Na^+-APs (Schiller et al., 1997). Alpha-amino-3-hydroxy-5-methyl-4-isoxazolepropionic acid (AMPA) and N-methyl-D-aspartate (NMDA) receptor activation are both necessary for synaptically-induced Ca^{2+}-Na^+-APs in the distal tuft (Schiller et al., 1997). Interestingly, high frequency bursts of Na^+-APs can also cause the initiation of apical dendrite Ca^{2+}-Na^+-APs (Larkum et al., 1999b). Therefore, the soma and distal apical dendrite are distinct zones that can separately integrate information and respond in a specialized manner. Synaptic inputs located at different points along the somato-dendritic membrane can have very different contributions to AP firing. For example, input to basal dendrites is integrated at the soma and if it is above threshold will evoke a Na^+-AP. If this is accompanied by input to the distal tuft that generates a Ca^{2+}-Na^+-AP that propagates to the soma, a burst of Na^+-APs can result (Larkum et al., 2004).

The propagation of both Ca^{2+}-Na^{+}-APs from the tuft to the soma, and Na^{+}-APs from the soma to tuft are regulated by proximal oblique dendrites that lie in between the two regions (Larkum et al., 2001). Thus, distal dendritic tufts regulate firing of the distal AP zone and basal dendrites regulate the firing of the somatic AP zone (Larkum et al., 2001). Synaptic activity or membrane potential change in the oblique dendrites, or 'coupling zone,' can influence the communication between the two AP initiation zones and resultant output pattern (Larkum et al., 2001).

Action Potential Backpropagation

Historically, the role of an AP in excitable cells is to propagate from the site of initiation, the axon initial segment (Fuortes et al., 1957), down the axon and depolarize the presynaptic terminal, evoking synaptic neurotransmitter release. The speed at which an AP propagates from the axon initial segment to the presynaptic terminal depends upon the axon diameter, presence of myelin, and distribution of voltage sensitive Na^{+} and K^{+} channels in the axon. Regulation of neurotransmitter release from the presynaptic terminal is determined by the temporal proximity of APs. A low frequency of APs will preferentially result in the release of small, 'clear' synaptic vesicles containing classical (i.e., small molecule) neurotransmitters, whereas a high frequency of APs will also result in the release of the much larger dense core vesicles often containing larger molecules such as neuropeptides (Hokfelt, 1991; Klyatchko and Jackson, 2002). However, it has more recently become clear that orthodromically-propagating APs that arise from the initial segment also antidromically invade the dendritic tree. This propagation into the dendritic tree is appropriately termed a backpropagating action potential (bAP) and can have profound consequences on neuronal activity and plasticity.

Backpropagating action potentials are regulated by both passive and active dendritic properties. Dendrites can be considered to be a complex arrangement of

compartmentalized electrical cables with constant (time- and voltage-independent) electrical parameters (Rall, 1959). Therefore, current flow along a cable, or dendrite, can be measured mathematically if passive membrane properties [axial resistance (R_i), membrane capacitance (C_m), membrane resistance (R_m)] and input current are known. The arrangement and branching pattern of dendrites also adds complexity to the degree of backpropagation. Mathematical modeling of AP propagation in dendritic trees of varying geometry has shown that the branching pattern is important for both forward and backpropagating action potentials (Vetter et al., 2001). As an example, the highly-branched dendrites of a cerebellar Purkinjie neuron will have a enhanced loss of backpropagation compared to that of an olfactory bulb mitral cell with nearly unbranched dendrites (Waters et al., 2005). Therefore, dendritic structure is a key component to the extent of backpropagation. However, active ionic conductances also have a profound role in the propagation of bAPs.

An active conductance is the influx or efflux of ions mediated via the opening of an ion channel in response to agonist binding or membrane potential change. Dendrites contain numerous active conductances mediated by synaptic input, both excitatory and inhibitory, and voltage-dependent ion channels (Stuart et al., 1997). In most neurons, backpropagation is decremental because of relatively low concentrations of Na^+ channels and high concentrations of K^+ channels in the dendrites (Huguenard et al., 1989; Korngreen and Sakmann, 2000; Waters et al., 2005). Some dendrites contain relatively uniform densities of Na^+ channels, which would support backpropagation, whereas others have a decreasing density with distance from the soma, which will restrict backpropagation. Properties of Na^+ channels such as rapidly developing and slowly recovering Na^+ channel inactivation in dendrites can also serve to limit backpropagation (Spruston et al., 1995; Stuart et al., 1997).

K^+ channels strongly regulate the shape and amplitude of bAPs (Johnston et al., 2000). There is a wide range of K^+ channels that can affect the efficacy of backpropagation including: Ca^{2+}-dependent potassium channels (BK-, SK-, and IK-types), and transient K^+ channels (A-type and D-type). In CA1 pyramidal neurons of the hippocampal formation, the A-type K^+ channel encoded by Kv 1.4, Kv 4.1, Kv 4.2, or Kv 4.3 genes (Coetzee et al., 1999; Serodio and Rudy, 1998) is a key regulator of backpropagation. In these neurons, A-type K^+ channels are present at increasing densities as the distance from the soma increases (Hoffman et al., 1997) and their activation can heavily decrease backpropagation into the distal dendritic tree, which in turn can have profound effects on synaptic plasticity (Chen et al., 2006). The downstream effects of dopamine, noradrenaline and acetylcholine can include the activation of kinases such as PKA, PKC, and MAPK, which can reduce activity of transient K^+ channels (Johnston et al., 2000) and promote synaptic plasticity. Modulation of A-type and D-type K^+ channels is thus an efficient method of regulating dendritic excitability which can have profound effects on the efficacy of forward and backpropagation.

Voltage-dependent Ca^{2+} channels have also been shown to be present in varying density and subtypes along the dendritic trees of pyramidal neurons (Johnston et al., 1996) and with sufficient local depolarization can be activated to also 'boost' the propagation of a bAP. A single bAP can lower the threshold for dendritically generated Ca^{2+}-Na^+- action potentials in L5 pyramidal neurons (Larkum et al., 1999a). Furthermore, in L5 pyramidal neurons, distal VDCCs are activated preferentially above a 'critical frequency' (CF) of bAPs and can produce a regenerative wave of depolarization. Larkum and colleagues demonstrated this in 1999b with simultaneous patch-clamp recordings of the soma, proximal and distal dendrites and Ca^{2+} imaging. They stimulated the soma with trains of 4 APs and progressively increased the frequency of APs from 20-200 Hz in

10 Hz increments. With an increase in frequency, the summation of the bAPs in the distal dendrites begins to overlap because of increased resistance in the smaller diameter dendrites. Above a CF ranging from about 70-100 Hz, there is sufficient depolarization to cross the threshold for a distally generated Ca^{2+}-Na^{+}-AP. The Ca^{2+}-Na^{+}-AP can then propagate forward and increase the afterdepolarization (ADP) at the soma (Fig. 1.5; Larkum et al., 1999b). This frequency- dependent distal Ca^{2+} influx is important for the regulation of plasticity (Kampa and Stuart, 2006) and is a physiological means by which gamma oscillations may potentially facilitate synaptic plasticity.

Synaptic activity can also modulate the efficacy of backpropagation-mediated activity. The pairing of a single, appropriately-timed bAP with an excitatory postsynaptic potential (EPSP) can elicit Ca^{2+}- Na^{+}-APs in distal dendrites of L5 pyramidal neurons (Larkum et al., 1999a) and CA1 pyramdial neurons (Stuart and Hausser, 2001). Conversely, the activation of L2/3 GABAergic interneurons that innervate the L5 dendrite can inhibit the generation of the Ca^{2+}-Na^{+}-AP (Larkum et al., 1999a). With population inhibitory postsynaptic potentials or activation of a single interneuron, inhibition of this distal regenerative Ca^{2+} current can occur (Larkum et al., 1999b). Distally generated Ca^{2+}- Na^{+}-APs require temporally organized synaptic and/or internal input and are heavily regulated by an inhibitory network.

Role of Backpropagating Action Potentials

Whereas the role of an AP is clear, to conduct frequency-encoded activity with high fidelity to the nerve terminal, where it can evoke neurotransmitter release according to the terminal's rules, the specific role of a backpropagating action potential is more difficult to define. Backpropagating action potentials have many proposed functions, including the priming of dendritic responsiveness, which can lead to short term and/or long term changes in synaptic efficacy (Stuart and Sakmann, 1994; Hausser et al., 1995;

Figure 1.5. Dendritic Regenerative Potentials are Frequency-Dependent and Blocked by Cd^{2+} .

(A) L5 pyramidal neuron reconstructed from biocytin. Simultaneous whole-cell recordings from the distal dendrite (670 μm from the soma) and the soma. (B) The top panel consists of recordings from the dendritic pipette. The solid line (above) is at a supracritical stimulation frequency of 90 Hz, whereas the dotted line (below) is at a subcritical frequency (80 Hz). Beneath is the simultaneous recording from the somatic pipette at 90 Hz. The arrow designates the afterdepolarization (ADP) that corresponds to the large dendritic response above. (C) Bath application of the voltage sensitive Ca^{2+} channel blocker Cd^{2+} inhibits the dendritic regenerative potential seen in B, and also prevents the ADP at the soma. In B-C the dotted line represents 0 mV. Adapted from Larkum et al., 1999b.

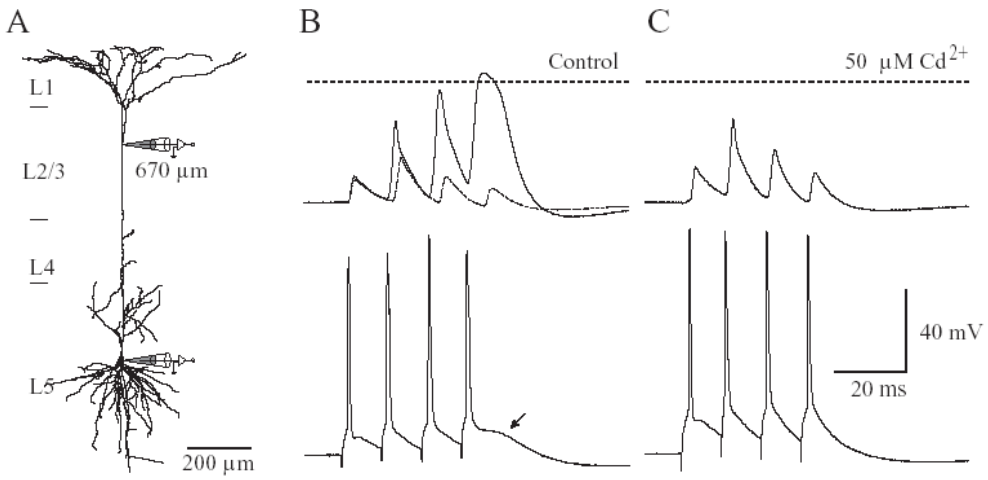
A
B
C
L1
L2/3
L4
L5
670 µm
200 µm
Control
50 µM Cd2+
40 mV
20 ms

Stuart et al. 1997), and the release of neurotransmitters from dendrites.

A bAP is an effective signal of neuronal output to electrotonically distinct regions of the cell, such as the dendrites. If this signal is appropriately timed with synaptic input the result can be a four-fold increase in dendritic amplitude that can propagate forward to the soma and produce an ADP (Stuart and Hausser, 2001). If the ADP is large enough, it can result in a burst of somatic APs (Stuart and Hausser, 2001). Intracellular Ca^{2+} influx into dendritic spines also depends on the temporal pairing of bAP and EPSPs (Koester and Sakmann, 1998). Thus, the opening of voltage-dependent ion channels can result in local alterations that promote or inhibit future synaptic input, which in turn can contribute to the computational power of the dendrites. Therefore, the attenuation of a regenerative current from the combination of EPSPs + bAPs will differ in each cell type due to the active and passive properties discussed above. In CA1 pyramidal neurons, decreasing the effectiveness of distal Na^{+} channels with locally applied TTX can prevent dendritic amplification, whereas decreasing distal A-type K^{+} channel activity with locally applied 4-AP can increase dendritic amplification (Stuart and Hausser, 2001). If the dendritic activity can reach the soma it can switch the firing mode of the neuron from single spiking to burst mode, which could have a variety of functions such as coding for a novel or significant stimuli (Cooper, 2002).

A long-term change in synaptic efficacy is another potential function of bAPs. With repeated pairing of appropriately timed pre- (EPSPs) and postsynaptic (bAPs) activity at high frequencies, LTP or long-term depression (LTD) can be induced (Kampa et al., 2006). This is termed 'spike-timing dependent plasticity' (STDP) and will be covered in detail later in this introduction.

Backpropagating action potentials can evoke the release of chemical messengers from dendrites. For example, dopamine is released from dendrites of neurons in the substantia nigra, GABA from dendrites of olfactory bulb granule cells, oxytocin and

vasopressin are secreted from dendrites in the supraoptic and paraventricular nuclei of the hypothalamus (Cuello, 2004). Endocannabinoids are also secreted from dendrites ubiquitously in the CNS that can notify the presynaptic terminal of postsynaptic activity and induce a change in subsequent glutamate or GABA release (Chevalyre et al., 2006). In the hippocampal formation and cortex endocannabinoid release from dendrites can diffuse across the synapse and act on presynaptic G-protein coupled CB1 receptors to decrease glutamate release and block LTP (Misner and Sullivan, 1999; Sokal et al., 2008) or induce LTD (Nevian and Sakmann, 2006). Dynorphin release from DGC dendrites can also block perforant pathway LTP (Simmons et al., 1995). Furthermore, bAPs are a candidate mechanism to provide sufficient Ca^{2+} entry for dendritic neurotransmitter release, which has recently been shown to occur *in vivo*. At high frequencies (>40 Hz) bAPs evoked from the medial forebrain bundle can inhibit the activity of VTA dopaminergic neurons via dendritic endocannabinoid release (Pillolla, et al., 2007).

Long-Term Potentiation

Use-dependent synaptic changes that correlate to learning and memory occur throughout the neural network and have been intensively studied in the hippocampal formation, and to a lesser extent, in the neocortex (Martin et al., 2000). The first evidence for a biological basis of learning and memory came from *in vivo* recordings of the dentate gyrus over 35 years ago. Bliss and Lømø (1973) placed electrodes in the perforant pathway of an anesthetized rabbit and after a high frequency stimulus train, recorded a stable potentiation in the dentate gyrus that lasted for hours. Long-term potentiation can be defined as a long-lasting increase in synaptic efficacy by brief high-frequency activation of afferent fibers or by pairing presynaptic activity with postsynaptic depolarization (Colino and Malenka, 1993; Martin et al., 2000). Conversely, a long-lasting decrease in synaptic efficacy is appropriately termed LTD and has its own set of

induction rules (Kemp and Manahan-Vaughan, 2007). Since the discovery of LTP there has been intense interest in its induction and maintenance mechanisms, whether it is a pre- or postsynaptic phenomenon, and whether it is necessary for the formation of a memory.

As described above, Bliss and Lømø (1973) used a protocol consisting of high-frequency afferent stimulation of the perforant pathway (15 Hz for 10 seconds, or 100 Hz for 4 seconds) to evoke LTP. This became a common method of increasing synaptic efficacy in the hippocampal formation, and is termed 'tetanic' stimulation. Many aspects of LTP induction and maintenance have been unraveled using this type of high-frequency afferent stimulation. In particular, the NMDA receptor seems to be necessary for LTP induction in both the medial and lateral perforant pathways (Colino and Malenka, 1993) and in area CA1, but not in the mossy fiber pathway (Nicoll and Malenka, 1995). Although tetanic stimulation has been useful in unraveling many interesting facets of LTP, evidence for this type of neural activity in the intact brain is uncommon, or observed only in an epileptic state (Paulsen and Sejnowski, 2000). This led researchers to a more physiological induction protocol that stimulates afferents with bursts at theta frequency. With theta-burst stimulation, LTP recordings have been maintained for hours *in vitro* (Diamond et al., 1988; Larson and Lynch, 1989) and for up to 5 weeks *in vivo* (Staubli and Lynch, 1987).

In both tetanic and theta-burst protocols the underlying LTP induction mechanism includes a sharp rise in presynaptic and/or postsynaptic Ca^{2+}. In most excitatory circuits these protocols act via stimulation of glutamatergic synapses that activate AMPA receptors that pass inward current into the dendritic spine. Sufficient depolarization will remove the Mg^{2+} block from NMDA receptors and allow ionic movement (Ca^{2+}, Na^{+}, and K^{+}) through the pore. NMDA receptors have been termed 'coincidence detectors' because they are both glutamate- and voltage-dependent

(MacDonald and Nowak, 1990). The necessity for a local elevation in postsynaptic Ca^{2+} has been confirmed by buffering intracellular calcium with 1,2-bis(2-aminophenoxy)ethane-N,N,N,N-tetraacetic acid (BAPTA), which prevents LTP induction (Colino and Malenka, 1993). There is also a temporal requirement for LTP induction; a transient increase of Ca^{2+} must occur for at least 1- to 3-s (Malenka and Nicoll, 1999). The Ca^{2+} is primarily considered to enter the spine via NMDA receptors, but can also move through VDCCs. For example, mice lacking N-type VDCCs have impaired long-term memory measured with the Morris water maze and show markedly decreased LTP in CA1, *in vitro* (Jeon et al., 2007). A rise in postsynaptic Ca^{2+} is clearly necessary for the induction of LTP in most models and can result in the initiation of a variety of signaling cascades. The most likely candidate is Ca^{2+}-calmodulin (CaM) that activates calcium-calmodulin dependent protein kinase II (CaMKII) which can autophosphorylate and maintain activity without the dependence of CaM, long after the LTP-protocol (Lisman, 1994). The pharmacological inhibition of CaMKII and genetic suppression of its activity both block LTP induction (Malinow et al., 1989; Hinds et al., 1998). However, protein kinase A (PKA), protein kinase C (PKC), mitogen-activated protein kinase (MAPK), and tyrosine kinases may also play a role (Suzuki et al., 1994). An increase in Ca^{2+}-mediated signaling cascades can then result in the long-term synaptic changes such as vesicle-mediated AMPA receptor insertion or clathrin-dependent AMPA receptor endocytosis (Man et al., 2000; Lu et al., 2001).

One of the most heated debates within the field of LTP has been whether LTP results from changes at a pre- or postsynaptic site. Those on the presynaptic side hypothesized that there was a change in *m*-the average number of quanta released from the presynaptic terminal, whereas those on the postsynaptic side hypothesized that there was a change in *n*-the number of functional synapses, or *q*- the postsynaptic effect of one released quanta (Poncer, 2003). Not until recently has there been a general consensus

that the postsynaptic membrane is the main site of LTP expression (Kerchner and Nicoll, 2008), however there is still good evidence for the contrary (Enoki et al., 2009).

Functional changes in dendritic spines occur with LTP, consistent with a postsynaptic mechanmism. The term 'silent synapse' refers to a spine contacted by an excitatory terminal with both NMDA receptors and AMPA receptors present. However, under basal conditions the AMPA receptors are not inserted into the membrane. With low levels of synaptic stimulation there will be no transmission because the only receptors present on the membrane are NMDA receptors that are blocked near the resting potential by Mg^{2+} ions and, therefore, the connection is referred to as 'silent'. The presence of silent synapses has been verified not only in the hippocampal formation, but also throughout the CNS and especially during development (Kerchner and Nicoll, 2008). Recent experimental evidence for the postsynaptic mechanism of LTP induction has been shown by pairing postsynaptic depolarization with the uncaging of glutamate, thus eliminating any presynaptic influence (Matsuzaki et al., 2004).

Despite convincing evidence that LTP is a postsynaptic mechanism at many synapses, there is also evidence for the contrary. In mossy fiber terminals it has been shown that LTP induction is much different from that seen at the perforant path-DGC and Schaffer collateral-CA1 pathways. In the MFs there is an increase in paired pulse facilitation (a presynaptic phenomenon) and a dependence on a presynaptic, not postsynaptic, Ca^{2+} increase that can cause presynaptic changes via activation of adenylyl cyclase (Nicoll and Malenka, 1995). A recent theory that may serve to dampen the debate suggests that LTP is primarily postsynaptic at immature and silent synapses and presynaptic in mature synapses with functional AMPA receptors (Enoki et al., 2009).

Considering the diversity of neurons, connectivity, intracellular mechanisms, and specificity of the nervous system, it is realistic that activity-dependent changes can occur

on both sides of the synapse and depend on the cell type, age of the neuron, and induction protocol.

Regardless of whether LTP occurs primarily pre-, or postsynaptically, the enhancement of synaptic strength after an appropriate LTP-protocol is difficult to refute. However, a criticism of LTP research is that the information stored in the synapse after induction is a representation or 'memory' of the electrical stimulation, and this does not necessarily represent a memory that would form in nature, or in humans. In the thousands of reports of LTP *in vitro* and *in vivo*, there have only been a few reports that have attempted to question whether learning is due to LTP *in vivo* (Moser et al., 1998; O'Carroll et al., 2006; Whitlock et al., 2006; Pastalkova et al., 2006). In an elegant study Whitlock and colleagues (2006) used a one-trial inhibitory avoidance (IA) learning paradigm in which training induces NMDA receptor-dependent phosphorylation of AMPA receptor subunit GluR1 at Ser831 and not Ser845, consistent with LTP induction via an increase in AMPA receptor insertion (Lee et al., 2000). In order to test whether the IA paradigm altered synaptic efficacy, Whitlock and colleagues (2006) next placed a multielectrode array in the apical dendritic layer of CA1, and a stimulating electrode on the Schaffer collaterals. They tested population activity by measuring the field EPSP (fEPSP) slope in the freely moving rats before and after IA training and found a persistent increase in 12 of 44 recording sites, compared to no change in control animals (144 sites). In a final experiment to determine if this heterogeneous increase in synaptic response was due to LTP, they trained animals as above and tested whether the IA enhanced potentiation would occlude high-frequency stimulation induced LTP. Indeed, the electrodes that showed an increase after IA exhibited less LTP (121.1%) compared to electrodes that had no enhancement with IA (136.1%; Whitlock et al., 2006). Thus, learning the inhibitory avoidance paradigm and high-frequency stimulation seem to enhance the synaptic response in the same manner, providing solid evidence that learning

is directly related to a change in synaptic efficacy. Taken together, to further the understanding of LTP and learning, future studies of LTP *in vitro* should include physiological means of stimulation that parallel naturally occurring electrical activity.

Spike-timing dependent plasticity

Spike-timing dependent plasticity is a "physiological" means of LTP induction that is likely to occur specifically in areas of the brain that generate or maintain high-frequencies of activity, such as the hippocampal formation and neocortex (Jung and McNaughton 1993; Larkum and Zhu, 2002; Leutgeb et al., 2007). The temporal dynamics that underlie the pairing of pre- and postsynaptic APs can result in a spectrum of changes in synaptic strength, consistent with the ideas of Donald Hebb. Hebb proposed that the paired and repeated firing of APs in two synaptically connected neurons would result in changes of synaptic strength between those two neurons (Hebb, 1949). One form of this is now termed STDP and is defined as the increase or decrease in synaptic strength due to the timing of paired pre- and postsynaptic activity. Classically, when repeated postsynaptic APs immediately (0 - ~20 ms) precede presynaptic EPSPs (post-pre) the result is LTD, whereas repeated EPSPs preceding APs (pre-post; 0 ~ 20 ms) results in LTP (Bi and Poo, 1998). Thus, there is a 'critical window' for the pairing of presynaptic input and postsynaptic activity that dictates whether potentiation or depression will occur. The exact timing and size of the window varies, but this general rule applies across neuronal subtypes (Dan and Poo, 2006). An important mechanism that regulates STDP is the depolarization of dendrites, that relieves NMDA receptors of their Mg^{2+} block (Mayer et al., 1984; Nowak et al., 1984) and activates VDCCs (Kampa et al., 2006), increasing postsynaptic Ca^{2+} entry into dendrites which can promote synaptic changes (Froemke et al., 2005; Nevian and Sakmann, 2006; Campanac and Debanne, 2008). Whether a high or low level of Ca^{2+} enters the dendrite

is thought to underlie the induction of LTP and LTD, respectively (Dan and Poo, 2006). Although this is a simplistic theory, there has been some evidence that pre-post spiking results in supralinear Ca^{2+} influx and LTP, whereas post-pre spiking evokes sublinear Ca^{2+} influx and LTD, as demonstrated in the spines of basal dendrites in L5 and L2/3 pyramidal neurons (Koester and Sakmann, 1998; Nevian and Sakmann, 2004). The amplitude and width of the STDP window in L2/3 pyramidal neurons also depends on the site of the input along the dendritic tree, with distal locations having smaller LTP and LTD windows compared to more proximal locations, due to the extent of Ca^{2+} influx (Fromke et al., 2005). The intracellular concentration of Ca^{2+} is also increased with Ca^{2+} release from intracellular stores (Emptage et al., 1999; Sandler and Barbara, 1999) and activation of downstream effectors that likely contribute to a supralinear Ca^{2+} signal. Because the sign and magnitude of plasticity seem to be tightly dependent upon postsynaptic levels of $[Ca^{2+}]_i$, modulatory changes of intracellular Ca^{2+} levels are capable of greatly affecting plasticity (Malinow et al., 1989; Hinds et al., 1998).

However, the theory that the relative Ca^{2+} influx will dictate the sign of plasticity does not come without a caveat. If the level of $[Ca^{2+}]_i$ is the sole determinant, then after a high level of $[Ca^{2+}]_i$ that triggers LTP, as the $[Ca^{2+}]_i$ declines back to rest, by definition it would cross the lower $[Ca^{2+}]_i$ threshold for LTD. According to this Ca^{2+}-based theory, LTD would occur soon after LTP on many occasions. Therefore, potential mechanisms of LTD include spiking induced afterhyperpolarization, NMDA receptor desensitization, and a second coincidence detector – activation of metabotropic glutamate receptors (Karmarkar and Buonomano 2002; Dan and Poo, 2006). LTP and LTD should not be considered parallel mechanisms, but instead separate phenomenon that can shape synaptic strength (Kemp and Managhan-Vaughan, 2007).

In apical dendrites of L5 pyramidal neurons, a single AP or low frequency train of bAPs is not sufficient to depolarize distal dendrites and allow STDP to occur because

of the decremental propagation present in these dendrites, and resultant lack of a dendritic Ca^{2+} spike (Kampa et al., 2006). However, a burst of high frequency bAPs can provide enough depolarization to activate distal VDCCs, produce a regenerative Ca^{2+} current and unblock distal NMDA receptors (Larkum et al., 1999b; Kampa et al., 2006). When these bursts are sufficient to evoke distal Ca^{2+} spikes and are paired with presynaptic input the result is robust LTP or LTD depending on the relative timing (Kampa et al., 2006). *In vivo* recordings of L5 pyramidal neurons during whisker stimulation have shown that bAPs can evoke complex potentials that are especially prominent with input from layer 1 (Larkum and Zhu, 2002). In granule cells of the dentate gyrus, high frequency bursts of APs have been recorded during exploratory behaviours (Jung and McNaughton, 1993; Leutgeb et al., 2007). These bursts could evoke supralinear Ca^{2+} influx if bAPs reach a CF, and if so, have a profound influence on plasticity (Kampa et al., 2006).

Are bAPs necessary for LTP induction? bAPs occur at high frequencies in many physiological circumstances and are likely to result in distal Ca^{2+} influx. For example, high AP frequencies that produce bAPs with relatively little attenuation into the distal dendrites have been recorded *in vivo* in the intact and awake rat (Bereshpolova et al., 2007). However, recent work with CA1 pyramidal neurons has demonstrated that bAPs are not necessary for LTP. Golding and colleagues (2002) locally applied tetrodotoxin (TTX) to the axon, soma, and proximal dendrites of CA1 pyramids during theta-burst pairing (repeated EPSP-AP pairs at theta frequency; TBP), and still observed LTP. This form of LTP does, however, require regenerative Ca^{2+} currents mediated by both VDCCs and NMDA receptors that work synergistically to generate a dendritic spike (Golding et al., 2002). Thus, in some circumstances, robust (Golding et al., 2002) or paired (Dudman et al., 2007) synaptic input can generate a dendritic Ca^{2+} spike that can lead to LTP without the influence of bAPs. In any case, the crucial signal is a significant distal Ca^{2+} influx, however generated. This input must be on a temporal scale that will result in

sufficient Ca^{2+} entry to induce LTP. Therefore, even a small alteration in Ca^{2+} influx can have profound consequences.

Neuropeptide Y

Neuropeptide Y (NPY) is a 36 amino acid peptide that is well conserved throughout the mammalian central nervous system (CNS) and peripheral nervous system (PNS). Tatemoto and colleagues (1982a) first isolated NPY from the porcine brain and discovered that its structure is fairly homologous to the previously identified pancreatic polypeptide (PP; Kimmel et al., 1968). It transpired that they are both members of a family of molecules that includes the gut hormone peptide YY (PYY; 70% homologous) and PP (50 % homologous; Tatemoto, 1982b). NPY, PYY, and PP, are each composed of 36 amino acid residues, 5 of which are tyrosines (4 in PP), an N-terminal tyrosine and a C-terminal tyrosine amide (Tatemoto et al., 1982b). This family of peptides is also constructed to contain what is know as the "Pancreatic Polypeptide-fold" (PP-fold) characterized by interdigitating proline (P) and Tyrosine (Y) residues (Blundell et al., 1981; Larhammar, 1996b), although this may not always occur in solution (Bettio et al., 2002). Neuropeptide tyrosine (NPY) is unique from the family because it is expressed almost exclusively in neurons (Lundberg et al., 1982; Adrian et al., 1983), whereas PYY and PP are found in higher concentrations in endocrine cells in the intestine and pancreas, as well as in some neurons in the enteric nervous system (Larhammar, 1996). In fact, Larhammer and colleagues (1993) reported that NPY was more evolutionarily conserved and likely older than PP, and thus the family should be appropriately named the 'NPY family.' Peptides belonging to the NPY family have been found throughout vertebrates with very high sequence homology in humans, cow, sheep, pig, rat, rabbit, guinea pig, chicken, alligator, European green frog, European common frog, African clawed toad, common goldfish, trout, European common dogfish, river lamprey (Larhammar, 1996),

and teleost fishes (Salaneck et al., 2005). As the most abundant peptide in the CNS of mammals with an extensive history throughout mammalian evolution, NPY is a very important neuromodulator with a variety of functions.

Evidence supporting NPY's role as a neuromodulator came from immunoelectron microscopy studies that discovered its localization in neurons in the soma, dendrites, and axon where it was associated with dense core vesicles (Pelletier et al., 1984). NPY is synthesized in the cell body where it is often colocalized in vesicles with other neurotransmitters. For example, noradrenaline and NPY are packaged in the same vesicles in the soma (Lundberg et al., 1982, 1983) and through fast axonal transport distributed to the terminals of the sciatic nerve (D'Hooge et al., 1990). In the central nervous system NPY can be colocalized with GABA (Hendry et al., 1984; Kohler et al., 1987), agouti-related protein (Menyhert et al., 2007), cocaine- and amphetamine-related transcript (Menyhert et al., 2007), noradrenaline (Everitt et al., 1984; Smialowska, 1988), and somatostatin (Kohler et al., 1987; Freund and Buzsaki, 1996). Whereas small classical neurotransmitters like acetylcholine and GABA can be found in small synaptic vesicles that are released with low frequencies of APs, neuropeptides are typically stored in larger dense core vesicles, often with classical neurotransmitters, and released preferentially with high frequencies (Hokfelt, 1991). Thus, the release of NPY can occur as a response to high frequencies or bursts of activity, which is important when considering the functional role (s) of NPY in the nervous system.

NPY is responsible for the regulation of a plethora of physiological states throughout the central nervous system such as; induction of food intake, regulation of anxiety state, memory retention, pain transmission, circadian rhythm regulation, vasoconstriction, neurogenesis, and regulation of ethanol consumption (Schwart et al., 2000; Pedrazzini et al., 2003). Recent advances in genetics have allowed the investigation of up- or down-regulation of NPY expression with transgenic and knock-

out models, respectively. Interestingly, NPY transgenic rats have normal growth, development, and lifespan but demonstrate a decreased fear response in the open-arm maze, and decreased spatial memory in the Morris water maze (Thorsell et al., 2000). Indeed, NPY is a very important component of CNS activity, however its role in learning and memory has not been fully explored.

NPY Receptors

NPY is widely distributed throughout the CNS and PNS where its biological effects are mediated by several subtypes of receptors. Y1, Y2, Y4, Y5 and y6 receptors have all been cloned (Gerald et al., 1996; Michel et al., 1998) and are present in mammals except for y6, which is present in the mouse and rabbit, but not rat and primates (Larhammar, 1996; Weinberg et al., 1996; Dumont et al., 1998; Mullins et al., 2000). Subtypes of NPY receptors each have a unique pharmacological profile and distribution throughout the CNS and PNS. NPY has an equal affinity for all subtypes of receptors, while PP, a weak agonist at best at Y1 and Y2, and modest affinity at the Y5 receptors has far higher affinity than does NPY at the Y4 receptor. Y receptors couple to $G_{i/o}$ signaling pathways and via a pertussis toxin sensitive mechanism can inhibit the production of cAMP (Larhammar et al., 1992; Mullins et al., 2000), mobilize intracellular Ca^{2+}, or modulate Ca^{2+} or K^{+} channels. It has also been shown that the $\beta\gamma$ subunit of the G-protein can directly inhibit VDCCs (Zamponi et al., 1997) which is a candidate mechanism for NPY action (Chee et al, 2008). A variety of methods have been used to characterize the structure, activity, and location of NPY binding sites in the mammalian CNS. Immunohistochemistry, *in situ* hybridization, and autoradiography have been used to determine receptor distribution throughout brain regions and across species. With the development of selective NPY receptor analogues and antagonists, physiological effects of the subtypes of NPY receptors have been explored (El Bahh et al., 2005; Sperk et al.,

2007). Cloning of the receptor subtypes has made it possible to generate knockout and transgenic models of specific subtypes of NPY receptors, which are also powerful tools to investigate the physiological role of each receptor subtype (Michel et al., 1998).

Y1 Receptor

The first subdivision of NPY receptors was proposed because of structural dissimilarities (Sheikh and Williams, 1990) and pharmacological differences (Wahlestedt et al., 1986) and resulted in the terms Y1 and Y2 receptor. Y1 receptors are glycoproteins about 70 kDa (Sheikh and Williams, 1990) with low affinity to long C-terminal fragments of NPY (e.g. NPY $^{13-36}$) and high affinity for Pro^{34} substituted, full-length analogs of NPY. Y1 receptor activation does require an intact N-terminal of NPY. Early on in the study of Y1 receptors it was postulated that it was primarily located postsynaptically, whereas the Y2 receptors were primarily located presynaptically (Lundberg et al., 1988). Indeed, this seems to be the case in the hippocampal formation and neocortex (McQuiston et al., 1996a; McQuiston et al., 1996b; Kopp et al., 2002), though not necessarily elsewhere (Pronchuk et al., 2002).

In an extensive study of the localization of the Y1 receptor, Kopp and colleagues (2002) used immunohistochemistry with a highly-selective Y1 antibody, together with Y1 knock-out mice, and *in situ* hybridization of Y1 receptor mRNA. Relevant to this thesis, the Y1 receptor was seen to be expressed at very high levels in the molecular layer of the dentate gyrus, and the DGCs showed extensive Y1 receptor immunoreactivity in their dendrites and somata (Fig. 1.6; Kopp et al., 2002). Furthermore, the Y1 receptor was also present on dendrites and somata of L5 pyramidal neurons. Y1-like immunoreactivity has also been shown in the dentate gyrus (Caberlotto, et al., 1997) and cortex (Statnick et al., 1997) in human post-mortem studies. Knockout models of the Y1 receptor have produced decreased neurogenesis in the dentate gyrus (Howell et al., 2003),

Figure 1.6. Y1 Receptor Immunoreactivity in the Hippocampus.

A rabbit polyclonal antibody was used to map the distribution of NPY1 receptors. A-E are confocal immunofluorescence micrographs of rat brain sections. (A) CA1 immunofluorescence. cc-corpus callosim, alv-alveus, sostratum oriens, sp-stratum pyramidale, sr-stratum radiatum. (B-C) Dentate gyrus immunofluorescence. mo-molecular layer, sg-stratum granulare, po-polymorph layer, alv-alveus. (D) Magnification of a single DGC with immunofluorescence in the dendrites, soma and axon. (E) Magnification of immunofluorescence in the axons making up the mossy fibre pathway. Scale bars = 100 μm (A-C), (E) 50 μm, (D) 10 μm. Modified from Kopp et al. 2002.

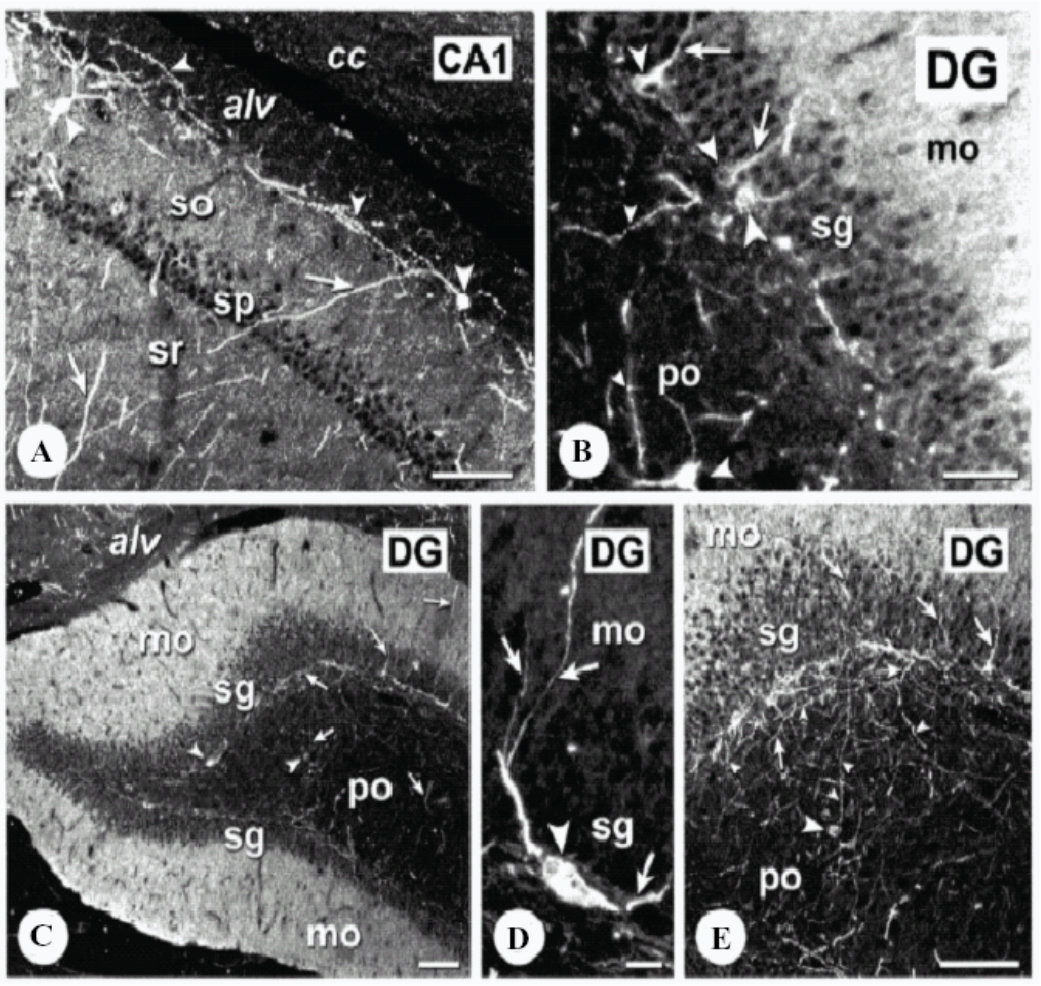
cc
CA1
alv
so
sp
sr
A
DG
mo
sg
po
B
alv
DG
mo
sg
po
sg
mo
C
DG
mo
sg
D
mo
DG
sg
po
E

increased algesia (Naveilhan et al., 2001) and decreased sensitivity to ethanol (Thiele et al., 2002). Taken together, these studies demonstrate the diverse role of the Y1 receptor in the brain.

Y2 Receptor

Y2 receptors are the most widely distributed of all NPY receptors in the brain (Aicher et al., 1991) and are primarily located presynaptically where they typically inhibit transmitter release (Colmers et al., 1985). Y2 receptors are smaller glycoproteins than Y1, at about 50 kDa (Sheikh and Williams, 1990), with high affinity for C-terminal fragments of NPY (Beck-Sickinger et al., 1994). NPY fragments without the N-terminus and small C-terminal truncated peptide fragments as small as 11 amino acids can also activate the Y2 receptor (Grundemar and Hakanson, 1990; Michel et al., 1998). BIIE 0246 is an extremely potent and specific antagonist of Y2 receptors (Dumont et al., 2000). This compound was very useful in determining that the anti-epileptic actions of NPY in hippocampal areas CA3 and CA1 were mediated by the Y2 receptor (El Bahh et al., 2005). In human post-mortem studies Y2 receptor mRNA has been found in high levels in layer 2 and 6 of the cortex, the polymorph layer of the dentate gyrus, basal ganglia, and amygdala (Caberlotto et al., 2000). Knockout of the Y2 receptor has also been useful in implicating the role of Y2 receptor actions in the CNS. A lack of Y2 receptors results in decreased body weight, decreased adiposity, no change in food intake, and decreased anxiety (Herzog, 2003).

Y4 Receptor

The Y4 receptor is often referred to as the PP receptor (Lundell et al., 1995) because of its preference of PP to NPY and PYY. There has been relatively little investigation of the Y4 receptor because the distribution of Y4 receptors is high in the

periphery compared to the CNS (Bard et al., 1995) where only small concentrations have been found, mainly in the hypothalamus, amygdala, and brainstem of the rat and mouse (Whitcomb et al., 1997; Tasan et al., 2009). Despite this low level of central Y4 receptors, Y4 knockout mice show marked behavioural changes such as decreased depression-like behaviour, decreased anxiety, increased novelty-induced motor activity (Tasan et al., 2009), and reduced adiposity (Lee et al., 2008). NPY's actions on the Y4 receptor may also be an orexigenic signal in humans (Batterham et al., 2003).

Y5 Receptor

The Y5 receptor is only distantly related to Y1 and Y2 and is activated by NPY and PYY without the first two amino acids (Michel et al., 1998). Y5 receptors have been found in the hypothalamus, thalamus, amygdala, cingulate cortex, area CA3 of the hippocampal formation (Gerald et al., 1996), and in the dentate gyrus where they are present on hilar neurons and granule cells (Parker et al. 1999). Knockout studies of the Y5 receptor have attempted to validate the theory that it is the 'feeding receptor' (Marsh et al., 1998). However, they have shown that without the Y5 receptor mice eat and store adipose tissue normally (Herzog, 2003). Furthermore, knocking out the Y5 receptor in obese (ob/ob) mice had no effect (Marsh et al., 1998). Although some Y5 antagonists have been shown to be anti-orexigenic it is likely that they are acting on a non-Y5 mediated mechanism (Levens and Della-Zuana, 2003).

y6 Receptor

This receptor is considered a part of the Y1 family because its sequence is closely related to the Y1 receptor. The y6 receptor has been studied in mice and rabbits *in vitro*, but is not present in the rat, primate, or human (Larhammar and Salaneck, 2004). The designation of "y" instead of "Y" was given by the International Union of Pharmacology

because it is a pseudogene and therefore is not expressed in higher mammals (Michel et al., 1998).

NPY Action on Mossy Fiber Terminals

As it does in area CA1 (Colmers et al., 1987, 1988, Colmers and Bleakman, 1994), NPY also negatively modulates synaptic transmission at the mossy fiber-to-CA3 synapse. Synaptic excitation, evoked by stimulation of the mossy fiber pathway, is potently and reversibly inhibited by bath application of NPY in a concentration-dependent manner (El Bahh et al., 2005; Guo et al., 2002; Klapstein and Colmers, 1993). The mechanism underlying this NPY-mediated inhibition of glutamate release from mossy fibers was first determined by quantal synaptic analysis. Measurements of the frequency and amplitude of spontaneous (sEPSC) and miniature (mEPSC) excitatory postsynaptic currents were made in CA3 pyramidal neurons in the whole-cell patch configuration. Application of NPY and the Y2-preferring agonist [ahx$^{5-24}$]NPY increased the interval and decreased the amplitude of sEPSCs, but had no effect on either parameter when mEPSCs were measured in the presence of TTX (McQuiston et al., 1996b). This indicates that Y2 receptors on mossy fiber terminals inhibit glutamate release and decrease excitatory input into CA3 pyramidal neurons. Subsequent experiments in area CA1 determined that NPY inhibits glutamate release via a suppression of presynaptic Ca^{2+} influx (Qian et al., 1997). Controversy developed because it was unclear whether the Y5 receptor also played a role in this inhibition (Guo et al., 2002). However, in experiments at the mossy fiber-CA3 and stratum radiatum-CA1 synapse in hippocampal slices, presynaptic inhibitory responses to the application either of the Y2-preferring agonist [ahx$^{5-24}$]NPY, or the Y5-preferring agonist, AlaAib NPY, were both blocked entirely by pretreatment with the potent and selective Y2 receptor antagonist, BIIE0246 (El Bahh et al., 2005). As this antagonist has no activity at the Y5 receptor (Doods et al.,

1999), this indicates that the Y2 receptor is the only one mediating this action of NPY, and that at high concentrations the Y5-preferring agonist has some activity at Y2 receptors (El Bahh et al., 2005). This conclusion is further supported by the observation that in hippocampal slices prepared from mutant mice lacking functional Y2 receptors, there is no inhibition of either the mossy fiber or stratum radiatum-evoked field EPSPs by NPY or the Y5-preferring agonist AlaAib NPY (El Bahh et al., 2005). The Y2 receptor is therefore responsible for NPY-mediated inhibition of glutamate release from mossy fiber terminals, most likely by suppression of voltage-dependent Ca^{2+} influx through presynaptic Ca^{2+} channels.

NPY Actions on Somata and Dendrites of Dentate Granule Cells

In the molecular layer of the dentate gyrus, the effect of NPY on EPSPs is, if anything, barely detectable. Stimulation of the perforant path or commissural inputs evokes EPSPs in the molecular layer that are either unaltered (Klapstein and Colmers, 1993), or show very minor inhibition (Bijak and Smialowska, 1995) with bath application of NPY. This apparent absence of NPY actions within the dentate gyrus itself was puzzling, given the significant levels of NPY receptor expression previously reported in this region (Chan-Palay et al., 1986; Kohler et al., 1986), and prompted further investigations**.**

Using patch clamp recording and simultaneous Ca^{2+} imaging, McQuiston and colleagues (1996a) evoked APs in rat DGCs in brain slices. Bath application of NPY did not alter resting Ca^{2+} levels in the soma or dendrites of the DGCs, but did significantly and reversibly decrease the depolarization-induced Ca^{2+} influx in the soma and dendrites of these same DGCs. Because voltage clamp conditions are less than ideal in neurons with their dendritic trees intact, as occurs in brain slices, mechanistic studies of this postsynaptic NPY action were undertaken in acutely-isolated DGCs, which are

electrically more tractable. Somatic Ca^{2+} currents were isolated pharmacologically and NPY and receptor subtype-preferring agonists were applied, as were selective blockers of different Ca^{2+}channel subtypes. Calcium currents were inhibited by the NPY Y1- and Y5-preferring agonist, [$Leu^{31}Pro^{34}$]NPY but were much less commonly inhibited by the NPY Y2- (and Y5)- preferring agonist, NPY13-36. These observations were consistent with the actions of NPY on Ca^{2+} influx preferentially occurring via Y1 receptor activation. Selective blockade of N-type Ca^{2+} channels occluded all actions of NPY, consistent with an action of Y1 receptors to selectively suppress current through this subtype of VDCC (McQuiston et al., 1996a). Functionally, the inhibition of calcium currents by NPY was postulated to regulate the release of dynorphin from DGC dendrites, which is mediated by L- and N- type VDCCs (Simmons et al. 1995), but this has not been investigated further. Certainly, the Y1 receptor does mediate the inhibition of N-type VDCCs in DGCs. Given the remarkable amounts of NPY in the dentate, particularly in the molecular layer, it is reasonable to presume that there will be some significant physiological consequences of Y1 receptor activation on the dendrites and soma of DGCs.

Dopamine

Dopamine is a neurochemical that is involved in movement, cognition, emotion, and the regulation of the endocrine system. It is synthesized from the amino acid L-tyrosine and classified as a catecholamine, along with noradrenaline and adrenaline. Dopamine can be converted to noradrenaline, and until the late 1950's, was thought of as solely an intermediate in this biosynthetic process (Blaschko, 1939). When dopamine was originally identified in the brain and was discovered in different regions than noradrenaline, this led to the proposal that dopamine could act on its own as a neurotransmitter. Soon thereafter, theories emerged that related dopamine to motor

control, and a lack of dopamine in the basal ganglia as the cause of Parkinson's disease (Bertler and Fosengren, 1959; Carlsson, 1958, 1959). The presence of dopamine in nerve cells was first demonstrated in snails (Dahl et al., 1966) and in the CNS of mammals (Haggendal and Malmfors, 1963) confirming the presence of a central dopaminergic system.

Dopamine is produced in four distinct cell systems including the mesencephalic, diencephalic, retinal and olfactory systems. The mesencephalic system comprises dopamine neurons in the VTA and *pars compacta*, *pars lateralis,* and adjacent areas of the substantia nigra (Swanson et al., 1982). The diencephalic system consists of dopamine neurons in the posterior, dorsal, periventricular and arcuate regions of the hypothalamus, caudal thalamus. The remaining dopaminergic cell systems are found throughout the olfactory bulb and in amacrine cells of the retina.

Dopamine Receptors

Dopamine acts upon binding to its receptors throughout the CNS and PNS. Evidence for endogenous dopamine receptors first arose in 1972 when it was shown that dopamine can activate adenylate-cyclase in the calf and rat retina (Brown and Makman, 1972). A dopamine-mediated increase in cAMP was also demonstrated in the rat caudate nucleus, an effect inhibited by the antagonists haloperidol and chlorpromazine (Kebabian et al., 1972). A few years later, dopamine receptors were discovered using the tritium-labelled compounds [^{3}H]dopamine and [^{3}H]haloperidol (Burt et al., 1975; Creese et al., 1975). In the late 1970's, discrepancies between the presence of dopamine receptors with autoradiography and an absence of dopamine mediated-cAMP increase in the same brain areas, led to the hypothesis that there were at least two receptors for dopamine – D1 and D2, whose effects differed, and were mediated via different signaling pathways (Cools

and van Rossum, 1976, Kebabian and Calne, 1979). Currently, dopamine receptors are broadly characterized as being D1-like (D1 and D5) and D2-like (D2, D3, and D4) according to their structure, genetic and pharmacological profile, and downstream effectors. All dopamine receptors are G-protein coupled receptors, containing seven transmembrane-spanning segments. Dopamine receptors can modulate the activity of ion channels such as VDCCs (Liu et al., 1992), A-type K^+ channels (Hoffman and Johnston, 1999), and Na^+ channels (Rosenkranz and Johnston, 2007). The activation of dopamine receptors can also modulate many signaling systems including adenylyl cyclase (Brown and Makman, 1972), arachidonic acid (Keefe et al., 1995), amiloride-sensitive Na^+/H^+ exchangers (Felder et al., 1993), and Na^+-K^+-ATPase (Bertorello and Aperia, 1990). The increase or decrease in activity of these downstream targets depends upon specific receptor subtype activated, cell type and brain region.

D1-like Receptors

The D1 receptor subfamily consists of the D1 and D5 receptors, based on their relatively high affinities for phenylbenzamines and ability to activate G_s proteins and stimulate adenylyl cyclase. The D1 subtype is the most abundant of all dopamine receptors in the CNS (Missale et al., 1998). D1-like receptors have been shown to regulate neuronal growth and development, mediate numerous behavioural responses, and modulate D2-receptor events.

With autoradiography, D1-like receptors are observed in human brain at a high density in the caudate nucleus, putamen, globus pallidus and substantia nigra, a moderate density in the amygdala, mammillary bodies, cerebral cortex and hippocampus (Cortes et al., 1989). This is similar to the pattern found in the rat brain, with the exception of very low or indetectable levels of D1 receptors in the stratum lacunosum moleculare of the rat

hippocampus (Wamsley et al., 1989). Relevant to this thesis, D1-like receptor density, observed with a combination of electron microscopy and immunohistochemistry, is often high in dendritic spines (Huang et al., 1992; Bergson et al., 1995). In the dentate gyrus of the rat D1 receptor mRNA is differentially distributed. Specifically, DGCs in dorsal hippocampal formation are prominently labeled, whereas in ventral hippocampal formation the labeling is sparse or non-existent. However, even in the ventral part of the dentate gyrus, other neurons in the molecular layer and hilus were shown to express D1R mRNA (Fremeau et al., 1991).

Immunocytochemistry has been used to investigate the location of D5 receptors in the brain because no pharmacological agent uniquely identifies the D5 receptor. D5 receptors have a different distribution from that of D1 and are typically present on the somata and dendrites of neurons of the cerebral cortex, basal ganglia, basal forebrain, hippocampus, diencephalon, brainstem and cerebellum of the rat and monkey (Ciliax et al., 2000). Another study using D5-specific antibodies has shown that, the localization of receptors is fairly homologous throughout the brains of rats and humans, with the exception of the hippocampus. In the rat hippocampus, D5 receptors are found only at the soma of pyramidal neurons in CA1 and CA3 and in DGCs, whereas in the human they are also found in the apical dendrites of pyramidal cells and DGCs (Khan et al., 2000). The distinctive distribution would imply that D5 receptors have a specific role in neurotransmission.

D2-like Receptors

The D2 receptor subfamily includes D2, D3 and D4 receptors, based on their mutual preference for butyphenones and substituted benzamines, their activation of G_i and G_o proteins (Lledo et al., 1992), and inhibition of adenylyl cyclase (Missale et al., 1998). D2, D3 and D4 receptors have also been shown to be coupled to phospholipase C,

PKC, and extracellular signal-regulated kinase (Luo et al., 1998; Zhen et al., 2001; Zhang et al., 2008).

Using a radiolabelled D2 agonist and antagonist, D2 like receptors are seen to be concentrated in the human caudate nucleus, nucleus accumbens, olfactory tubercle and substantia nigra, and at lower levels in the globus pallidus, hippocampus and amygdala (Camps et al., 1989). This distribution is very similar to that which is found in the rat with the exception of a lack of D2 receptors in the cerebral cortex, accessory amygdala, and the dentate gyrus (Wamsley et al., 1989).

Dopamine Action in the Hippocampus

There are only a few reports of dopaminergic actions in the hippocampus, although it is known that D1-like receptors are important for synaptic plasticity. In area CA1, D1/D5 agonists can enhance LTP (Navakkode et al., 2007) and when applied alone can induce a protein-synthesis dependent, late LTP (Huang and Kandel, 1995). Both of these actions are mediated via an increase in cAMP-mediated by adenlyl cyclase activity (Frey et al., 1993). These results are consistent with a study using D1 knockout mice that showed the D1, but not D5 receptor, was necessary for LTP induction. Interestingly, these mice also had impaired spatial learning in a water maze task (Granado et al., 2008). Furthermore, compared with those of control animals, place cells in area CA1 of D1R knockout animals have impaired firing patterns in novel spatial environments, but not familiar environments (Tran et al., 2008). Dopamine also increases the amplitude of EPSPs at mossy fiber-CA3 neuron synapses likely via an increase in presynaptic glutamate release. This mechanism is also mediated by a D1R-mediated increase in cAMP, and is not affected by blockade of GABA receptors (Kobayashi and Suzuki, 2007).

In the dentate gyrus of anesthetized rats, LTP can be induced during the activation of D1-like receptors by a previously subthreshold stimulation of the perforant pathway (Kusuki et al., 1997). Perforant pathway LTP seems to be enhanced with D1-like receptor activation, however, this is contrary to reports of LTP in the basolateral amygdala to dentate gyrus pathway. In this pathway, D2-like receptors, rather than D1-like receptors, are responsible for the facilitation of LTP induction (Abe et al., 2008). In general, the role of the D1-like receptor in the hippocampus seems to be an enhancement of synaptic plasticity, likely via increases in cAMP. However, the mechanism(s) that underlie the induction of LTP and the presence of dopamine-induced LTP in the dentate gyrus *in vitro* are unknown.

Calcium Imaging

Calcium is responsible for the regulation for many cellular functions ranging from neuronal excitation and exocytosis to the contraction of muscles to bone formation (Berridge, 1993). The concentration of the calcium ion, Ca^{2+}, inside neurons is precisely controlled because even nanomolar or low micromolar increases can have dramatic effects (Thomas et al., 2000). Thus the measurement of intracellular calcium has been intensively developed using various approaches including electrophysiology and chemical and bioluminescent fluorescent indicators.

A fluorescent indicator is a molecule with a chemical structure which, when excited by an appropriate wavelength of light, can emit light of a longer specific wavelength. 'Fluorescence' is considered this process of light absorption and light emission. The synthetic fluorescent dyes murexide, the azo dyes (Arsenazo I-III), and chlorotetracycline were first used to monitor intracellular Ca^{2+} in the 1960's but were not popular because each has substantial limitations (Rudolf et al., 2003). The first monitoring of free intracellular Ca^{2+} concentration with a protein-based fluorescent

calcium indicator was performed by Ridgway and Ashley (1967) who injected the photoprotein aequorin into a giant muscle fibre. However, the measurement of intracellular Ca^{2+} with fluorescent probes did not become widespread until the 1980's when Tsien and colleagues (Tsien et al., 1980; Grynkiewicz et al., 1985; Minta et al., 1989) developed a wide range of now commercially-available Ca^{2+} indicator dyes. The relatively high signal-to-noise ratio and high affinity of these molecules, coupled with the low background signal afforded by epifluorescence made the accurate measurement of $[Ca^{2+}]_i$ readily accessible to many more investigators than had been the case with previous methods. The majority of these Ca^{2+} indicators are chemical fluorescent probes that are related to the Ca^{2+} chelators EGTA and BAPTA. The choice of an appropriate Ca^{2+} indicator will depend on a multitude of factors.

There are two main categories of calcium indicators: ratiometric (dual-wavelength) dyes (e.g. Fura-2, Indo-1), and non-ratiometric (single-wavelength) dyes (e.g. Fluo-4, OGB-1).

A ratiometric dye responds to the binding of Ca^{2+} by changing either its excitation or emission spectra. For example, the peak excitation wavelength of Fura-2 changes when it binds Ca^{2+}. As increasing levels of Ca^{2+} are bound, the measurement of fluorescence emission at two suitably chosen wavelengths on either side of the isosbestic point of the dye (the wavelength at which there is no change in fluorescence with Ca^{2+} binding), will increase in emission at one wavelength and decrease at the another (Grynkiewicz et al., 1985). A calculation can then be made of the ratio of fluorescence at the peak excitation wavelengths for the Ca^{2+}-bound and Ca^{2+}-unbound states (Grynkiewicz et al., 1985). As this is a ratiometric measure, it is relatively independent of dye concentration and cell thickness. This method can permit a calibration of ion concentration, using a variety of methods, providing measurements closer to absolute concentrations of $[Ca^{2+}]_i$, but is more cumbersome to implement than the single-

wavelength dye method. Furthermore, many of these dyes require short (UV range) excitation wavelengths, limiting the depth of penetration and elevating phototoxicity (Molecular Probes Handbook, 2005).

By contrast, a single-wavelength dye emits fluorescence at one specified wavelength in proportion to the concentration of free $[Ca^{2+}]_i$. No ratiometric measurements are generally possible with these dyes, although a combination of 2 single-wavelength dyes, such as Fura Red and fluo-3, with sufficiently separated emission peaks, can mimic single-dye ratiometry (e.g. Molecular Probes Handbook Ch. 19.3, 2005). Long-wavelength indicators, such as OGB-1, have some advantages such as emission spectra that are out of the range of most cellular autofluorescence (reducing background noise), reduced light scattering (longer wavelengths are scattered less by tissue), and an excitation spectra that is lower in energy, thus reducing potential photodamage. Many of these dyes have an excitation spectrum that is well-suited for use with most lasers (Molecular Probes Handbook, 2005). However, in some paradigms single wavelength dyes are not preferred because of difficulty in measuring absolute $[Ca^{2+}]_i$, although under specific circumstances it is possible (Maravall et al., 2000).

Ca^{2+} indicators are available in membrane-impermeant and membrane-permeant forms. A membrane-impermeant indicator must be invasively loaded into the cell, most commonly via an intracellular pipette. This can be an advantage or a disadvantage, depending on the experiment to be performed. A membrane-permeant form includes an acetoxymethyl ester (AM) moiety that makes the molecule sufficiently hydrophobic to readily pass through the cell membrane. Once inside the cell, the ester is cleaved from the remainder of the molecule by intracellular esterases, thus trapping the now cell-impermeant indicator inside the cell. Membrane permeant indicators allow for the simultaneous loading of a large population of cells.

Another important factor in the choice of an appropriate Ca^{2+} indicator is the affinity of the dye for Ca^{2+} (or dissociation constant, K_d). Low affinity (high K_d) and high affinity (low K_d) dyes both have advantages and disadvantages. A high-affinity dye will buffer more Ca^{2+}, and become saturated at concentrations below those of a low-affinity dye. Saturation can lead to underestimates of $[Ca^{2+}]_i$, and an inability to reliably record large Ca^{2+} transients (Takahashi et al., 1999). Temporal dynamics are also an important property of indicators and are related to K_d. The on- and off-rates of Ca^{2+}-binding to the indicator will determine the speed at which a Ca^{2+} transient can be measured. Therefore, high affinity indicators are considered "slow" and low affinity indicators are considered "fast," and better for temporal accuracy (Poenie, 2006).

The choice of an appropriate Ca^{2+} indicator will invariably depend on the question of interest. As mentioned above, a single- or dual-wavelength dye, membrane impermeant or permeant forms, and Ca^{2+}-binding affinity are important factors to consider. Other factors include the the specificity of the indicator for Ca^{2+} versus other divalent cations (Zn^{2+}, Mn^{2+}, Mg^{2+}), the excitation and emission spectrum, the free Ca^{2+} range, the sensitivity to photobleaching, and the maximum fluorescence intensity of the dye (Takahashi et al., 1999).

Methods commonly used to record changes in the emission or excitation of fluorescent indicators includes conventional epifluorescence microscopy and confocal laser scanning microscopy (CLSM). In both types of microscopy the area of interest is illuminated by wavelengths of light that are reflected from a dichroic filter (which reflects light of a specific range of wavelengths and allows a separate range of longer wavelengths to pass through it) through the objective and onto the specimen. To excite the area of interest, epifluorescence systems filter a noncoherent beam of light at the excitation wavelength. Any emitted fluorescence will pass back through the objective and dichroic filter and can be viewed by the eye, or sent to a detector, which is

conventionally a cooled charge-coupled device (CCD). A CCD camera system consists of a two-dimensional array of millions of silicon structures (pixels) that gather light and convert brightness into an electrical signal. This signal is then digitized into a binary form, stored for a short period of time, then sent to a computer for further processing. Epifluorescence microscopy requires the use of excitation, dichroic, and emission filters that are chosen to suit the fluorophore used in the experiment. A limitation of epifluorescence microscopy is light scattering caused by the large field of illumination, and light coming from structures outside the plane of focus. Thus, with this conventional approach, very fine structures like dendritic spines have a low spatial resolution (Denk et al., 1996), which has led to the development of more advanced imaging technology.

CLSM uses one or more tightly-focused beams of light from a laser to scan the specimen and obtain optical sections. Compared to the large beam of illumination used in conventional epifluorecence systems, CLSM uses a tuned, coherent laser beam that scans parts of the specimen pixel-by-pixel and line-by-line in horizontal sections. This eliminates out-of-plane light and greatly decreases unwanted fluorescence from regions in the focal plane away from the region of interest. Fluorescence is detected by a photomultiplier tube or captured with a CCD and the intensity signal is processed by a computer to provide the image (Paddock, 2000). The optical sectioning method is a noninvasive way to view a specific portion of the specimen in a specific horizontal plane. Another advantage of CLSM is a decreased background fluorescence compared to epifluorescence microscopy. This results in increased contrast and clarity of the image. CLSM also allows fine spatial resolution along the vertical axis. Therefore, it is also possible to construct three-dimensional images. A disadvantage of CLSM is the small range of excitation wavelengths produced by argon or argon-krypton lasers (Takahashi et al., 1999).

Purpose

The purpose of this thesis was to investigate the modulation of dendritic excitability in principal neurons of the dentate gyrus and in the somatosensory cortex. This thesis can be broken down into two major sections that will investigate properties of dendritic electrogenesis in either DGCs or L5 pyramidal neurons.

Section 1: Dentate Granule Cells

Hypothesis 1a: Dentate granule cell dendrites can support frequency-dependent activity. Backpropagating action potentials have not been investigated *in vitro* or *in vivo* in DGCs, nor have high-frequency trains of pre-synaptic activity. Therefore, I sought to determine whether frequency-dependent regenerative activity is present in DGCs.

Hypothesis 1b: The efficacy of backpropagation activated Ca^{2+} currents is dependent on a complex interplay of voltage-dependent Ca^{2+} and K^{+} channels. Dendrites contain various distributions of ion channels that can affect the degree of signal propagation (Johnston et al., 1996; Stuart et al., 1997). I hypothesize that the blockade of specific K^{+} channels will increase, whereas the blockade of specific Ca^{2+} channels will decrease, dendritic regenerative activity.

Hypothesis 1c: Neuropeptide Y1 receptors can inhibit frequency-dependent Ca^{2+} electrogenesis. NPY1 receptors have been shown to inhibit N-type VDCCs on dendrites and the soma of DGCs (McQuiston et al., 1996a). NPYergic cell bodies with projections to the molecular layer are located in the hilus of the DG where they are positioned to provide negative feedback to DGCs (Chan-Palay et al., 1986; Kohler et al., 1986).

Therefore, I hypothesize that Y1 receptors can limit frequency-dependent Ca^{2+} currents in DGCs.

Hypothesis 1d: Dopamine can potentiate frequency-dependent Ca^{2+} electrogenesis. Ventral tegmental area afferents synapse on to dendrites of DGCs in the molecular layer (Leranth and Hajszan, 2007). D1 receptor activation is classically known to stimulate adenylate cyclase, which can lead to an increase in excitability (Greengard, 2001; Chen et al., 2007). I hypothesize that D1 receptor activation will potentiate frequency-dependent activity.

Hypothesis 1e: Dopamine and NPY will have opposing effects on synaptic plasticity. Dentate granule cells are prone to LTP after the appropriate pairing of pre- and postsynaptic input at theta frequencies (Schmidt-Hieber et al., 2004). I hypothesize that dopamine will potentiate, and NPY will inhibit theta-burst pairing induced LTP.

Hypothesis 1f: Human DGCs will also demonstrate frequency-dependent electrogenesis, modulation by NPY, and dopamine induced long-term potentiation. The few studies reporting electrical properties of human DGCs from the epileptic hippocampus have observed a subset of neurons with preserved properties similar to non-epileptic rodents (Dietrich et al., 1999). Therefore, I hypothesize that results from human DGCs will be comparable to those from the rat.

Section Two: Layer 5 Pyramidal Neurons

Hypothesis 2a: NPY1 receptors will increase the critical frequency and decrease the afterdepolarization. With paired somatic and dendritic whole-cell recordings it has been shown that distal Ca^{2+} spikes are generated above a critical frequency of backpropagating action potentials (Larkum et al., 1999b). I hypothesize that Y1 receptors will inhibit this Ca^{2+} electrogenesis.

Hypothesis 2b: NPY acts postsynaptically to inhibit Ca^{2+} electrogenesis. The few reports of NPY action in the cortex report pre-synaptic activity (Bacci et al., 2002; Wang, 2005). However, there is a dense distribution of NPY1 receptors on dendrites of L5 pyramidal neurons (Kopp et al., 2002) whose physiological significance is unknown. I hypothesize that NPY can act via postsynaptic receptors.

Hypothesis 2c: The action of NPY is mediated by receptors on the distal apical dendrite. Since the distal apical dendrite is the location of dendritic Ca^{2+} spike generation (Larkum et al., 1999a, 1999b; Perez-Garci et al., 2006), I hypothesize that a local application of NPY at the distal dendrites will affect the critical frequency, whereas a somatic application will not.

Hypothesis 2d: Suprathreshold activity from the pairing of an EPSP and a bAP will be inhibited by NPY. In L5 pyramidal neurons dendritic Ca^{2+} spikes can occur as a result of the appropriate timing of a presynaptic EPSP and a postsynaptic bAP (Larkum et al. 1999a). I hypothesize that NPY will decrease this coupling.

REFERENCES

Abe, K., Niikura, Y., Fujimoto, T., Akaishi, T., and Misawa, M. (2008). Involvement of dopamine D2 receptors in the induction of long-term potentiation in the basolateral amygdala-dentate gyrus pathway of anesthetized rats. Neuropharmacology *55*, 1419-1424.

Acsady, L., Kamondi, A., Sik, A., Freund, T., and Buzsaki, G. (1998). GABAergic cells are the major postsynaptic targets of mossy fibers in the rat hippocampus. J Neurosci *18*, 3386-3403.

Adrian, T.E., Allen, J.M., Bloom, S.R., Ghatei, M.A., Rossor, M.N., Roberts, G.W., Crow, T.J., Tatemoto, K., and Polak, J.M. (1983). Neuropeptide Y distribution in human brain. Nature *306*, 584-586.

Aicher, S.A., Springston, M., Berger, S.B., Reis, D.J., and Wahlestedt, C. (1991). Receptor-selective analogs demonstrate NPY/PYY receptor heterogeneity in rat brain. Neurosci Lett *130*, 32-36.

Aimone, J.B., Wiles, J., and Gage, F.H. (2006). Potential role for adult neurogenesis in the encoding of time in new memories. Nat Neurosci *9*, 723-727.

Amaral, D.G. (1978). A Golgi study of cell types in the hilar region of the hippocampus in the rat. J Comp Neurol *182*, 851-914.

Amaral, D.G. (1979). Synaptic extensions from the mossy fibers of the fascia dentata. Anat Embryol (Berl) *155*, 241-251.

Amaral, D.G., and Witter, M.P. (1989). The three-dimensional organization of the hippocampal formation: a review of anatomical data. Neuroscience *31*, 571-591.

Amaral, D.G. (1993). Emerging principles of intrinsic hippocampal organization. Curr Opin Neurobiol *3*, 225-229.

Amaral, D.G., Scharfman, H.E., and Lavenex, P. (2007). The dentate gyrus: fundamental neuroanatomical organization (dentate gyrus for dummies). Prog Brain Res *163*, 3-22.

Andersen, P., Bliss, T.V., and Skrede, K.K. (1971). Unit analysis of hippocampal polulation spikes. Exp Brain Res *13*, 208-221.

Bannister, A.P. (2005). Inter- and intra-laminar connections of pyramidal cells in the neocortex. Neurosci Res *53*, 95-103.

Bard, J.A., Walker, M.W., Branchek, T.A., and Weinshank, R.L. (1995). Cloning and functional expression of a human Y4 subtype receptor for pancreatic polypeptide, neuropeptide Y, and peptide YY. J Biol Chem *270*, 26762-26765.

Batterham, R.L., Le Roux, C.W., Cohen, M.A., Park, A.J., Ellis, S.M., Patterson, M., Frost, G.S., Ghatei, M.A., and Bloom, S.R. (2003). Pancreatic polypeptide reduces appetite and food intake in humans. J Clin Endocrinol Metab *88*, 3989-3992.

Beck-Sickinger, A.G., Wieland, H.A., Wittneben, H., Willim, K.D., Rudolf, K., and Jung, G. (1994). Complete L-alanine scan of neuropeptide Y reveals ligands binding to Y1 and Y2 receptors with distinguished conformations. Eur J Biochem *225*, 947-958.

Bereshpolova, Y., Amitai, Y., Gusev, A.G., Stoelzel, C.R., and Swadlow, H.A. (2007). Dendritic backpropagation and the state of the awake neocortex. J Neurosci *27*, 9392-9399.

Berger, T., Larkum, M.E., and Luscher, H.R. (2001). High I(h) channel density in the distal apical dendrite of layer V pyramidal cells increases bidirectional attenuation of EPSPs. J Neurophysiol *85*, 855-868.

Bergson, C., Mrzljak, L., Smiley, J.F., Pappy, M., Levenson, R., and Goldman-Rakic, P.S. (1995). Regional, cellular, and subcellular variations in the distribution of D1 and D5 dopamine receptors in primate brain. J Neurosci *15*, 7821-7836.

Berridge, M.J. (1993). Inositol trisphosphate and calcium signalling. Nature *361*, 315-325.

Bertler, A., and Rosengren, E. (1959). Occurrence and distribution of dopamine in brain and other tissues. Experientia *15*, 10-11.

Bertorello, A.M., Hopfield, J.F., Aperia, A., and Greengard, P. (1990). Inhibition by dopamine of (Na(+)+K+)ATPase activity in neostriatal neurons through D1 and D2 dopamine receptor synergism. Nature *347*, 386-388.

Bettio, A., Dinger, M.C., and Beck-Sickinger, A.G. (2002). The neuropeptide Y monomer in solution is not folded in the pancreatic-polypeptide fold. Protein Sci *11*, 1834-1844.

Bi, G.Q., and Poo, M.M. (1998). Synaptic modifications in cultured hippocampal neurons: dependence on spike timing, synaptic strength, and postsynaptic cell type. J Neurosci *18*, 10464-10472.

Bijak, M., and Smialowska, M. (1995). Effects of neuropeptide Y on evoked potentials in the CA1 region and the dentate gyrus of the rat hippocampal slice. Pol J Pharmacol *47*, 333-338.

Blackstad, T.W. (1956). Commissural connections of the hippocampal region in the rat, with special reference to their mode of termination. J Comp Neurol *105*, 417-537.

Blaschko, H. (1939). The specific action of 1-dopa decarboxylase. J. Physiol. (Lond) *96,* 5O-51.

Bliss, T.V., and Lømø , T. (1973). Long-lasting potentiation of synaptic transmission in the dentate area of the anaesthetized rabbit following stimulation of the perforant path. J Physiol *232*, 331-356.

Blundell, T.L., Pitts, J.E., Tickle, I.J., and Wood, S.P. (1981). The conformation and receptor binding of pancreatic hormones. Biochem Soc Trans *9*, 31-32.

Boss, B.D., Peterson, G.M., and Cowan, W.M. (1985). On the number of neurons in the dentate gyrus of the rat. Brain Res *338*, 144-150.

Bragin, A., Jando, G., Nadasdy, Z., Hetke, J., Wise, K., and Buzsaki, G. (1995). Gamma (40-100 Hz) oscillation in the hippocampus of the behaving rat. J Neurosci *15*, 47-60.

Brown, J.H., and Makman, M.H. (1972). Stimulation by dopamine of adenylate cyclase in retinal homogenates and of adenosine-3':5'-cyclic monophosphate formation in intact retina. Proc Natl Acad Sci U S A *69*, 539-543.

Buckmaster, P.S., Strowbridge, B.W., and Schwartzkroin, P.A. (1993). A comparison of rat hippocampal mossy cells and CA3c pyramidal cells. J Neurophysiol *70*, 1281-1299.

Burt, D.R., Enna, S.J., Creese, I., and Snyder, S.H. (1975). Dopamine receptor binding in the corpus striatum of mammalian brain. Proc Natl Acad Sci U S A *72*, 4655-4659.

Buzsaki, G. (2002). Theta oscillations in the hippocampus. Neuron *33*, 325-340.

Buzsaki, G., Horvath, Z., Urioste, R., Hetke, J., and Wise, K. (1992). High-frequency network oscillation in the hippocampus. Science *256*, 1025-1027.

Caberlotto, L., Fuxe, K., and Hurd, Y.L. (2000). Characterization of NPY mRNA-expressing cells in the human brain: co-localization with Y2 but not Y1 mRNA in the cerebral cortex, hippocampus, amygdala, and striatum. J Chem Neuroanat *20*, 327-337.

Caberlotto, L., Fuxe, K., Sedvall, G., and Hurd, Y.L. (1997). Localization of neuropeptide Y Y1 mRNA in the human brain: abundant expression in cerebral cortex and striatum. Eur J Neurosci *9*, 1212-1225.

Campanac, E., and Debanne, D. (2008). Spike timing-dependent plasticity: a learning rule for dendritic integration in rat CA1 pyramidal neurons. J Physiol *586*, 779-793.

Camps, M., Cortes, R., Gueye, B., Probst, A., and Palacios, J.M. (1989). Dopamine receptors in human brain: autoradiographic distribution of D2 sites. Neuroscience *28*, 275-290.

Canto, C.B., Wouterlood, F.G., and Witter, M.P. (2008). What does the anatomical organization of the entorhinal cortex tell us? Neural Plast *2008*, 381243.

Carlsson, A. (1959). Detection and assay of dopamine. Pharmacol Rev *11*, 300-304.

Carlsson, A., and Waldeck, B. (1958). A fluorimetric method for the determination of dopamine (3-hydroxytyramine). Acta Physiol Scand *44*, 293-298.

Chan-Palay, V., Kohler, C., Haesler, U., Lang, W., and Yasargil, G. (1986). Distribution of neurons and axons immunoreactive with antisera against neuropeptide Y in the normal human hippocampus. J Comp Neurol *248*, 360-375.

Chee, M.J., Colmers, W.F. (2008). Y eat? Nutrition *24*, 869-877.

Chen, X., Yuan, L.L., Zhao, C., Birnbaum, S.G., Frick, A., Jung, W.E., Schwarz, T.L., Sweatt, J.D., and Johnston, D. (2006). Deletion of Kv4.2 gene eliminates dendritic A-type K+ current and enhances induction of long-term potentiation in hippocampal CA1 pyramidal neurons. J Neurosci *26*, 12143-12151.

Chevaleyre, V., Takahashi, K.A., and Castillo, P.E. (2006). Endocannabinoid-mediated synaptic plasticity in the CNS. Annu Rev Neurosci *29*, 37-76.

Chrobak, J.J., and Buzsaki, G. (1994). Selective activation of deep layer (V-VI) retrohippocampal cortical neurons during hippocampal sharp waves in the behaving rat. J Neurosci *14*, 6160-6170.

Chrobak, J.J., and Buzsaki, G. (1996). High-frequency oscillations in the output networks of the hippocampal-entorhinal axis of the freely behaving rat. J Neurosci *16*, 3056-3066.

Chrobak, J.J., Lorincz, A., and Buzsaki, G. (2000). Physiological patterns in the hippocampo-entorhinal cortex system. Hippocampus *10*, 457-465.

Ciliax, B.J., Nash, N., Heilman, C., Sunahara, R., Hartney, A., Tiberi, M., Rye, D.B., Caron, M.G., Niznik, H.B., and Levey, A.I. (2000). Dopamine D(5) receptor immunolocalization in rat and monkey brain. Synapse *37*, 125-145.

Claiborne, B.J., Amaral, D.G., and Cowan, W.M. (1986). A light and electron microscopic analysis of the mossy fibers of the rat dentate gyrus. J Comp Neurol *246*, 435-458.

Claiborne, B.J., Amaral, D.G., and Cowan, W.M. (1990). Quantitative, three-dimensional analysis of granule cell dendrites in the rat dentate gyrus. J Comp Neurol *302*, 206-219.

Coetzee, W.A., Amarillo, Y., Chiu, J., Chow, A., Lau, D., McCormack, T., Moreno, H., Nadal, M.S., Ozaita, A., Pountney, D.*, et al.* (1999). Molecular diversity of K+ channels. Ann N Y Acad Sci *868*, 233-285.

Colino, A., and Malenka, R.C. (1993). Mechanisms underlying induction of long-term potentiation in rat medial and lateral perforant paths in vitro. J Neurophysiol *69*, 1150-1159.

Colmers, W.F., Lukowiak, K., and Pittman, Q.J. (1985). Neuropeptide Y reduces orthodromically evoked population spike in rat hippocampal CA1 by a possibly presynaptic mechanism. Brain Res *346*, 404-408.

Colmers, W.F., Lukowiak, K., and Pittman, Q.J. (1987). Presynaptic action of neuropeptide Y in area CA1 of the rat hippocampal slice. J Physiol *383*, 285-299.

Colmers, W.F., Lukowiak, K., and Pittman, Q.J. (1988). Neuropeptide Y action in the rat hippocampal slice: site and mechanism of presynaptic inhibition. J Neurosci *8*, 3827-3837.

Colmers, W.F., and Bleakman, D. (1994). Effects of neuropeptide Y on the electrical properties of neurons. Trends Neurosci *17*, 373-379.

Connors, B.W., Gutnick, M.J., and Prince, D.A. (1982). Electrophysiological properties of neocortical neurons in vitro. J Neurophysiol *48*, 1302-1320.

Connors, B.W., and Gutnick, M.J. (1990). Intrinsic firing patterns of diverse neocortical neurons. Trends Neurosci *13*, 99-104.

Cooper, D.C. (2002). The significance of action potential bursting in the brain reward circuit. Neurochem Int *41*, 333-340.

Cools, A.R., Boudier, A.J., and Rossum, J.M. (1976). Dopamine receptors: selective agonists and antagonists of functionally distinct types within the feline brain. Eur J Pharmacol *37*, 283-293.

Cortes, R., Gueye, B., Pazos, A., Probst, A., and Palacios, J.M. (1989). Dopamine receptors in human brain: autoradiographic distribution of D1 sites. Neuroscience *28*, 263-273.

Creese, I., Burt, D.R., and Snyder, S.H. (1975). Dopamine receptor binding: differentiation of agonist and antagonist states with 3H-dopamine and 3H-haloperidol. Life Sci *17*, 933-1001.

Csicsvari, J., Hirase, H., Czurko, A., Mamiya, A., and Buzsaki, G. (1999). Fast network oscillations in the hippocampal CA1 region of the behaving rat. J Neurosci *19*, RC20.

Csicsvari, J., Jamieson, B., Wise, K.D., and Buzsaki, G. (2003). Mechanisms of gamma oscillations in the hippocampus of the behaving rat. Neuron *37*, 311-322.

Cuello, A.C. (2004). Dendritic neurotransmitter release, from early days to today's challenges. In: Dendritic Neurotransmitter release. (Ed: Ludwig, M.). pp 1-11.

D'Hooge, R., De Deyn, P.P., Verzwijvelen, A., De Block, J., and De Potter, W.P. (1990). Storage and fast transport of noradrenaline, dopamine beta-hydroxylase and neuropeptide Y in dog sciatic nerve axons. Life Sci *47*, 1851-1859.

Dahl, E., Falck, B., von Mecklenburg, C., Myhrberg, H., and Rosengren, E. (1966). Neuronal localization of dopamine and 5-hydroxytryptamine in some mollusca. Z Zellforsch Mikrosk Anat *71*, 489-498.

Dan, Y., and Poo, M.M. (2006). Spike timing-dependent plasticity: from synapse to perception. Physiol Rev *86*, 1033-1048.

Deller, T., Martinez, A., Nitsch, R., and Frotscher, M. (1996). A novel entorhinal projection to the rat dentate gyrus: direct innervation of proximal dendrites and cell bodies of granule cells and GABAergic neurons. J Neurosci *16*, 3322-3333.

Denk, W., Yuste, R., Svoboda, K., and Tank, D.W. (1996). Imaging calcium dynamics in dendritic spines. Curr Opin Neurobiol *6*, 372-378.

Diamond, D.M., Dunwiddie, T.V., and Rose, G.M. (1988). Characteristics of hippocampal primed burst potentiation in vitro and in the awake rat. J Neurosci *8*, 4079-4088.

Doods, H., Gaida, W., Wieland, H.A., Dollinger, H., Schnorrenberg, G., Esser, F., Engel, W., Eberlein, W., and Rudolf, K. (1999). BIIE0246: a selective and high affinity neuropeptide Y Y(2) receptor antagonist. Eur J Pharmacol *384*, R3-5.

Douglas, R.J., and Martin, K.A. (2004). Neuronal circuits of the neocortex. Annu Rev Neurosci *27*, 419-451.

Douglas, R.J., and Martin, K.A. (2007). Recurrent neuronal circuits in the neocortex. Curr Biol *17*, R496-500.

Dudman, J.T., Tsay, D., and Siegelbaum, S.A. (2007). A role for synaptic inputs at distal dendrites: instructive signals for hippocampal long-term plasticity. Neuron *56*, 866-879.

Dumont, Y., Cadieux, A., Doods, H., Pheng, L.H., Abounader, R., Hamel, E., Jacques, D., Regoli, D., and Quirion, R. (2000). BIIE0246, a potent and highly selective non-peptide neuropeptide Y Y(2) receptor antagonist. Br J Pharmacol *129*, 1075-1088.

Dumont, Y., Jacques, D., Bouchard, P., and Quirion, R. (1998). Species differences in the expression and distribution of the neuropeptide Y Y1, Y2, Y4, and Y5 receptors in rodents, guinea pig, and primates brains. J Comp Neurol *402*, 372-384.

Dvorak-Carbone, H., and Schuman, E.M. (1999). Patterned activity in stratum lacunosum moleculare inhibits CA1 pyramidal neuron firing. J Neurophysiol *82*, 3213-3222.

Eichenbaum, H., and Cohen, N.J. (1988). Representation in the hippocampus: what do hippocampal neurons code? Trends Neurosci *11*, 244-248.

Eichenbaum, H. (1998). Using olfaction to study memory. Ann N Y Acad Sci *855*, 657-669.

El Bahh, B., Balosso, S., Hamilton, T., Herzog, H., Beck-Sickinger, A.G., Sperk, G., Gehlert, D.R., Vezzani, A., and Colmers, W.F. (2005). The anti-epileptic actions of neuropeptide Y in the hippocampus are mediated by Y and not Y receptors. Eur J Neurosci *22*, 1417-1430.

Emptage, N., Bliss, T.V., and Fine, A. (1999). Single synaptic events evoke NMDA receptor-mediated release of calcium from internal stores in hippocampal dendritic spines. Neuron *22*, 115-124.

Enoki, R., Hu, Y.L., Hamilton, D., and Fine, A. (2009). Expression of long-term plasticity at individual synapses in hippocampus is graded, bidirectional, and mainly presynaptic: optical quantal analysis. Neuron *62*, 242-253.

Everitt, B.J., Hokfelt, T., Terenius, L., Tatemoto, K., Mutt, V., and Goldstein, M. (1984). Differential co-existence of neuropeptide Y (NPY)-like immunoreactivity with catecholamines in the central nervous system of the rat. Neuroscience *11*, 443-462.

Felder, C.C., Albrecht, F.E., Campbell, T., Eisner, G.M., and Jose, P.A. (1993). cAMP-independent, G protein-linked inhibition of Na+/H+ exchange in renal brush border by D1 dopamine agonists. Am J Physiol *264*, F1032-1037.

Ferbinteanu, J., Holsinger, R.M., and McDonald, R.J. (1999). Lesions of the medial or lateral perforant path have different effects on hippocampal contributions to place learning and on fear conditioning to context. Behav Brain Res *101*, 65-84.

Fremeau, R.T., Jr., Duncan, G.E., Fornaretto, M.G., Dearry, A., Gingrich, J.A., Breese, G.R., and Caron, M.G. (1991). Localization of D1 dopamine receptor mRNA in brain supports a role in cognitive, affective, and neuroendocrine aspects of dopaminergic neurotransmission. Proc Natl Acad Sci U S A *88*, 3772-3776.

Freund, T.F., and Buzsaki, G. (1996). Interneurons of the hippocampus. Hippocampus *6*, 347-470.

Frey, U., Huang, Y.Y., and Kandel, E.R. (1993). Effects of cAMP simulate a late stage of LTP in hippocampal CA1 neurons. Science *260*, 1661-1664.

Froemke, R.C., Poo, M.M., and Dan, Y. (2005). Spike-timing-dependent synaptic plasticity depends on dendritic location. Nature *434*, 221-225.

Frotscher, M. (1985). Mossy fibres form synapses with identified pyramidal basket cells in the CA3 region of the guinea-pig hippocampus: a combined Golgi-electron microscope study. J Neurocytol *14*, 245-259.

Fu, L.Y., and van den Pol, A.N. (2007). GABA excitation in mouse hilar neuropeptide Y neurons. J Physiol *579*, 445-464.

Fuortes, M.G., Frank, K., and Becker, M.C. (1957). Steps in the production of motoneuron spikes. J Gen Physiol *40*, 735-752.

Gasbarri, A., Packard, M.G., Campana, E., and Pacitti, C. (1994). Anterograde and retrograde tracing of projections from the ventral tegmental area to the hippocampal formation in the rat. Brain Res Bull *33*, 445-452.

Gerald, C., Walker, M.W., Criscione, L., Gustafson, E.L., Batzl-Hartmann, C., Smith, K.E., Vaysse, P., Durkin, M.M., Laz, T.M., Linemeyer, D.L., *et al.* (1996). A receptor subtype involved in neuropeptide-Y-induced food intake. Nature *382*, 168-171.

Gilbert, C.D., and Sigman, M. (2007). Brain states: top-down influences in sensory processing. Neuron *54*, 677-696.

Gilbert, P.E., Kesner, R.P., and Lee, I. (2001). Dissociating hippocampal subregions: double dissociation between dentate gyrus and CA1. Hippocampus *11*, 626-636.

Golding, N.L., Staff, N.P., and Spruston, N. (2002). Dendritic spikes as a mechanism for cooperative long-term potentiation. Nature *418*, 326-331.

Golgi, C. (1886). *Sulla Fina Anatomia Degli Organi Centrali del Sistema Nervose*, Milano: U. Hoepli.

Granado, N., Ortiz, O., Suarez, L.M., Martin, E.D., Cena, V., Solis, J.M., and Moratalla, R. (2008). D1 but not D5 dopamine receptors are critical for LTP, spatial learning, and LTP-Induced arc and zif268 expression in the hippocampus. Cereb Cortex *18*, 1-12.

Grynkiewicz, G., Poenie, M., and Tsien, R.Y. (1985). A new generation of Ca2+ indicators with greatly improved fluorescence properties. J Biol Chem *260*, 3440-3450.

Green, E.J., and Juraska, J.M. (1985). The dendritic morphology of hippocampal dentate granule cells varies with their position in the granule cell layer: a quantitative Golgi study. Exp Brain Res *59*, 582-586.

Green, J.D., and Arduini, A.A. (1954). Hippocampal electrical activity in arousal. J Neurophysiol *17*, 533-557.

Grundemar, L., and Hakanson, R. (1990). Effects of various neuropeptide Y/peptide YY fragments on electrically-evoked contractions of the rat vas deferens. Br J Pharmacol *100*, 190-192.

Guo, H., Castro, P.A., Palmiter, R.D., and Baraban, S.C. (2002). Y5 receptors mediate neuropeptide Y actions at excitatory synapses in area CA3 of the mouse hippocampus. J Neurophysiol *87*, 558-566.

Gutierrez, R. (2003). The GABAergic phenotype of the "glutamatergic" granule cells of the dentate gyrus. Prog Neurobiol *71*, 337-358.

Gutnick, M.J., and Friedman, A. (1986). Synaptic and intrinsic mechanisms of synchronization and epileptogenesis in the neocortex. Exp. Brain Res. *114*: 327-335.

Haas, H.L. (1983). Amine neurotransmitter actions in the hippocampus. In: Seifert W (ed) Neurobiology of the hippocampus. Academic Press, New York, p 147.

Haeggendal, J., and Malmfors, T. (1963). Evidence of Dopamine-Containing Neurons in the Retina of Rabbits. Acta Physiol Scand *59*, 295-296.

Hanse, E., and Gustafsson, B. (1992). Long-term Potentiation and Field EPSPs in the Lateral and Medial Perforant Paths in the Dentate Gyrus In Vitro: a Comparison. Eur J Neurosci *4*, 1191-1201.

Hausser, M., Stuart, G., Racca, C., and Sakmann, B. (1995). Axonal initiation and Neuron *15*, 637-647.

Hebb, D. O. (*1949*). The Organization of Behavior: A neuropsychological theory. New York: Wiley.

Helmchen, F., Svoboda, K., Denk, W., and Tank, D.W. (1999). In vivo dendritic calcium dynamics in deep-layer cortical pyramidal neurons. Nat Neurosci *2*, 989-996.

Hendry, S.H., Jones, E.G., DeFelipe, J., Schmechel, D., Brandon, C., and Emson, P.C. (1984). Neuropeptide-containing neurons of the cerebral cortex are also GABAergic. Proc Natl Acad Sci U S A *81*, 6526-6530.

Henze, D.A., Urban, N.N., and Barrionuevo, G. (2000). The multifarious hippocampal mossy fiber pathway: a review. Neuroscience *98*, 407-427.

Herzog, H. (2003). Neuropeptide Y and energy homeostasis: insights from Y receptor knockout models. Eur J Pharmacol *480*, 21-29.

Hinds, H.L., Tonegawa, S., and Malinow, R. (1998). CA1 long-term potentiation is diminished but present in hippocampal slices from alpha-CaMKII mutant mice. Learn Mem *5*, 344-354.

Hjorth-Simonsen, A. (1973). Some intrinsic connections of the hippocampus in the rat: an experimental analysis. J Comp Neurol *147*, 145-161.

Hoffman, D.A., Magee, J.C., Colbert, C.M., and Johnston, D. (1997). K+ channel regulation of signal propagation in dendrites of hippocampal pyramidal neurons. Nature *387*, 869-875.

Hoffman, D.A., and Johnston, D. (1998). Downregulation of transient K+ channels in dendrites of hippocampal CA1 pyramidal neurons by activation of PKA and PKC. J Neurosci *18*, 3521-3528.

Hokfelt, T. (1991). Neuropeptides in perspective: the last ten years. Neuron *7*, 867-879.

Howell, O.W., Scharfman, H.E., Herzog, H., Sundstrom, L.E., Beck-Sickinger, A., and Gray, W.P. (2003). Neuropeptide Y is neuroproliferative for post-natal hippocampal precursor cells. J Neurochem *86*, 646-659.

Huang, Q., Zhou, D., Chase, K., Gusella, J.F., Aronin, N., and DiFiglia, M. (1992). Immunohistochemical localization of the D1 dopamine receptor in rat brain reveals its axonal transport, pre- and postsynaptic localization, and prevalence in the basal ganglia, limbic system, and thalamic reticular nucleus. Proc Natl Acad Sci U S A *89*, 11988-11992.

Huang, Y.Y., and Kandel, E.R. (1995). D1/D5 receptor agonists induce a protein synthesis-dependent late potentiation in the CA1 region of the hippocampus. Proc Natl Acad Sci U S A *92*, 2446-2450.

Huguenard, J.R., Hamill, O.P., and Prince, D.A. (1989). Sodium channels in dendrites of rat cortical pyramidal neurons. Proc Natl Acad Sci U S A *86*, 2473-2477.

Huguenard, J.R, McCormick, D.A., and Coulter, D.C. (1995). Thalamocortical Interactions. In: The Cortical Neuron. (Ed: Gutnick, M.J. and Mody, I.) Oxford press. pp. 157-173.

Jeon, D., Kim, C., Yang, Y.M., Rhim, H., Yim, E., Oh, U., and Shin, H.S. (2007). Impaired long-term memory and long-term potentiation in N-type Ca2+ channel-deficient mice. Genes Brain Behav *6*, 375-388.

Johnston, D., Magee, J.C., Colbert, C.M., and Cristie, B.R. (1996). Active properties of neuronal dendrites. Annu Rev Neurosci *19*, 165-186.

Johnston, D., Hoffman, D.A., Magee, J.C., Poolos, N.P., Watanabe, S., Colbert, C.M., and Migliore, M. (2000). Dendritic potassium channels in hippocampal pyramidal neurons. J Physiol *525 Pt 1*, 75-81.

Jones, E.G. (1975). Varieties and distribution of non-pyramidal cells in the somatic sensory cortex of the squirrel monkey. J Comp Neurol *160*, 205-267.

Jones, E.G. (1993). GABAergic neurons and their role in cortical plasticity in primates. Cereb Cortex *3*, 361-372.

Jung, M.W., and McNaughton, B.L. (1993). Spatial selectivity of unit activity in the hippocampal granular layer. Hippocampus *3*, 165-182.

Kampa, B.M., Letzkus, J.J., and Stuart, G.J. (2006). Requirement of dendritic calcium spikes for induction of spike-timing-dependent synaptic plasticity. J Physiol *574*, 283-290.

Kampa, B.M., Letzkus, J.J., and Stuart, G.J. (2007). Dendritic mechanisms controlling spike-timing-dependent synaptic plasticity. Trends Neurosci *30*, 456-463.

Karmarkar, U.R., and Buonomano, D.V. (2002). A model of spike-timing dependent plasticity: one or two coincidence detectors? J Neurophysiol *88*, 507-513.

Kebabian, J.W., and Calne, D.B. (1979). Multiple receptors for dopamine. Nature *277*, 93-96.

Kebabian, J.W., Petzold, G.L., and Greengard, P. (1972). Dopamine-sensitive adenylate cyclase in caudate nucleus of rat brain, and its similarity to the "dopamine receptor". Proc Natl Acad Sci U S A *69*, 2145-2149.

Keefe, K.A., and Gerfen, C.R. (1995). D1-D2 dopamine receptor synergy in striatum: effects of intrastriatal infusions of dopamine agonists and antagonists on immediate early gene expression. Neuroscience *66*, 903-913.

Kemp, A., and Manahan-Vaughan, D. (2007). Hippocampal long-term depression: master or minion in declarative memory processes? Trends Neurosci *30*, 111-118.

Kerchner, G.A., and Nicoll, R.A. (2008). Silent synapses and the emergence of a postsynaptic mechanism for LTP. Nat Rev Neurosci *9*, 813-825.

Khan, Z.U., Gutierrez, A., Martin, R., Penafiel, A., Rivera, A., and de la Calle, A. (2000). Dopamine D5 receptors of rat and human brain. Neuroscience *100*, 689-699.

Kim, H.G., and Connors, B.W. (1993). Apical dendrites of the neocortex: correlation between sodium- and calcium-dependent spiking and pyramidal cell morphology. J Neurosci *13*, 5301-5311.

Kimmel, J.R., Pollock, H.G., and Hazelwood, R.L. (1968). Isolation and characterization of chicken insulin. Endocrinology *83*, 1323-1330.

Klapstein, G.J., and Colmers, W.F. (1993). On the sites of presynaptic inhibition by neuropeptide Y in rat hippocampus in vitro. Hippocampus *3*, 103-111.

Klyachko, V.A., and Jackson, M.B. (2002). Capacitance steps and fusion pores of small and large-dense-core vesicles in nerve terminals. Nature *418*, 89-92.

Kobayashi, K., and Suzuki, H. (2007). Dopamine selectively potentiates hippocampal mossy fiber to CA3 synaptic transmission. Neuropharmacology *52*, 552-561.

Koester, H.J., and Sakmann, B. (1998). Calcium dynamics in single spines during coincident pre- and postsynaptic activity depend on relative timing of back-propagating action potentials and subthreshold excitatory postsynaptic potentials. Proc Natl Acad Sci U S A *95*, 9596-9601.

Kohler, C., Eriksson, L., Davies, S., and Chan-Palay, V. (1986). Neuropeptide Y innervation of the hippocampal region in the rat and monkey brain. J Comp Neurol *244*, 384-400.

Kohler, C., Eriksson, L.G., Davies, S., and Chan-Palay, V. (1987). Co-localization of neuropeptide tyrosine and somatostatin immunoreactivity in neurons of individual subfields of the rat hippocampal region. Neurosci Lett *78*, 1-6.

Kopp, J., Xu, Z.Q., Zhang, X., Prazzini, T., Herzog, H., Kresse, A., Wong, H., Walsh, J.H., and Hokfelt, T. (2002). Expression of the neuropeptide Y Y1 receptor in the CNS of rat and of wild-type and Y1 receptor knock-out mice. Focus on immunohistochemical localization. Neuroscience *111*, 443-532.

Korngreen, A., and Sakmann, B. (2000). Voltage-gated K+ channels in layer 5 neocortical pyramidal neurones from young rats: subtypes and gradients. J Physiol *525 Pt 3*, 621-639.

Kusuki, T., Imahori, Y., Ueda, S., and Inokuchi, K. (1997). Dopaminergic modulation of LTP induction in the dentate gyrus of intact brain. Neuroreport *8*, 2037-2040.

Larhammar, D. (1996a). Evolution of neuropeptide Y, peptide YY and pancreatic polypeptide. Regul Pept *62*, 1-11.

Larhammar, D. (1996b). Structural diversity of receptors for neuropeptide Y, peptide YY and pancreatic polypeptide. Regul Pept *65*, 165-174.

Larhammar, D., Blomqvist, A.G., Yee, F., Jazin, E., Yoo, H., and Wahlested, C. (1992). Cloning and functional expression of a human neuropeptide Y/peptide YY receptor of the Y1 type. J Biol Chem *267*, 10935-10938.

Larhammar, D., Blomqvist, A.G., and Soderberg, C. (1993). Evolution of neuropeptide Y and its related peptides. Comp Biochem Physiol C *106*, 743-752.

Larhammar, D., and Salaneck, E. (2004). Molecular evolution of NPY receptor subtypes. Neuropeptides *38*, 141-151.

Larkman, A., and Mason, A. (1990). Correlations between morphology and electrophysiology of pyramidal neurons in slices of rat visual cortex. I. Establishment of cell classes. J Neurosci *10*, 1407-1414.

Larkman, A.U. (1991). Dendritic morphology of pyramidal neurones of the visual cortex of the rat: I. Branching patterns. J Comp Neurol *306*, 307-319.

Larkum, M.E., Zhu, J.J., and Sakmann, B. (1999a). A new cellular mechanism for coupling inputs arriving at different cortical layers. Nature *398*, 338-341.

Larkum, M.E., Kaiser, K.M., and Sakmann, B. (1999b). Calcium electrogenesis in distal apical dendrites of layer 5 pyramidal cells at a critical frequency of back-propagating action potentials. Proc Natl Acad Sci U S A *96*, 14600-14604.

Larkum, M.E., Zhu, J.J., and Sakmann, B. (2001). Dendritic mechanisms underlying the coupling of the dendritic with the axonal action potential initiation zone of adult rat layer 5 pyramidal neurons. J Physiol *533*, 447-466.

Larkum, M.E., and Zhu, J.J. (2002). Signaling of layer 1 and whisker-evoked Ca2+ and Na+ action potentials in distal and terminal dendrites of rat neocortical pyramidal neurons in vitro and in vivo. J Neurosci *22*, 6991-7005.

Larkum, M.E., Senn, W., and Luscher, H.R. (2004). Top-down dendritic input increases the gain of layer 5 pyramidal neurons. Cereb Cortex *14*, 1059-1070.

Larson, J., and Lynch, G. (1989). Theta pattern stimulation and the induction of LTP: the sequence in which synapses are stimulated determines the degree to which they potentiate. Brain Res *489*, 49-58.

Larson, J., Xiao, P., and Lynch, G. (1993). Reversal of LTP by theta frequency stimulation. Brain Res *600*, 97-102.

Laurberg, S., and Sorensen, K.E. (1981). Associational and commissural collaterals of neurons in the hippocampal formation (hilus fasciae dentatae and subfield CA3). Brain Res *212*, 287-300.

Lee, H.K., Barbarosie, M., Kameyama, K., Bear, M.F., and Huganir, R.L. (2000). Regulation of distinct AMPA receptor phosphorylation sites during bidirectional synaptic plasticity. Nature *405*, 955-959.

Lee, N.J., Enriquez, R.F., Boey, D., Lin, S., Slack, K., Baldock, P.A., Herzog, H., and Sainsbury, A. (2008). Synergistic attenuation of obesity by Y2- and Y4-receptor double knockout in ob/ob mice. Nutrition *24*, 892-899.

Leranth, C. and Hajszan, T. (2007). Extrinsic afferent systems to the dentate gyrus. In The Dentate gyrus: A Comprehensive Guide to Structure, Function, and Clinical Implications, H. Scharfman, ed. (Amsterdam, NL: Elsevier) pp. 63-84.

Leutgeb, J.K., Leutgeb, S., Moser, M.B., and Moser, E.I. (2007). Pattern separation in the dentate gyrus and CA3 of the hippocampus. Science *315*, 961-966.

Levens, N.R., and Della-Zuana, O. (2003). Neuropeptide Y Y5 receptor antagonists as anti-obesity drugs. Curr Opin Investig Drugs *4*, 1198-1204.

Lewis, F.T. (1923). The significance of the term *Hippocampus*. J. Comp. Neurol. 35, pp. 213–230.

Li, X.G., Somogyi, P., Ylinen, A., and Buzsaki, G. (1994). The hippocampal CA3 network: an in vivo intracellular labeling study. J Comp Neurol *339*, 181-208.

Liao, D., Hessler, N.A., and Malinow, R. (1995). Activation of postsynaptically silent synapses during pairing-induced LTP in CA1 region of hippocampal slice. Nature *375*, 400-404.

Lin, Y.W., Yang, H.W., Wang, H.J., Gong, C.L., Chiu, T.H., and Min, M.Y. (2006). Spike-timing-dependent plasticity at resting and conditioned lateral perforant path synapses on granule cells in the dentate gyrus: different roles of N-methyl-D-aspartate and group I metabotropic glutamate receptors. Eur J Neurosci *23*, 2362-2374.

Lisman, J. (1994). The CaM kinase II hypothesis for the storage of synaptic memory. Trends Neurosci *17*, 406-412.

Liu, Y.F., Civelli, O., Zhou, Q.Y., and Albert, P.R. (1992). Cholera toxin-sensitive 3',5'-cyclic adenosine monophosphate and calcium signals of the human dopamine-D1 receptor: selective potentiation by protein kinase A. Mol Endocrinol *6*, 1815-1824.

Lledo, P.M., Homburger, V., Bockaert, J., and Vincent, J.D. (1992). Differential G protein-mediated coupling of D2 dopamine receptors to K+ and Ca2+ currents in rat anterior pituitary cells. Neuron *8*, 455-463.

Lorente de Nó, R. (1934). Studies on the structure of the cerebral cortex. II. Continuation of the study of the ammonic system. J. Psychol. Neurol. *46*, pp. 113–117.

Lorincz, A., Notomi, T., Tamas, G., Shigemoto, R., and Nusser, Z. (2002). Polarized and compartment-dependent distribution of HCN1 in pyramidal cell dendrites. Nat Neurosci *5*, 1185-1193.

Loy, R. (1980). Development of afferent lamination in Ammon's horn of the rat. Anat Embryol (Berl) *159*, 257-275.

Lu, W., Man, H., Ju, W., Trimble, W.S., MacDonald, J.F., and Wang, Y.T. (2001). Activation of synaptic NMDA receptors induces membrane insertion of new AMPA receptors and LTP in cultured hippocampal neurons. Neuron *29*, 243-254.

Lundberg, J.M., Terenius, L., Hokfelt, T., Martling, C.R., Tatemoto, K., Mutt, V., Polak, J., Bloom, S., and Goldstein, M. (1982). Neuropeptide Y (NPY)-like immunoreactivity in peripheral noradrenergic neurons and effects of NPY on sympathetic function. Acta Physiol Scand *116*, 477-480.

Lundberg, J.M., Terenius, L., Hokfelt, T., and Goldstein, M. (1983). High levels of neuropeptide Y in peripheral noradrenergic neurons in various mammals including man. Neurosci Lett *42*, 167-172.

Lundberg, J.M., Hemsen, A., Larsson, O., Rudehill, A., Saria, A., and Fredholm, B.B. (1988). Neuropeptide Y receptor in pig spleen: binding characteristics, reduction of cyclic AMP formation and calcium antagonist inhibition of vasoconstriction. Eur J Pharmacol *145*, 21-29.

Lundell, I., Blomqvist, A.G., Berglund, M.M., Schober, D.A., Johnson, D., Statnick, M.A., Gadski, R.A., Gehlert, D.R., and Larhammar, D. (1995). Cloning of a human receptor of the NPY receptor family with high affinity for pancreatic polypeptide and peptide YY. J Biol Chem *270*, 29123-29128.

Luo, Y., Kokkonen, G.C., Wang, X., Neve, K.A., and Roth, G.S. (1998). D2 dopamine receptors stimulate mitogenesis through pertussis toxin-sensitive G proteins and Ras-involved ERK and SAP/JNK pathways in rat C6-D2L glioma cells. J Neurochem *71*, 980-990.

MacDonald, J.F., and Nowak, L.M. (1990). Mechanisms of blockade of excitatory amino acid receptor channels. Trends Pharmacol Sci *11*, 167-172.

Magee, J.C., and Johnston, D. (1995). Characterization of single voltage-gated Na+ and Ca2+ channels in apical dendrites of rat CA1 pyramidal neurons. J Physiol *487 (Pt 1)*, 67-90.

Malenka, R.C., and Nicoll, R.A. (1999). Long-term potentiation--a decade of progress? Science *285*, 1870-1874.

Malinow, R., Schulman, H., and Tsien, R.W. (1989). Inhibition of postsynaptic PKC or CaMKII blocks induction but not expression of LTP. Science *245*, 862-866.

Man, H.Y., Lin, J.W., Ju, W.H., Ahmadian, G., Liu, L., Becker, L.E., Sheng, M., and Wang, Y.T. (2000). Regulation of AMPA receptor-mediated synaptic transmission by clathrin-dependent receptor internalization. Neuron *25*, 649-662.

Marin-Padilla, M. (1967). Number and distribution of the apical dendritic spines of the layer V pyramidal cells in man. J Comp Neurol *131*, 475-490.

Markram, H., and Sakmann, B. (1994). Calcium transients in dendrites of neocortical neurons evoked by single subthreshold excitatory postsynaptic potentials via low-voltage-activated calcium channels. Proc Natl Acad Sci U S A *91*, 5207-5211.

Markram, H., Lubke, J., Frotscher, M., and Sakmann, B. (1997). Regulation of synaptic efficacy by coincidence of postsynaptic APs and EPSPs. Science *275*, 213-215.

Marsh, D.J., Hollopeter, G., Kafer, K.E., and Palmiter, R.D. (1998). Role of the Y5 neuropeptide Y receptor in feeding and obesity. Nat Med *4*, 718-721.

Martin, S.J., Grimwood, P.D., and Morris, R.G. (2000). Synaptic plasticity and memory: an evaluation of the hypothesis. Annu Rev Neurosci *23*, 649-711.

Matsuzaki, M., Honkura, N., Ellis-Davies, G.C., and Kasai, H. (2004). Structural basis of long-term potentiation in single dendritic spines. Nature *429*, 761-766.

Mayer, M.L., Westbrook, G.L., and Guthrie, P.B. (1984). Voltage-dependent block by Mg2+ of NMDA responses in spinal cord neurones. Nature *309*, 261-263.

McCormick, D.A., Connors, B.W., Lighthall, J.W., and Prince, D.A. (1985). Comparative electrophysiology of pyramidal and sparsely spiny stellate neurons of the neocortex. J Neurophysiol *54*, 782-806.

McNaughton, N., and Morris, R.G. (1987). Chlordiazepoxide, an anxiolytic benzodiazepine, impairs place navigation in rats. Behav Brain Res *24*, 39-46.

McQuiston, A.R., Petrozzino, J.J., Connor, J.A., and Colmers, W.F. (1996a). Neuropeptide Y1 receptors inhibit N-type calcium currents and reduce transient calcium increases in rat dentate granule cells. J Neurosci *16*, 1422-1429.

McQuiston, A.R., and Colmers, W.F. (1996b). Neuropeptide Y2 receptors inhibit the frequency of spontaneous but not miniature EPSCs in CA3 pyramidal cells of rat hippocampus. J Neurophysiol *76*, 3159-3168.

Menyhert, J., Wittmann, G., Lechan, R.M., Keller, E., Liposits, Z., and Fekete, C. (2007). Cocaine- and amphetamine-regulated transcript (CART) is colocalized with the orexigenic neuropeptide Y and agouti-related protein and absent from the anorexigenic alpha-melanocyte-stimulating hormone neurons in the infundibular nucleus of the human hypothalamus. Endocrinology *148*, 4276-4281.

Michel, M.C., Beck-Sickinger, A., Cox, H., Doods, H.N., Herzog, H., Larhammar, D., Quirion, R., Schwartz, T., and Westfall, T. (1998). XVI. International Union of Pharmacology recommendations for the nomenclature of neuropeptide Y, peptide YY, and pancreatic polypeptide receptors. Pharmacol Rev *50*, 143-150.

Minta, A., Kao, J.P., and Tsien, R.Y. (1989). Fluorescent indicators for cytosolic calcium based on rhodamine and fluorescein chromophores. J Biol Chem *264*, 8171-8178.

Misner, D.L., and Sullivan, J.M. (1999). Mechanism of cannabinoid effects on long-term potentiation and depression in hippocampal CA1 neurons. J Neurosci *19*, 6795-6805.

Miyawaki, A., Llopis, J., Heim, R., McCaffery, J.M., Adams, J.A., Ikura, M., and Tsien, R.Y. (1997). Fluorescent indicators for Ca2+ based on green fluorescent proteins and calmodulin. Nature *388*, 882-887.

Molecular Probes. (2005). The Handbook—A Guide to Fluorescent Probes and Labeling Technologies**.** Eugene, OR.

Moga, D.E., Shapiro, M.L., and Morrison, J.H. (2006). Bidirectional redistribution of AMPA but not NMDA receptors after perforant path simulation in the adult rat hippocampus in vivo. Hippocampus *16*, 990-1003.

Moser, E.I., Krobert, K.A., Moser, M.B., and Morris, R.G. (1998). Impaired spatial learning after saturation of long-term potentiation. Science *281*, 2038-2042.

Mountcastle, V.B. (1998). Perceptual neuroscience. The cerebral cortex. Cambridge, MA: Harvard University Press.

Mullins, D.E., Guzzi, M., Xia, L., and Parker, E.M. (2000). Pharmacological characterization of the cloned neuropeptide Y y(6) receptor. Eur J Pharmacol *395*, 87-93.

Navakkode, S., Sajikumar, S., and Frey, J.U. (2007). Synergistic requirements for the induction of dopaminergic D1/D5-receptor-mediated LTP in hippocampal slices of rat CA1 in vitro. Neuropharmacology *52*, 1547-1554.

Naveilhan, P., Hassani, H., Lucas, G., Blakeman, K.H., Hao, J.X., Xu, X.J., Wiesenfeld-Hallin, Z., Thoren, P., and Ernfors, P. (2001). Reduced antinociception and plasma extravasation in mice lacking a neuropeptide Y receptor. Nature *409*, 513-517.

Nevian, T., and Sakmann, B. (2004). Single spine Ca2+ signals evoked by coincident EPSPs and backpropagating action potentials in spiny stellate cells of layer 4 in the juvenile rat somatosensory barrel cortex. J Neurosci *24*, 1689-1699.

Nevian, T., and Sakmann, B. (2006). Spine Ca2+ signaling in spike-timing-dependent plasticity. J Neurosci *26*, 11001-11013.

Nicoll, R.A., and Malenka, R.C. (1995). Contrasting properties of two forms of long-term potentiation in the hippocampus. Nature *377*, 115-118.

Nowak, L., Bregestovski, P., Ascher, P., Herbet, A., and Prochiantz, A. (1984). Magnesium gates glutamate-activated channels in mouse central neurones. Nature *307*, 462-465.

O'Carroll, C.M., Martin, S.J., Sandin, J., Frenguelli, B., and Morris, R.G. (2006). Dopaminergic modulation of the persistence of one-trial hippocampus-dependent memory. Learn Mem *13*, 760-769.

O'Keefe, J., and Dostrovsky, J. (1971). The hippocampus as a spatial map. Preliminary evidence from unit activity in the freely-moving rat. Brain Res *34*, 171-175.

Paddock, S.W. (2000). Principles and practices of of laser scanning confocal microscopy. Mol Biotech, *16,* 127-149.

Parent, J.M. (2007). Adult neurogenesis in the intact and epileptic dentate gyrus. Prog Brain Res *163*, 529-540.

Parker, D., Soderberg, C., Zotova, E., Shupliakov, O., Langel, U., Bartfai, T., Larhammar, D., Brodin, L., and Grillner, S. (1998). Co-localized neuropeptide Y and GABA have complementary presynaptic effects on sensory synaptic transmission. Eur J Neurosci *10*, 2856-2870.

Parker, R.M., and Herzog, H. (1999). Regional distribution of Y-receptor subtype mRNAs in rat brain. Eur J Neurosci *11*, 1431-1448.

Pastalkova, E., Serrano, P., Pinkhasova, D., Wallace, E., Fenton, A.A., and Sacktor, T.C. (2006). Storage of spatial information by the maintenance mechanism of LTP. Science *313*, 1141-1144.

Paulsen, O., and Sejnowski, T.J. (2000). Natural patterns of activity and long-term synaptic plasticity. Curr Opin Neurobiol *10*, 172-179.

Pedrazzini, T., Pralong, F., and Grouzmann, E. (2003). Neuropeptide Y: the universal soldier. Cell Mol Life Sci *60*, 350-377.
Pelletier, G. (1984). [Coexistence of peptides and classical neurotransmitters]. Ann Endocrinol (Paris) *45*, 173-174.

Perez-Garci, E., Gassmann, M., Bettler, B., and Larkum, M.E. (2006). The GABAB1b isoform mediates long-lasting inhibition of dendritic Ca2+ spikes in layer 5 somatosensory pyramidal neurons. Neuron *50*, 603-616.

Pillolla, G., Melis, M., Perra, S., Muntoni, A.L., Gessa, G.L., and Pistis, M. (2007). Medial forebrain bundle stimulation evokes endocannabinoid-mediated modulation of ventral tegmental area dopamine neuron firing in vivo. Psychopharmacology (Berl) *191*, 843-853.

Poenie M. (2006). Calcium Signalling. 2nd ed. Ed: Putney J.W. Ch 1:1-50.

Poncer, J.C. (2003). Hippocampal long term potentiation: silent synapses and beyond. J Physiol Paris *97*, 415-422.

Pronchuk, N., Beck-Sickinger, A.G., and Colmers, W.F. (2002). Multiple NPY receptors Inhibit GABA(A) synaptic responses of rat medial parvocellular effector neurons in the hypothalamic paraventricular nucleus. Endocrinology *143*, 535-543.

Qian, J., Colmers, W.F., and Saggau, P. (1997). Inhibition of synaptic transmission by neuropeptide Y in rat hippocampal area CA1: modulation of presynaptic Ca2+ entry. J Neurosci *17*, 8169-8177.

Rall, W. (1959). Branching dendritic trees and motoneuron membrane resistivity. Exp Neurol *1*, 491-527.

Ranck, J.B., Jr. (1973). Studies on single neurons in dorsal hippocampal formation and septum in unrestrained rats. I. Behavioral correlates and firing repertoires. Exp Neurol *41*, 461-531.

Ranganath, C., Heller, A., Cohen, M.X., Brozinsky, C.J., and Rissman, J. (2005). Functional connectivity with the hippocampus during successful memory formation. Hippocampus *15*, 997-1005.

Ridgway, E.B., and Ashley, C.C. (1967). Calcium transients in single muscle fibers. Biochem Biophys Res Commun *29*, 229-234.

Rosenkranz, J.A., and Johnston, D. (2007). State-dependent modulation of amygdala inputs by dopamine-induced enhancement of sodium currents in layer V entorhinal cortex. J Neurosci *27*, 7054-7069.

Rubio-Garrido, P., Perez-de-Manzo, F., Porrero, C., Galazo, M.J., and Clasca, F. (2009). Thalamic Input to Distal Apical Dendrites in Neocortical Layer 1 Is Massive and Highly Convergent. Cereb Cortex.

Rudolf, R., Mongillo, M., Rizzuto, R., and Pozzan, T. (2003). Looking forward to seeing calcium. Nat Rev Mol Cell Biol *4*, 579-586.

Salaneck, E., Larson, E.T., Larsson, T.A., and Larhammar, D. (2005). Effects of a teleost tetraploidization on neuropeptide Y receptor gene repertoire in ray-finned fishes. Ann N Y Acad Sci *1040*, 457-459.

Sandler, V.M., and Barbara, J.G. (1999). Calcium-induced calcium release contributes to action potential-evoked calcium transients in hippocampal CA1 pyramidal neurons. J Neurosci *19*, 4325-4336.

Scharfman, H.E. (1991). Dentate hilar cells with dendrites in the molecular layer have lower thresholds for synaptic activation by perforant path than granule cells. J Neurosci *11*, 1660-1673.

Scharfman, H.E. (1993). Spiny neurons of area CA3c in rat hippocampal slices have similar electrophysiological characteristics and synaptic responses despite morphological variation. Hippocampus *3*, 9-28.

Scharfman, H.E. (1994). Evidence from simultaneous intracellular recordings in rat hippocampal slices that area CA3 pyramidal cells innervate dentate hilar mossy cells. J Neurophysiol *72*, 2167-2180.

Scharfman, H.E. (1995). Electrophysiological evidence that dentate hilar mossy cells are excitatory and innervate both granule cells and interneurons. J Neurophysiol *74*, 179-194.

Schiller, J., Schiller, Y., Stuart, G., and Sakmann, B. (1997). Calcium action potentials restricted to distal apical dendrites of rat neocortical pyramidal neurons. J Physiol *505 (Pt 3)*, 605-616.

Schmidt-Hieber, C., Jonas, P., and Bischofberger, J. (2004). Enhanced synaptic plasticity in newly generated granule cells of the adult hippocampus. Nature *429*, 184-187.

Scoville, W.B., and Milner, B. (1957). Loss of recent memory after bilateral hippocampal lesions. J Neurol Neurosurg Psychiatry *20*, 11-21.

Seress, L. (2007). Comparative anatomy of the hippocampal dentate gyrus in adult and developing rodents, non-human primates and humans. Prog Brain Res *163*, 23-41.

Serodio, P., and Rudy, B. (1998). Differential expression of Kv4 K+ channel subunits mediating subthreshold transient K+ (A-type) currents in rat brain. J Neurophysiol *79*, 1081-1091.

Sheikh, S.P., and Williams, J.A. (1990). Structural characterization of Y1 and Y2 receptors for neuropeptide Y and peptide YY by affinity cross-linking. J Biol Chem *265*, 8304-8310.

Simic, G., Kostovic, I., Winblad, B., and Bogdanovic, N. (1997). Volume and number of neurons of the human hippocampal formation in normal aging and Alzheimer's disease. J Comp Neurol *379*, 482-494.

Simmons, M.L., Terman, G.W., Gibbs, S.M., and Chavkin, C. (1995). L-type calcium channels mediate dynorphin neuropeptide release from dendrites but not axons of hippocampal granule cells. Neuron *14*, 1265-1272.

Sjöström, P.J., and Hausser, M. (2006). A cooperative switch determines the sign of synaptic plasticity in distal dendrites of neocortical pyramidal neurons. Neuron *51*, 227-238.

Smialowska, M., and Bajkowska, M. (1998). Reserpine induces increase in neuropeptide Y immunoreactivity in rat amygdala neurons. Pol J Pharmacol *50*, 443-447.

Smith, D.M., and Mizumori, S.J. (2006). Hippocampal place cells, context, and episodic memory. Hippocampus *16*, 716-729.

Sokal, D.M., Benetti, C., Girlanda, E., and Large, C.H. (2008). The CB1 receptor antagonist, SR141716A, prevents high-frequency stimulation-induced reduction of feedback inhibition in the rat dentate gyrus following perforant path stimulation in vivo. Brain Res *1223*, 50-58.

Spruston, N., Schiller, Y., Stuart, G., and Sakmann, B. (1995). Activity-dependent action potential invasion and calcium influx into hippocampal CA1 dendrites. Science *268*, 297-300.

Spruston, N. (2008). Pyramidal neurons: dendritic structure and synaptic integration. Nat Rev Neurosci *9*, 206-221.

Statnick, M.A., Schober, D.A., Mayne, N.G., Burnett, J.P., and Gehlert, D.R. (1997). Analysis of NPY receptor subtypes in the human frontal cortex reveals abundant Y1 mRNA and binding sites. Peptides *18*, 137-143.

Staubli, U., and Lynch, G. (1987). Stable hippocampal long-term potentiation elicited by 'theta' pattern stimulation. Brain Res *435*, 227-234.

Steward, O., and Scoville, S.A. (1976). Cells of origin of entorhinal cortical afferents to the hippocampus and fascia dentata of the rat. J Comp Neurol *169*, 347-370.

Stuart, G.J., and Sakmann, B. (1994). Active propagation of somatic action potentials into neocortical pyramidal cell dendrites. Nature *367*, 69-72.

Stuart, G., Spruston, N., Sakmann, B., and Hausser, M. (1997). Action potential initiation and backpropagation in neurons of the mammalian CNS. Trends Neurosci *20*, 125-131.

Stuart, G.J., and Hausser, M. (2001). Dendritic coincidence detection of EPSPs and action potentials. Nat Neurosci *4*, 63-71.

Suzuki, T. (1994). Protein kinases involved in the expression of long-term potentiation. Int J Biochem *26*, 735-744.

Swanson, L.W., Wyss, J.M., and Cowan, W.M. (1978). An autoradiographic study of the organization of intrahippocampal association pathways in the rat. J Comp Neurol *181*, 681-715.

Swanson, L.W. (1982). The projections of the ventral tegmental area and adjacent regions: a combined fluorescent retrograde tracer and immunofluorescence study in the rat. Brain Res Bull *9*, 321-353.

Takahashi, A., Camacho, P., Lechleiter, J.D., and Herman, B. (1999). Measurement of intracellular calcium. Physiol Rev *79*, 1089-1125.

Tasan, R.O., Lin, S., Hetzenauer, A., Singewald, N., Herzog, H., and Sperk, G. (2009). Increased novelty-induced motor activity and reduced depression-like behavior in neuropeptide Y (NPY)-Y4 receptor knockout mice. Neuroscience *158*, 1717-1730.

Tatemoto, K., Carlquist, M., and Mutt, V. (1982a). Neuropeptide Y--a novel brain peptide with structural similarities to peptide YY and pancreatic polypeptide. Nature *296*, 659-660.

Tatemoto, K. (1982b). Neuropeptide Y: complete amino acid sequence of the brain peptide. Proc Natl Acad Sci U S A *79*, 5485-5489.

Thiele, T.E., Koh, M.T., and Pedrazzini, T. (2002). Voluntary alcohol consumption is controlled via the neuropeptide Y Y1 receptor. J Neurosci *22*, RC208.

Thomas, D., Tovey, S.C., Collins, T.J., Bootman, M.D., Berridge, M.J., and Lipp, P. (2000). A comparison of fluorescent Ca2+ indicator properties and their use in measuring elementary and global Ca2+ signals. Cell Calcium *28*, 213-223.

Thorsell, A., Michalkiewicz, M., Dumont, Y., Quirion, R., Caberlotto, L., Rimondini, R., Mathe, A.A., and Heilig, M. (2000). Behavioral insensitivity to restraint stress, absent fear suppression of behavior and impaired spatial learning in transgenic rats with hippocampal neuropeptide Y overexpression. Proc Natl Acad Sci U S A *97*, 12852-12857.

Towers, S.K., LeBeau, F.E., Gloveli, T., Traub, R.D., Whittington, M.A., and Buhl, E.H. (2002). Fast network oscillations in the rat dentate gyrus in vitro. J Neurophysiol *87*, 1165-1168.

Tran, A.H., Uwano, T., Kimura, T., Hori, E., Katsuki, M., Nishijo, H., and Ono, T. (2008). Dopamine D1 receptor modulates hippocampal representation plasticity to spatial novelty. J Neurosci *28*, 13390-13400.

Tsien, R.Y. (1980). New calcium indicators and buffers with high selectivity against magnesium and protons: design, synthesis, and properties of prototype structures. Biochemistry *19*, 2396-2404.

Vanderwolf, C.H. (1969). Hippocampal electrical activity and voluntary movement in the rat. Electroencephalogr Clin Neurophysiol *26*, 407-418.

Vetter, P., Roth, A., and Hausser, M. (2001). Propagation of action potentials in dendrites depends on dendritic morphology. J Neurophysiol *85*, 926-937.

Wahlestedt, C., Yanaihara, N., and Hakanson, R. (1986). Evidence for different pre-and post-junctional receptors for neuropeptide Y and related peptides. Regul Pept *13*, 307-318.

Wamsley, J.K., Gehlert, D.R., Filloux, F.M., and Dawson, T.M. (1989). Comparison of the distribution of D-1 and D-2 dopamine receptors in the rat brain. J Chem Neuroanat *2*, 119-137.

Waters, J., Schaefer, A., and Sakmann, B. (2005). Backpropagating action potentials in neurones: measurement, mechanisms and potential functions. Prog Biophys Mol Biol *87*, 145-170.

Weinberg, D.H., Sirinathsinghji, D.J., Tan, C.P., Shiao, L.L., Morin, N., Rigby, M.R., Heavens, R.H., Rapoport, D.R., Bayne, M.L., Cascieri, M.A., *et al.* (1996). Cloning and expression of a novel neuropeptide Y receptor. J Biol Chem *271*, 16435-16438.

Whitcomb, D.C., Puccio, A.M., Vigna, S.R., Taylor, I.L., and Hoffman, G.E. (1997). Distribution of pancreatic polypeptide receptors in the rat brain. Brain Res *760*, 137-149.

Whitlock, J.R., Heynen, A.J., Shuler, M.G., and Bear, M.F. (2006). Learning induces long-term potentiation in the hippocampus. Science *313*, 1093-1097.

Whittaker, E., Vereker, E., and Lynch, M.A. (1999). Neuropeptide Y inhibits glutamate release and long-term potentiation in rat dentate gyrus. Brain Res *827*, 229-233.

Witter, M.P. (1986). A survey of the anatomy of the hippocampal formation, with emphasis on the septotemporal organization of its intrinsic and extrinsic connections. Adv Exp Med Biol *203*, 67-82.

Witter, M.P. (2002). The parahippocampal region: past, present, and future. In: The Parahippocampal Region, Organization and Role in Cognitive Functions (Witter and Wouterlood eds). Oxford Univ Press. pp 3-20.

Witter, M.P., and Amaral, D.G. (1991). Entorhinal cortex of the monkey: V. Projections to the dentate gyrus, hippocampus, and subicular complex. J Comp Neurol *307*, 437-459.

Yuste, R., and Denk, W. (1995). Dendritic spines as basic functional units of neuronal integration. Nature *375*, 682-684.

Yuste, R., Gutnick, M.J., Saar, D., Delaney, K.R., and Tank, D.W. (1994). Ca2+ accumulations in dendrites of neocortical pyramidal neurons: an apical band and evidence for two functional compartments. Neuron *13*, 23-43.

Zamponi, G.W., Bourinet, E., Nelson, D., Nargeot, J., and Snutch, T.P. (1997). Crosstalk between G proteins and protein kinase C mediated by the calcium channel alpha1 subunit. Nature *385*, 442-446.

Zhang, J., Xiong, B., Zhen, X., and Zhang, A. (2009). Dopamine D1 receptor ligands: where are we now and where are we going. Med Res Rev *29*, 272-294.

Zhen, X., Zhang, J., Johnson, G.P., and Friedman, E. (2001). D(4) dopamine receptor differentially regulates Akt/nuclear factor-kappa b and extracellular signal-regulated kinase pathways in D(4)MN9D cells. Mol Pharmacol *60*, 857-864.

Zimmer, J. (1971). Ipsilateral afferents to the commissural zone of the fascia dentata, demonstrated in decommissurated rats by silver impregnation. J Comp Neurol *142*, 393-416.

Zola-Morgan, S., Squire, L.R., and Amaral, D.G. (1986). Human amnesia and the medial temporal region: enduring memory impairment following a bilateral lesion limited to field CA1 of the hippocampus. J Neurosci *6*, 2950-2967.

CHAPTER 2

Dopamine and Neuropeptide Y Modulate Dendritic Excitability and Synaptic Plasticity in Dendrites of Rat and Human Dentate Granule Cells

INTRODUCTION

As an animal explores a specific location, place cells in the dentate gyrus of the hippocampus fire bursts of action potentials (APs; Jung and McNaughton, 1993) that can result in the formation of a new, long-term contextual memory (Smith and Mizumori, 2006). The principal neurons of the dentate gyrus, dentate granule cells (DGCs), respond preferentially to the high frequency gamma oscillations (30-100 Hz) from the perforant pathway that have been recorded in the dentate gyrus of freely moving rats during exploratory behaviours (Bragin et al., 1995; Csicsvari et al., 2003; Leutgeb et al., 2007). To balance this high frequency excitatory input, DGCs receive substantial tonic feedback inhibition from local GABAergic interneurons (Staley and Mody, 1992). During states of prolonged perforant pathway stimulation this inhibitory influence can be overridden and the dentate can become hyperexcitable (Scharfman and Schwartzkroin, 1990). There has been much emphasis on the epileptiform activity that can result when the inhibitory "gate" of the dentate gyrus is overwhelmed (Brenner et al., 2005; Sperk et al., 2007). However, little is known about the response of individual DGCs to high-frequency perforant pathway information, or the consequences of DGC excitability changes in normal physiology. As in neocortical and CA1 pyramidal neurons, frequency-dependent properties in DGCs that contribute to synaptic integration and information processing are likely of paramount importance in the context of memory formation.

In pyramidal neurons of neocortical layers 2/3 (L2/3) and layer 5 (L5), trains of backpropagating action potentials (bAPs) can result in supralinear, dendritic Ca^{2+} electrogenesis - a mechanism for linearizing, integrating and associating synaptic input, particularly repetitive or coincident responses (Stuart and Hausser, 2001; Waters et al., 2005). Trains of APs above a critical frequency (CF) backpropagating into the dendritic tree can elicit a regenerative, forward-propagating Ca^{2+} response originating in the distal dendrite (Larkum et al., 1999a; Larkum et al., 1999b). Functionally, bAPs can inform

dendrites of neuronal output, strengthen active synapses in a Hebbian manner, and are a candidate mechanism participating in memory formation (Stuart et al., 1997; Kampa and Stuart, 2006; Sjöström et al., 2008). Despite the postulated contribution of this mechanism in the hippocampal formation (Sjöström et al., 2008), only a single, in silico, modeling study has considered the role of bAPs in DGCs (Vetter et al., 2001). Based upon dendritic morphology and dendritic Na^+/K^+ channel ratio, this model suggests that backpropagation in DGCs should be comparable to that in pyramidal neurons of hippocampal area CA1 and neocortex (Vetter et al., 2001). Action potential backpropagation might thus depolarize DGC dendrites, promote Ca^{2+} influx, and thereby participate in synaptic plasticity such as long-term potentiation (LTP) in the dentate gyrus, the earliest physiological model of memory formation (Bliss and Lømø, 1973).

The perforant pathway, predominantly comprising projections from stellate and pyramidal neurons in layer 2 of the entorhinal cortex, provides the bulk of the glutamatergic excitation to DGCs and is heavily regulated by intrinsic and extrinsic neurotransmitters and neuropeptides (Leranth and Hajszan, 2007). Perforant path fibers synapse onto the outer two-thirds of DGC dendrites in the molecular layer of the dentate gyrus. The excitation provided by these afferents can be modulated by interneurons of the molecular layer and hilus that release GABA and neuropeptides, such as neuropeptide Y (NPY; Sperk et al., 2007). NPY1 receptors (Y1R) on DGC soma and dendrites have been shown to inhibit N-type VDCCs (McQuiston et al., 1996); however, the physiological role of NPY in dentate gyrus remains unclear (Sperk et al., 2007). Neuropeptides such as NPY are more efficiently released during prolonged stimulation, or high-frequency activity (Bartfai et al., 1988). Perforant pathway gamma oscillations, in the 30-100 Hz range (Csicsvari et al., 2003), are thus potentially ideal stimuli for neuropeptide release. In addition to GABA and glutamate inputs, DCG dendrites also receive extrinsic inputs, including dopaminergic axons from the ventral tegmental area (VTA) that modulate

excitability (O'Sullivan et al., 2008) and synaptic plasticity (Kulla and Manahan-Vaughan, 2000). Here, we first determined that backpropagation can occur in rat and human DGCs, and identified frequency-dependent Ca^{2+} electrogenesis originating in distal dendrites. During high-frequency (> 60 Hz) activity, a compartmentalized, supralinear Ca^{2+} influx can occur in DGC dendrites, and this response can be differentially modulated by the postsynaptic actions of both NPY and dopamine. Finally, we paired pre- and postsynaptic bursts at hippocampal theta frequencies and found that LTP induction is sharply facilitated by dopamine D1-receptor (D1R) activation in both human and rat DGCs.

METHODS

Slice Preparation

Animal procedures were in accordance with Canadian Council of Animal Care guidelines (protocol approved by the University of Alberta Health Sciences Laboratory Animal Committee) and relevant international laws and policies (EEC Council Directive 86/609, OJ L 358, 1, Dec. 12, 1987; Guide for the Care and Use of Laboratory Animals, U.S. National Research Council, 1996).

Rat experiments were performed in hippocampal slices from 3-5 week old male (or female where indicated) Sprague-Dawley rats as described previously (Klapstein et al., 1997). Rats were decapitated and the brains were removed and placed into an ice-cold (0-4°C) slicing solution containing (mM): 124 NaCl, 3 KCl, 1.4 NaH_2PO_4, 1.3 $MgSO_4$, 26 $NaHCO_3$, 1.5 $CaCl_2$, 10 glucose, 1 kynurenic acid (Sigma, St. Louis, MO), and saturated with 5% CO_2, 95% O_2 (carbogen). All extracellular solutions had an osmolarity of 300 ± 2 mOsm. Transverse slices (300 μm thick; Klapstein et al., 1993) were cut with a Vibroslicer HR-2 (Sigmann-Elektronik, Huffenhardt, Germany) and placed in a 32-34°C artificial cerebrospinal fluid (aCSF) solution containing (mM): 124 NaCl, 3 KCl, 1.4 NaH_2PO_4, 1.3 $MgSO_4$, 26 $NaHCO_3$, 1.5 $CaCl_2$, 10 glucose, and saturated with 5% CO_2, 95% O_2 (carbogen), for 15 mins, then maintained at room temperature for an additional 30 mins before experimentation.

Electrophysiology

Hippocampal slices were submerged in a continuous flow (2.5-3.5 ml/min) of aCSF at near physiological temperature (33.0 ± 1.0°C) on the stage of an upright microscope (Axioskop FS2, Carl Zeiss, Germany). DGCs were visually identified with 20-, 40- (Carl Zeiss) or 60X (Olympus) water-immersion objectives and IR-DIC optics.

Whole-cell patch clamp recordings were obtained using borosilicate glass pipettes (4-6 MΩ) filled with an intracellular solution containing (mM): K-Gluconate 135, 7 KCl, 10 HEPES, 10 Na-phosphocreatine, 4 Mg-ATP, 0.3 GTP, 10 EGTA (unless otherwise indicated), and 0.02 % neurobiotin, pH 7.1-7.3, 292-296 mOsm. Recordings from DGCs were made using an Axoclamp 2A amplifier (Axon Instruments, Palo Alto, CA) in current-clamp configuration. Trains of APs were evoked with 1 ms depolarizing square pulses of 1-5 nA current injections at typically at frequencies from 20-200 Hz.

Calcium Imaging

Dentate granule cells in hippocampal slices under the same conditions as above were loaded with the membrane-impermeant fluorescent Ca^{2+} indicator Oregon Green 488 BAPTA-1 (OGB-1; Invitrogen, Carlsbad, CA) via the whole-cell pipette. The intracellular solution was the same as above with the exception of (mM): 0 EGTA, 0.1 $CaCl_2$, 0.1 OGB-1 (Invitrogen), and 0.05 to 0.1 Alexa 594. In most experiments, 30 mins of OGB-1 loading was sufficient for measurable Ca^{2+} signals in dendrites up to 250 μm from the soma. Fluorescence was imaged with an image-intensified frame-transfer CCD video camera (Pentamax, Princeton Instruments, New Jersey). Data were recorded using MetaFluor 6.3 (Molecular Devices) acquired at frame rates of 25-50 Hz. Relative changes in intracellular Ca^{2+} levels were determined offline by selecting regions of interest (ROI) along the dendrite of interest, and subtracting background fluorescence from an average of 2 ROIs of equal dimensions in areas away from the neuron. ΔF/F was calculated by dividing the change in fluorescence (ΔF) by the fluorescence intensity before stimulation (F).

Immunohistochemistry

After recordings, slices were fixed in 4% paraformaldehyde for at least 48 hrs then washed in a potassium phosphate buffer solution (KPBS) containing KH_2PO_4 (3.57 mM),K_2HPO_4 (anhydrous; 16.43 mM), and NaCl (15.4 mM), and dehydrated in 25% sucrose for 48-72 hrs. Slices were then incubated in SA conjugated Alexa 555 (Molecular Probes), 2% normal goat serum (Rockland), and 0.3% triton X-100 (Sigma St. Louis, MO) for 2 hrs. After washout with KPBS slices were mounted on slides with Prolong Gold antifade reagent (Invitrogen) and imaged with an upright confocal microscope.

Drugs

All drugs and peptides were dissolved in aCSF and bath-applied to on slices with a flow rate of 2.5-3.5 ml/min. Human NPY (NPY) was purchased from Peptidec Technologies (Pierrefonds, Quebec). The receptor preferring agonists: [ahx$^{5-24}$]NPY, F^{7}P^{34}NPY, and [hPP$^{1-17}$,Ala^{31},Aib^{32}]hNPY, were made by solid-state synthesis, as described previously (El Bahh et al., 2005). In some experiments 50 μM DL-2-Amino-5-phosphopentanoic acid (APV; Tocris, Ellisville, MO), 1 mM kynurenic acid (Sigma), 100 μM picrotoxin (Sigma, St. Louis, MO), 50 μM cadmium chloride (Sigma), 5 μM nifedipine (Sigma), 5 μM ω-conotoxin-GVIA (Sigma), 10 μM D1R agonist SKF 81297 hydrobromide (Tocris), or dibutyrl cAMP (db-cAMP;10 μM; Tocris), were applied to the bath. Local application experiments were performed using borosilicate glass pipettes (1-2 MΩ) filled with aCSF, the compound of interest, and 0.5-1 μM of Alexa 594 and pressure injected on to the location of interest.

Theta-burst Pairing Protocol

EPSPs were evoked via a bipolar stimulating electrode in the MPP (1 ms square pulse, 0-50 V). The theta-burst pairing protocol (TBP) consisted of the pairing of a

medial perforant path EPSP (presynaptic) with an AP (postsynaptic; EPSP - AP; 5 msec interval). Ten trials each consisting of five EPSP - AP pairs at 100 Hz were repeated eight times at theta frequency (5 Hz). Stimulus- intensity response curves for EPSP amplitude were constructed before TBP; and stimuli set to 50 % maximum used to evoke EPSPs for the remainder of the experiment. EPSPs were recorded as an average of 5 sweeps (5 sec inter-stimulus interval) every minute. All DGCs were in the inner or middle GCL.

Statistical Analysis

All values presented are means ± s.e.m unless otherwise indicated, with "n" being the number of neurons analyzed. For comparisons of group values, Student's paired or unpaired t-tests were used with alpha values of 0.05. One-sample t-tests were used to compare column means with the hypothetical value of 0 or 100. We used multiple t-tests and not an ANOVA because of the small sample sizes and because we were *a priori* interested in particular comparisons and did not conduct all possible pairwise comparisons. Pearson correlations were calculated with two-tailed P values. All statistics were calculated with GraphPad Prism 4 software.

Human Slices

Human hippocampal slices were prepared from biopsies obtained during surgical resection from 10 female patients (35-62 years old) and one male patient (36 years old) with medically-intractable temporal lobe epilepsy, under a protocol approved by the Health Research Ethics Board of the University of Alberta. Transverse slices containing the hippocampus were cut at 350-400 μM within 5 mins of tissue biopsy in a room adjacent the operating room. All other procedures were the same as in experiments with rat tissue.

RESULTS

To investigate the impact of high frequency input to the dentate gyrus, we stimulated the medial perforant path with trains of 4 sub-threshold EPSPs while recording whole-cell membrane potential from DGCs (Fig. 2.1A). As the frequency was increased from 20-150 Hz (10 Hz increments) the synaptic response was routinely observed to be non-linear at upper frequencies (Fig. 2.1B). We hypothesized that this was due to an increased influx of postsynaptic Ca^{2+} through VDCCs and/or NMDA receptors in the soma and/or dendrites of the DGCs. NPY fibers from hilar interneurons form a dense projection to the outer 2/3rds of the dentate gyrus molecular layer, where they innervate dendrites of DGCs whose membranes express high levels of NPY1 receptors (Kopp et al, 2002), however, their physiological role in the dentate gyrus is unknown (Sperk et al., 2007). Therefore, NPY which is known to inhibit only N-type VDCCs, acting completely postsynaptically in the dentate gyrus (Klapstein and Colmers, 1993; McQuiston et al., 1996) was applied. To block $GABA_A$ receptors and decrease activation of NMDA receptors, we tested it in the presence of picrotoxin (100 μM) and elevated Mg^{2+} (to 5 mM), respectively. NPY (1 μM) significantly decreased the non-linear response in the presence of picrotoxin and enhanced Mg^{2+} (Fig. 2.1C).

Next, we tested whether we could potentiate the non-linear response with another endogenous compound. Dopamine fibers from the VTA carry reward-based information (Lisman and Grace, 2005) to the dentate gyrus (Leranth and Hajszan, 2007), which is important in place memory formation (Jung and McNaughton, 1993). Because DGCs are known to have D1Rs, (Mansour et al., 1992), we tested whether D1R activation would affect the frequency-dependent response. The D1-receptor agonist SKF 81297 (10 μM) enhanced the synaptic nonlinearity in these cells (Fig. 2.1D). These results indicate that

Figure 2.1. Frequency-Dependence of Synaptic Activity.

(A) Recording configuration of a neurobiotin filled DGC with a somatic whole-cell recording and stimulation electrode in the medial perforant pathway (MPP). (B) Nonlinear summation with increasing frequency of normalized responses to synaptic trains in DGC neurons. The time-voltage integral of the entire synaptic train was divided by the time-voltage integral of the first EPSP in the train to give the integral normalized to the first EPSP (●). The black line represents a linear relationship of frequency and synaptic response. (n = 10). (inset) Sample recording at 120 Hz in control conditions. (C) DGC synaptic responses to higher frequency stimulus trains are sensitive to NPY. The time-voltage integral of the entire synaptic train was normalized to the first EPSP as in B. Picrotoxin (PTX; 100 μM) and increased (5 mM) Mg^{2+} (●) were used to isolate glutamatergic synaptic responses by blocking $GABA_A$ receptors and reducing NMDA receptor conductance to prevent epileptiform activity in dentate gyrus. NPY (1 μM) application is shown in red (■). (inset) 120 Hz traces in PTX and elevated Mg^{2+} (black) and with the addition of NPY (1 μM; red). (n = 9). *P<0.05, (paired t-test). (D) D1 agonist (SKF 81297; 10 μM; orange ■) was applied under control conditions similar to (B). (inset) 150 Hz traces in control conditions (black) and with the addition of SKF (10 μM; orange). (n = 6). *P<0.05, (paired t-test).

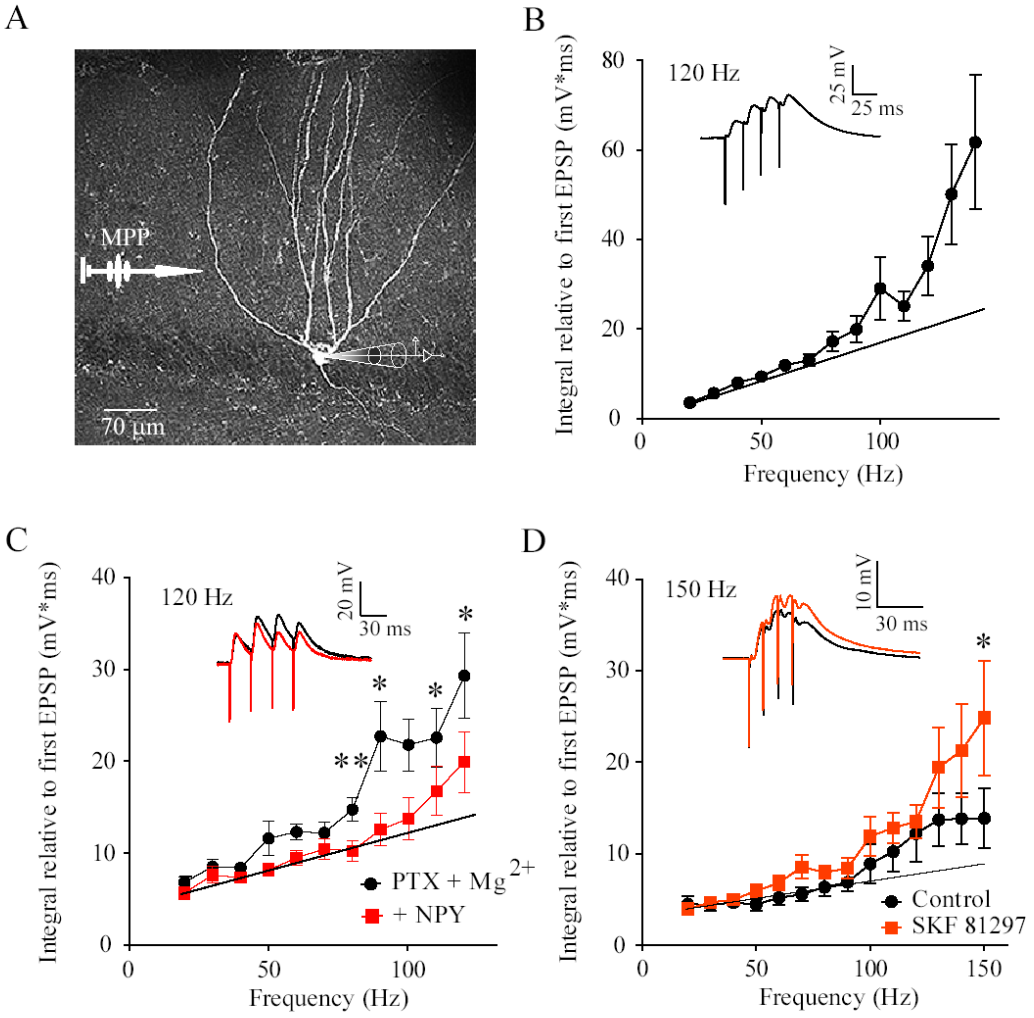
A
MPP
70 µm
B
120 Hz
25 mV
25 ms
Integral relative to first EPSP (mV*ms)
Frequency (Hz)
C
120 Hz
20 mV
30 ms
PTX + Mg 2+
+ NPY
Integral relative to first EPSP (mV*ms)
Frequency (Hz)
D
150 Hz
10 mV
30 ms
Control
SKF 81297
Integral relative to first EPSP (mV*ms)
Frequency (Hz)

this specialized response to high frequency input involves activation of postsynaptic VDCCs and is subject to modulation by local chemical messengers.

Frequency-Dependent Activity in Distal Dendrites

In many mammalian neurons, APs propagate backward from the initial segment into their dendritic tree (Stuart et al., 1997; Waters et al., 2005). As mentioned earlier, backpropagation has only been studied previously with simulations in DGCs (Vetter et al., 2001) because of the inherent difficulty in performing recordings on the fine distal dendrites. To examine dendritic consequences of high-frequency postsynaptic activity in DGCs, we next emulated bursting behaviour with trains of 4 somatic APs (40-150 Hz) in DGCs filled via the patch pipette with the Ca^{2+} indicator dye, OGB-1. First, we compared 5 ROIs along a granule cell dendrite (Fig. 2.2A), and normalized the Ca^{2+} transient to $\Delta F/F$ measurements obtained following a subthreshold (40 Hz) train of APs in each ROI. Normalized Ca^{2+} transients did not increase with AP frequency in the most proximal dendritic compartments, but more distal ROIs did exhibit frequency-dependent increases (Fig. 2.2B,C). In all cells tested (n=3), the most distal ROI had the largest relative increase in Ca^{2+} transient with a high frequency stimulus (150 Hz). Although the absolute rise in fluorescence was much smaller in distal ROIs than in proximal ROIs the distal ROIs showed an increased relative sensitivity to high frequency stimulation (Fig. 2.2B,C). Measurement of the integral of somatic depolarization after the 4^{th} action potential, a well-validated method of quantifying regenerative dendritic activity in neocortical pyramidal neurons (Larkum et al., 1999b), showed only a small but non-significant increase across all frequencies in the same DGCs (Fig. 2.2D).

Figure 2.2. Electrical Compartmentalization of Dentate Granule Cell Dendrites.
(A) Fluorescence image of a dendrite filled with OGB-1 (100 μM) via recording pipette. (x) is 44 μm from the soma. Colours correspond to (C) Scale bar, 20 μm. (B) Ca^{2+} influx measured as ΔF/F at 5 ROIs on the dendrite after trains of bAPs that correspond to those in (A). (C) Ca^{2+} rise normalized to 40 Hz measurements and compared to frequencies up to 150 Hz. (n = 3). *P<0.05, RO1 1 compared to ROI 5, (paired t-test). (D) Normalized integral of the 4^{th} action potential recorded at the soma. Normalized to 40 Hz measurements in the same DGCs as (C) and compared to frequencies up to 150 Hz.

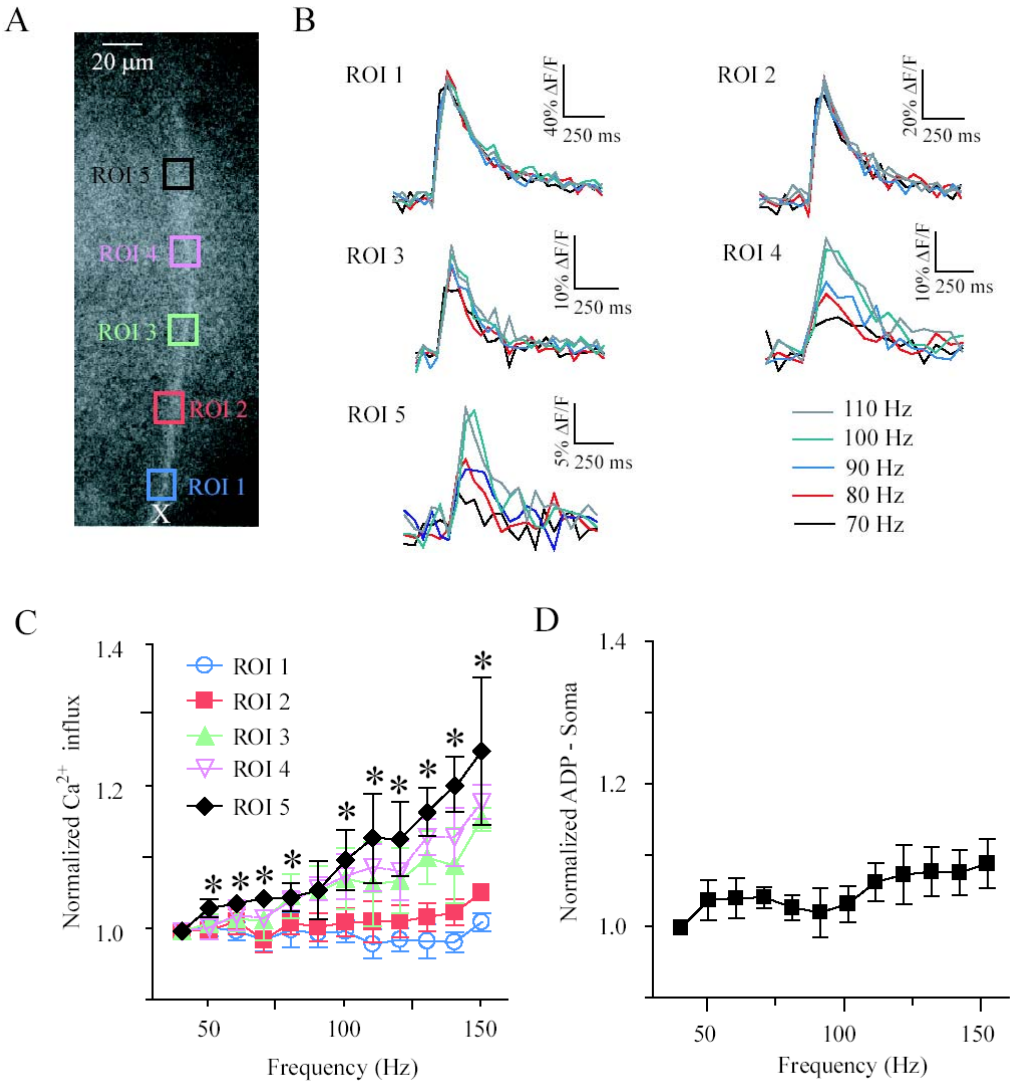
A
20 µm
ROI 5
ROI 4
ROI 3
ROI 2
ROI 1
X
B
ROI 1
40% ΔF/F
250 ms
ROI 2
20% ΔF/F
250 ms
ROI 3
10% ΔF/F
250 ms
ROI 4
10% ΔF/F
250 ms
ROI 5
5% ΔF/F
250 ms
110 Hz
100 Hz
90 Hz
80 Hz
70 Hz
C
Normalized Ca2+ influx
1.4
1.2
1.0
ROI 1
ROI 2
ROI 3
ROI 4
ROI 5
50
100
150
Frequency (Hz)
D
Normalized ADP - Soma
1.4
1.2
1.0
50
100
150
Frequency (Hz)

4-AP Sensitive K^+ Channels Prevent Soma-Dendrite Coupling

It was next hypothesized that the efficiency of coupling between the distal dendrite and the soma could be reduced by conductances from ongoing dendritic synaptic input (Staley and Mody, 1992) or by a subset of K^+ channels. Because A- and D-type potassium channels have been shown to modulate dendritic excitability in the hippocampus and neocortex (Golding et al., 1999; Kampa and Stuart, 2006; Metz et al., 2007), we added a modest concentration of 4-aminopyridine (4-AP; 100 μM) in addition to a cocktail of antagonists, including picrotoxin (100 μM), APV (50 μM), kynurenic acid (1 mM), and elevated Mg^{2+} (5 mM) to block GABAergic and glutamatergic synaptic currents, respectively. Under these conditions, trains of bAPs above a CF (Larkum et al., 1999b) evoked supralinear Ca^{2+} transients at a distance >175 μm from the soma, coincident with the appearance of a large somatic ADP (Fig. 2.3A,B). We calculated the CF by determining the frequency at half-maximal amplitude of the relationship between AP frequency and either the time-voltage integral of the 4^{th} action potential (ADP) or the amplitude of the dendritic Ca^{2+} transient (Larkum et al., 1999b; Larkum et al., 2007). Comparisons of mean CFs determined from distal dendritic Ca^{2+} signals and those determined from ADP magnitudes measured in DGC somata revealed no significant difference in these compartments (dendrite: 121 ± 8 Hz, soma: 128 ± 9 Hz; n=10, $P<0.09$); these two frequencies were also strongly correlated in individual neurons (Fig. 2.3C; $r^2=0.8258$, $P<0.0001$). Thus, in the presence of 4-AP, trains of bAPs at supracritical frequencies induce a distal dendritic Ca^{2+} influx that is tightly coupled to the somatic ADP.

We next asked whether the synaptic blockers helped prolong the ADP and support the appearance of a CF. Fig. 2.3D,E illustrate that no increase of ADP was seen in the presence of the synaptic blockers unless 4-AP (100 μM) was also present in the extracellular solution. In the presence of 4-AP, robust, frequency-dependent ADPs were

Figure 2.3. 4-AP Unmasks Frequency-Dependent Afterdepolarizations.

(A) Recording configuration of a neurobiotin-filled, mature DGC. Rectangle represents a typical ROI for calcium imaging experiments. Scale bar, 70 μm. (B) Dendritic Ca^{2+} transients recorded at a minimum of 150 μm from the soma (above) in the presence of 4-AP (100 μM) and synaptic blockers (Syn Blk; picrotoxin, 100 μM; APV, 50 μM; kynurenic acid, 100 μM; and increased Mg^{2+}, to 5 mM) become supracritical at the same frequencies as the 4th action potential ADP (120 Hz; below). (C) Correlation of dendrite and soma CFs recorded simultaneously from the same DGCs (n=12). r^2=0.8258, P<0.0001, --- 95% confidence intervals (linear regression). (D) Trains of APs at 80 Hz (i. and ii.) and 90 Hz (iii. and iv.) evoked in a DGC with somatic current pulses (1 ms) with synaptic transmission blocked (Syn Blk; i. and iii.). Shaded grey areas represent the voltage-time integral of the 4th action potential ADP. (E) Integral increases sharply with frequency in the presence of 4-AP (100 μM), in addition to synaptic blockers listed in B (n=16). *P <0.05, ***P <0.001, Syn Blk compared to + 4-AP, (paired t-test). (F) Distribution of CFs in the presence of 100 μM 4-AP, n=138.

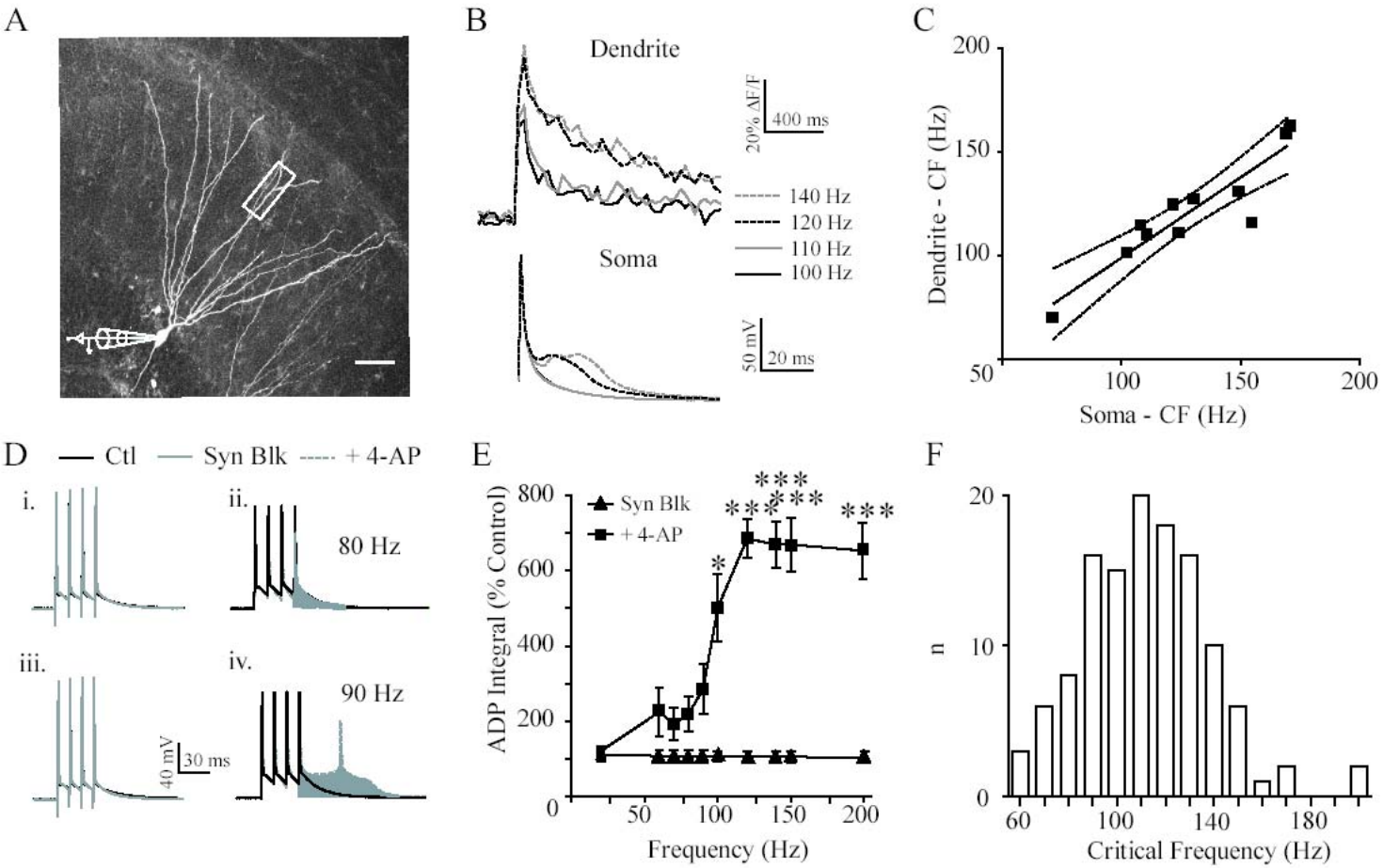
A
B
Dendrite
20% ΔF/F
400 ms
140 Hz
120 Hz
110 Hz
100 Hz
Soma
50 mV
20 ms
C
Dendrite - CF (Hz)
Soma - CF (Hz)
D
Ctl
Syn Blk
+ 4-AP
i.
ii.
80 Hz
iii.
iv.
90 Hz
40 mV
30 ms
E
ADP Integral (% Control)
Syn Blk
+ 4-AP
Frequency (Hz)
F
n
Critical Frequency (Hz)

seen in 91% (138 of 151) of DGCs. Above threshold, ADP magnitudes were independent of the amplitude of the current pulse, and were occasionally sufficient to trigger a somatic AP (Fig.2.3D,iv; Larkum et al., 1999b). Above the CF, the time-voltage integral of the ADP increased with frequency to an upper limit (Fig. 2.3E), although in a few neurons we observed the failure of ADPs at very high frequencies (≥ 200 Hz). Critical frequencies were distributed in a Gaussian manner and varied from 60-200 Hz (Fig. 2.3F; mean: 109 ± 3 Hz, n=138). 4-AP also induced complex spikes during long current injections (Appendix Figure 1). Taken together, these results suggest that 4-AP can increase intrinsic DGC excitability and facilitate large somatic ADPs above a CF of somatic bAPs.

A-type K^+ Channels Likely Mediate Soma-Dendrite Coupling

Next, we sought to identify the potassium channels that govern the frequency-dependent somato-dendritic coupling in DGC dendrites. First, we tested the D-type blocker α-dendrotoxin (DTX; Kv1.1, 1.2, 1.6; Alexander et al., 2008) and found significant but very modest effects with a high dose (500 nM; Fig.2.4A,B), that were however not frequency-dependent. Second, we tested TEA (Kv1.x, Kv2.x, Kv3.x, KCa1.1; Alexander et al., 2008) and saw very modest effects that were not frequency-dependent at concentrations up to 1 mM (Fig 2.4C) and effects equivalent to 100 μM 4-AP at 3 mM TEA (Fig.2.4D,E). We also found no significant effects of apamin (KCa2.1 and 2.3; Alexander et al., 2008; Fig 2.4F), charybdotoxin (KCa3.1 Alexander et al., 2008; Fig. 2.4G), or paxilline (KCa 1.1, "Maxi-K"; Alexander et al., 2008; Fig 2.4H), all with 0 mM EGTA in the intracellular solution (Appendix Figure 2), ruling out K_{Ca} channels. A number of reports confirm the presence of A-type channels in DGCs (Serôdio et al, 1998; Rüschenschmidt et al., 2006). Thus, it is likely that the effect of 4-AP is on a Kv1.4, or Kv 4.2, but not Kv1.1-3 or 1.6 because of a lack of effect from low doses of TEA (up to 1

Figure 2.4. **A-type K^+ Channels Likely Mediate Soma-Dendrite Coupling.**
(A) Trains of square pulse current injections at the soma at 150 Hz in the presence of a cocktail of antagonists (Syn Blk) containing picrotoxin (100 µM), APV (50 µM), kynurenic acid (1 mM), and elevated Mg^{2+} (to 5 mM). α-dendrotoxin (DTX; 500 nM) was applied via the bath. (B) Somatic APs were evoked (as in A) from 50-200 Hz in the presence of the PTX solution (●). DTX (■) increases the ADP integral at all lower and some higher frequencies compared to the PTX solution and had no CF (n=5). * P<0.05, **P<0.01 (paired t-test). (C) Tetraethylammonium (TEA; ■; 1 mM)) increases the ADP integral at all lower frequencies compared to PTX solution (●) and had no CF (n=6). * P<0.05, **P<0.01 (paired t-test). (D) Trains of square pulse current injections at the soma at 150 Hz in the presence of the PTX solution. TEA (3 mM) was applied via the bath and unmasked a robust ADP. (E) High concentrations of TEA (■; 3 mM) increased the ADP compared to PTX solution and unmasked a CF in all cells tested (n=7). * P<0.05, **P<0.01, ***P<.001 (paired t-test). (F) Apamin (■; 1 µM) has no effect on the ADP across all frequencies tested (50-150 Hz; n=8). (G) Paxilline (■; 5 µM) has no effect on the ADP across all frequencies tested (50-150 Hz; n=8). (H) Charybdotoxin (■; 50 nM) has no effect on the ADP across all frequencies tested (50-150 Hz; n=5).

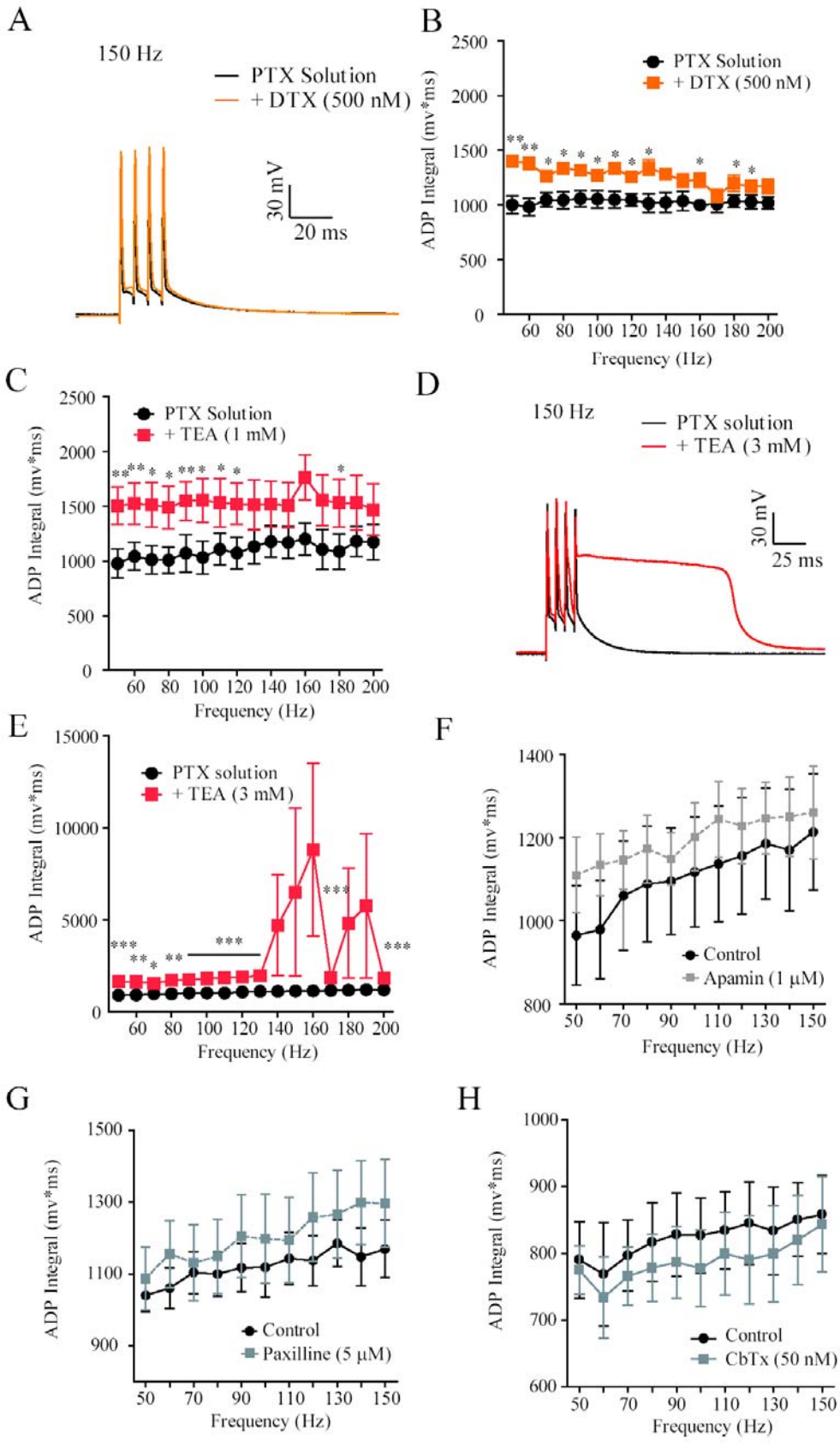
A
150 Hz
PTX Solution
+ DTX (500 nM)
30 mV
20 ms
B
PTX Solution
+ DTX (500 nM)
ADP Integral (mv*ms)
Frequency (Hz)
C
PTX Solution
+ TEA (1 mM)
ADP Integral (mv*ms)
Frequency (Hz)
D
150 Hz
PTX solution
+ TEA (3 mM)
30 mV
25 ms
E
PTX solution
+ TEA (3 mM)
ADP Integral (mv*ms)
Frequency (Hz)
F
Control
Apamin (1 µM)
ADP Integral (mv*ms)
Frequency (Hz)
G
Control
Paxilline (5 µM)
ADP Integral (mv*ms)
Frequency (Hz)
H
Control
CbTx (50 nM)
ADP Integral (mv*ms)
Frequency (Hz)

mM) and non-significant effects of high doses of α-dendrotoxin.

Critical Frequency Increases with Dentate Granule Cell Maturity

Because there is an ongoing recruitment of new DGCs from the subgranular zone into mature dentate gyrus, and young DGCs differ from mature ones in their excitability (Schmidt-Heiber et al., 2004), we examined whether the CFs varied with DGC maturity. First, we compared the input resistance (IR) of neurons in three visually-defined regions of the granule cell layer (GCL): the inner third (adjacent to the hilus), middle third, and outer third (adjacent to the molecular layer, Fig. 2.5A). Although previous studies classified subpopulations of granule cells as 'mature' (IR between 0.1-1 GΩ), and 'young' (IR between 1-10 GΩ; Schmidt-Heiber et al., 2004), our studies focused on cells within the GCL and not in the subgranular zone. We rarely saw a neuron with an IR greater than 1 GΩ, indicating the population we studied was primarily 'mature.' Nevertheless, even within this population of 'mature' neurons within the GCL, IR decreased significantly in DGCs with somata in the outer third vs. the inner third (Fig. 2.5B; outer: 225.6 ± 9.9 MΩ, n = 68; middle: 297.4 ± 11.8 MΩ, n = 117; inner: 463.5 ± 39.5 MΩ, n = 58; all $P < 0.0001$). This is consistent with the postulated maturation of DGCs in a gradient from the inner to outer GCL (Piatti et al., 2006). When we compared the CFs in the three regions of the GCL (in the presence of 4-AP), the outermost granule cells had a significantly higher CF than did DGCs in the innermost GCL (Fig. 2.5C; outer: 115.6 ± 4.7 Hz; n = 36; middle: 109.3 ± 4.0 Hz; n = 76; inner: 100.4 ± 5.1 Hz; n = 26) and there was a small, but significant correlation between input resistance and CF (Fig. 2.5D; $r^2 = 0.05$, $P=0.0092$). These data suggest a gradient of neuronal CF tuning from inner to outer GCL.

Figure 2.5. Dentate Granule Cell Critical Frequency Varies with Location in the Granule Cell Layer.

(A) A comparision of the input resistance (IR) of neurons in three visually-defined regions of the granule cell layer (GCL): the inner third (adjacent to the hilus), middle third, and outer third (adjacent to the molecular layer). Pipette indicates one neuron in the middle layer. (B) IR decreases significantly in DGCs with somata in the outer third vs. the inner third (outer: 225.6 ± 9.9 MΩ, n=68; middle: 297.4 ± 11.8 MΩ, n=117; inner: 463.5 ± 39.5 MΩ, n=58). ***P< 0.0001 (paired t-test). (C) CFs in neurons from the three regions of the GCL were compared. In the presence of 4-AP, the outermost granule cells (those with the lowest IR) had a significantly higher CF than did DGCs in the innermost GCL (outer: 116 ± 5 Hz; n = 36; middle: 109 ± 4 Hz; n = 76; inner: 100 ± 5 Hz; n = 26). *P< 0.05 (paired t-test). (D) CFs were binned by 10 Hz intervals and plotted against IR (n=127). There was a small, but significant correlation between input resistance and CF. $r^2 = 0.05$, P=0.0092 (linear regression).

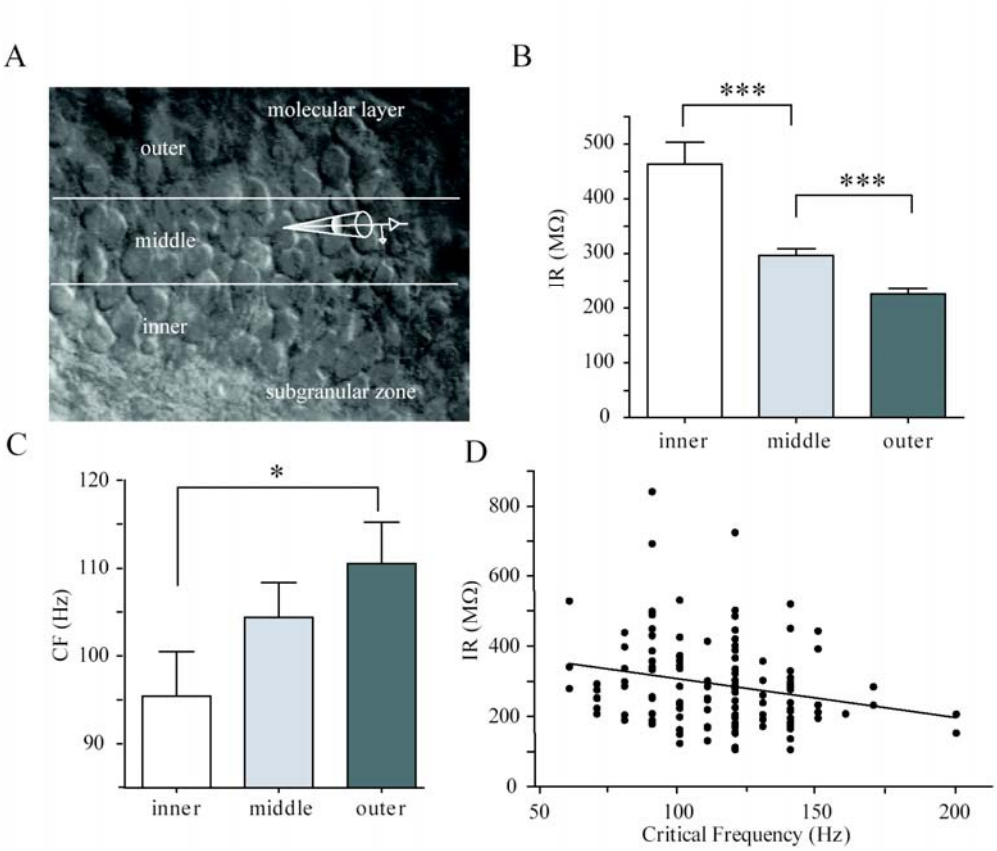
A
molecular layer
outer
middle
inner
subgranular zone
B
***
***
IR (MΩ)
500
400
300
200
100
0
inner
middle
outer
C
*
CF (Hz)
120
110
100
90
inner
middle
outer
D
IR (MΩ)
800
600
400
200
0
50
100
150
200
Critical Frequency (Hz)

Ca^{2+} Channels are Essential for the Afterdepolarization

We next investigated the mechanism underlying this nonlinear electrogenic behavior in 'mature' DGCs from the middle and outer GCLs. DGCs express N-, L-, and T-type VDCCs, (Jones et al., 1997; Schmidt-Heiber et al., 2004; Tippens et al., 2008). Blockade of VDCCs with Cd^{2+} (50 μM) virtually abolished somatic ADP responses at all frequencies tested (Fig. 2.6A,B). To determine more specifically whether N-, L-, or T-type VDCCs contribute to the ADP, we applied, respectively, either ω-conotoxin GVIA (5 μM), nifedipine (5 μM), or Ni^{2+} (50 μM) in separate experiments. To quantify the effect of these compounds, we calculated the change in CF with each treatment. Fig. 2.6C illustrates the CF change induced by nifedipine, ω-conotoxin GVIA, and Ni^{2+} (25 ± 6 Hz; n=9, $P<0.01$; 31 ± 10 Hz; n=6, $P<0.05$; 27 ± 6 Hz; n=9, $P<0.01$; respectively). We observed a significant, but incomplete, reduction of the ADP at the CF with each of the three blockers (Fig. 2.6D-F). Thus, the pronounced somatic ADP seen with 4-AP present depends on a combination of L-, N-, and T-type VDCCs, similar to that seen in L5 pyramidal neurons (Larkum et al., 1999b). The robust ADP observed at the soma requires unmasking with 4-AP, and suggests that somato-dendritic coupling is kept relatively low in DGCs by the presence of a subset of strongly 4-AP-sensitive K^+ channels, likely A-type.

Because distal Ca^{2+} responses were significantly more sensitive to bAP frequency than proximal ones (Fig. 2.2), we hypothesized that Ca^{2+} influx through VDCCs in the distal dendrites mediates the CF response in DGCs. To address this, we unmasked somatic ADPs with 4-AP as above, then applied Cd^{2+} locally to block Ca^{2+} influx at either the soma, the proximal (50-100 μm from the soma), or distal dendrites (120-250 μm from the soma). aCSF containing Cd^{2+} (100 μM) and Alexa 594 (500 nM) was pressure-ejected under visual guidance from an applicator pipette onto DGCs also loaded with Alexa 594 (5 μM; Fig. 2.7A). We first applied Cd^{2+} at the soma,

Figure 2.6 Critical Frequencies are Shifted by Voltage-Dependent Ca^{2+} Channel Blockers.

(A) Cadmium (Cd^{2+}; 50 μM) did not affect the 4th action potential voltage-time integral below the CF (80 Hz), inhibits the ADP above the CF (150 Hz), and washes out in the presence of 4-AP (Wash). (B) Cd^{2+} significantly inhibits the ADP across all supracritical frequencies (n=12) and washes out (n=4) in the presence of 4-AP (Wash). ***P<0.005, 4-AP compared to + Cd^{2+}, (paired t-test). (C) Mean change in CF (Δ CF) for nifedipine (5 μM; 25 ± 6 Hz; n=9), CgTx (5 μM; 31 ± 10 Hz; n=6), and nickel (50 μM; 27 ± 6 Hz; n=9). *P<0.05, **P<0.01, difference from 0, (one sample t test). (D) Nifedipine (5 μM) significantly reduces the ADP integral at, and above, the CF with 4-AP (100 μM) present. *P<0.05, **P<0.01, ***P<0.005, 4-AP compared to + Nif, (paired t-test). (E) ω-conotoxin GVIA (CgTx; 5 μM) significantly reduces the ADP integral at, and above, the CF with 4-AP (100 μM) present. *P<0.05, **P<0.01, 4-AP compared to + CgTx, (paired t-test). (F) Nickel (50 μM) significantly reduces the ADP integral at, and above, the CF with 4-AP (100 μM) present. **P<0.01, 4-AP compared to + Ni^{2+}, (paired t-test).

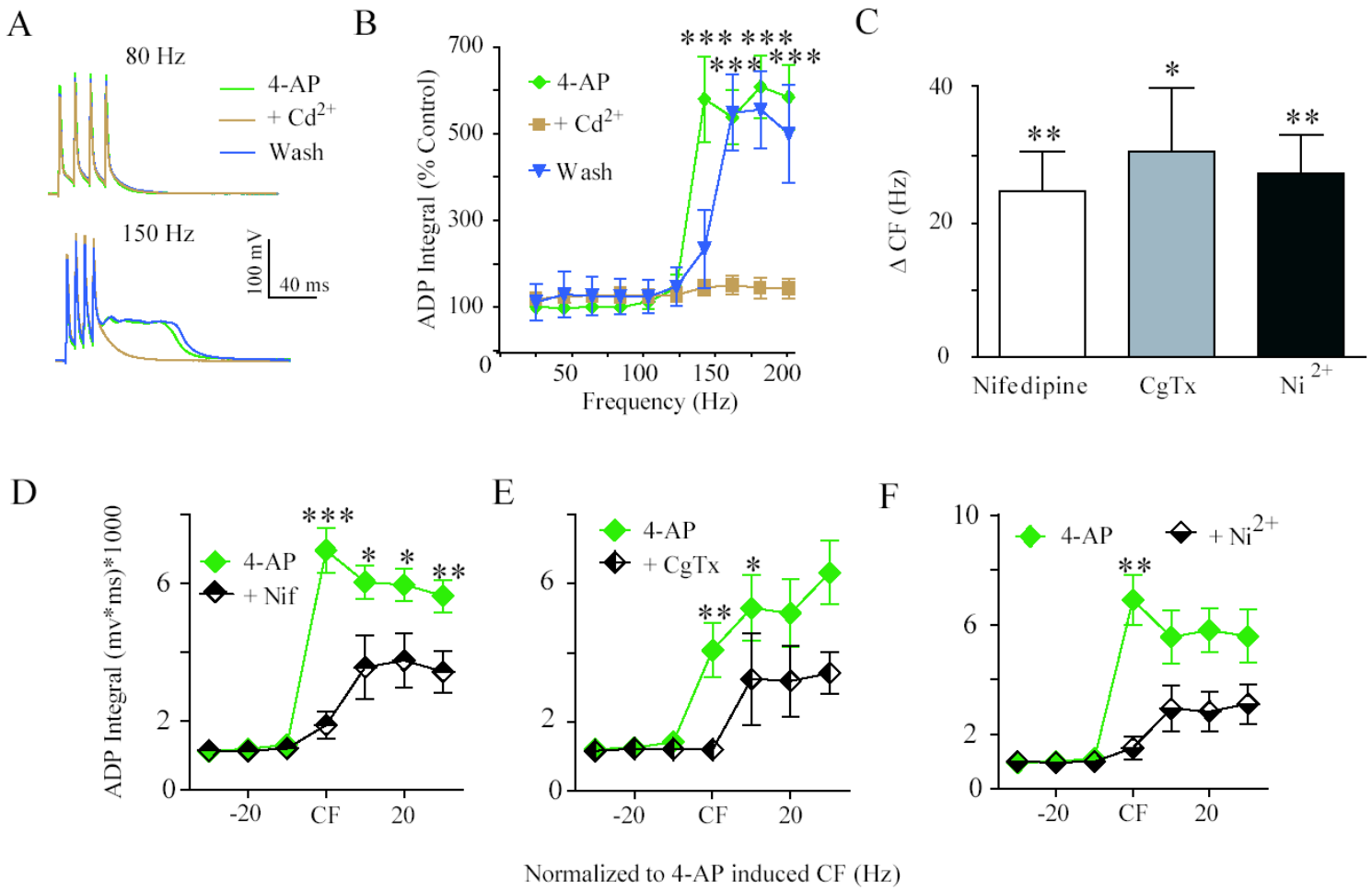
A
80 Hz
4-AP
+ Cd2+
Wash
150 Hz
100 mV
40 ms
B
ADP Integral (% Control)
700
500
300
100
0
4-AP
+ Cd2+
Wash
50
100
150
200
Frequency (Hz)
C
Δ CF (Hz)
40
20
0
Nifedipine
CgTx
Ni 2+
D
ADP Integral (mv*ms)*1000
6
2
0
4-AP
+ Nif
-20
CF
20
E
4-AP
+ CgTx
F
10
4-AP
+ Ni2+
Normalized to 4-AP induced CF (Hz)

Figure 2.7. Distal Ca^{2+} Currents Mediate the Critical Frequency.

(A) DGCs were filled with Alexa 594 (5 μM), somatic CFs were recorded in the presence of 4-AP and synaptic blockers, and Cd^{2+} (100 μM) was applied locally from a puffer pipette also containing Alexa 594 (500 nM). (B) Plot of ADP integral in a single DGC as a function of frequency. The Sigmoidal fit was used to determine the CF (shown) for responses in 4-AP (Ctl, black), and with subsequent local applications of Cd^{2+} to the soma (red), proximal (Prox, grey) and distal dendrites (orange). (C) Change in CF after local Cd^{2+} application to the soma (-5 Hz ± 2; n=9) proximal dendrite (7 ± 5 Hz; n=5), distal dendrite (19 ± 4 Hz; n=8), and during washout after distal application in the presence of 4-AP (3 ± 4 Hz; n=7). *$P<0.05$, difference from 0, (one sample t test).

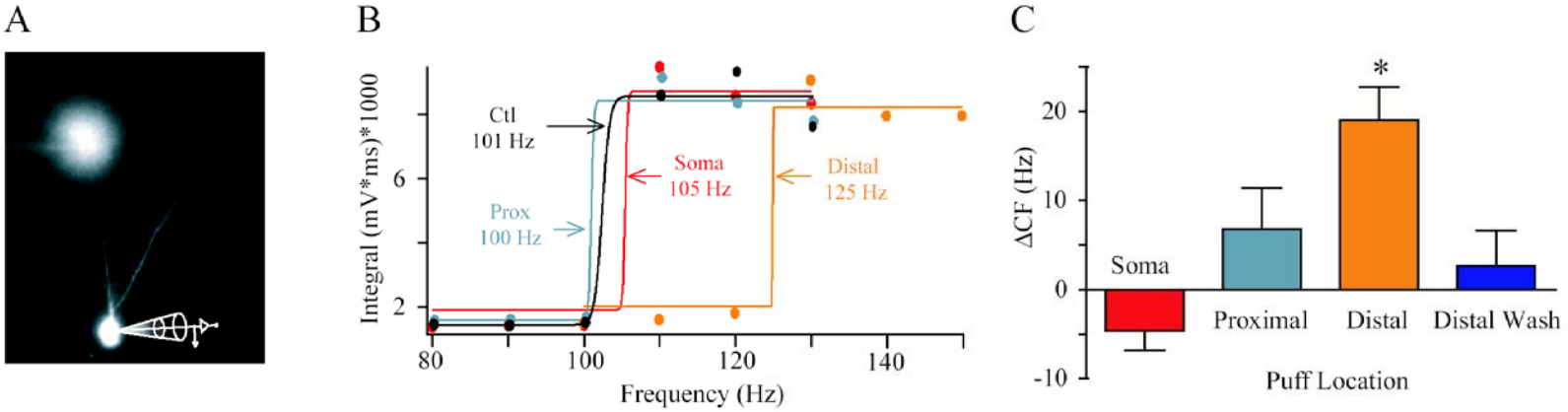
A
B
C
Integral (mV*ms)*1000
6
2
80
100
120
140
Frequency (Hz)
Ctl
101 Hz
Prox
100 Hz
Soma
105 Hz
Distal
125 Hz
ΔCF (Hz)
20
10
0
-10
*
Soma
Proximal
Distal
Distal Wash
Puff Location

then at the proximal dendrite (in some DGCs), and finally at a distal dendritic locus. Cd^{2+} only inhibited the ADP and altered the CF when it was applied distally (Fig. 2.7B), where it resulted in a mean CF change of 19 ± 4 Hz (Fig. 2.7C; n=8; P=0.0014). This suggests that distal dendritic VDCCs can generate local, frequency-dependent, regenerative responses. In the presence of 4-AP, these appear sufficient to propagate into the soma as the ADP.

Modulation of Dendritic Ca^{2+} Electrogenesis by NPY

The Colmers laboratory has previously demonstrated that NPY inhibits N-type VDCCs in the somata and dendrites of DGCs (McQuiston et al., 1996). This led us to hypothesize that NPY will regulate bAP-induced regenerative activity by acting on VDCCs at distal dendritic sites. Using Ca^{2+}imaging as above, we simultaneously observed distal dendritic Ca^{2+} transients and somatic V_m during sweeps of bAP frequency, in the absence and presence of NPY. Without 4-AP present, bAPs resulted in modest but significant, frequency-dependent increases in Ca^{2+} influx into distal dendrites that were reduced by bath application of NPY (Fig. 2.8A). Specifically, bath- applied NPY (1 μM) reversibly decreased distal Ca^{2+} influx and increased the dendritic CF by 33 ± 5 Hz (Fig. 2.8B). In the presence of 4-AP, NPY also reduced distal dendritic Ca^{2+} influx in response to bAPs at or above the CF, while simultaneously inhibiting the ADP recorded at the soma (Fig. 2.8C). Based on this concordance, we used somatic recordings of ADP amplitudes recorded in the presence of 4-AP as a proxy for dendritic CF responses for most of the data in this section. NPY significantly, and reversibly, reduced the magnitude of the ADP for frequencies between 90 and 200 Hz in somatic recordings from 8 DGCs without Ca^{2+} imaging (Fig. 2.8D).

In rats and humans, NPY can bind to at least 4 receptor subtypes, Y1, Y2, Y4 and

Figure 2.8. NPY Inhibits the Afterdepolarization, Distal Dendrite Ca^{2+} Currents, and Shifts the Critical Frequency.

(A) One DGC filled with OGB-1 via the patch pipette and distal Ca^{2+} influx recorded as % ΔF/F. Trains of 4 bAPs (40-200 Hz; not shown) were evoked and recorded electrically as before. 70 Hz (above) and 100 Hz (below). Distal Ca^{2+} measurements demonstrate a CF but no CF was seen at the soma (control ----)**.** The amplitude of the dendritic Ca^{2+} transients decreases with NPY (----), and returns to control levels with washout in 4-AP (----). (B) Summary of experiments in 5 DGCs (without 4-AP). NPY shifts the mean CF significantly in the distal dendrites. **P<0.01, Control compared to NPY, (paired t-test). (C) In the presence of 4-AP a subcritical 90 Hz train (above) and a supracritical train 100 Hz (below) recorded simultaneously at the soma and distal dendrite (----). NPY application inhibits the distal Ca^{2+} current and somatic ADP above the CF (----) and reverses with washout in the presence of 4-AP (----). (D) NPY and receptor-preferring agonists (all at 1 μM) were bath applied after 4-AP (100 μM) unmasked BACs seen at the soma (■). NPY (▲) decreases the average integral of the 4th action potential (n=8) and reverses in 4-AP (wash, ▼; n=6). *P<0.05, **P<0.01, ***P<0.005, 4-AP compared to + NPY, (paired t-test). (E) Y1 agonist (F^7P^{34}NPY; △) decreases the average integral (n=10) like NPY in (D) and reverses with washout in 4-AP (▼; n=7). *P<0.05, **P<0.01, 4-AP compared to + Y1 agonist, (paired t-test). (F) Y2 agonist ([ahx^{5-24}]NPY; △) has no effect on the integral of the 4th action potential (n=9). After Y2 agonist application, NPY(▲) has its usual effect (n=4). *P<0.05, 4-AP compared to + NPY, (paired t-test). (G) CF change for all compounds applied in A-D and washout for NPY and Y1 agonist both in the presence of 4-AP. Y5 agonist, n=5. *P<0.05, difference from 0, (one sample t test).

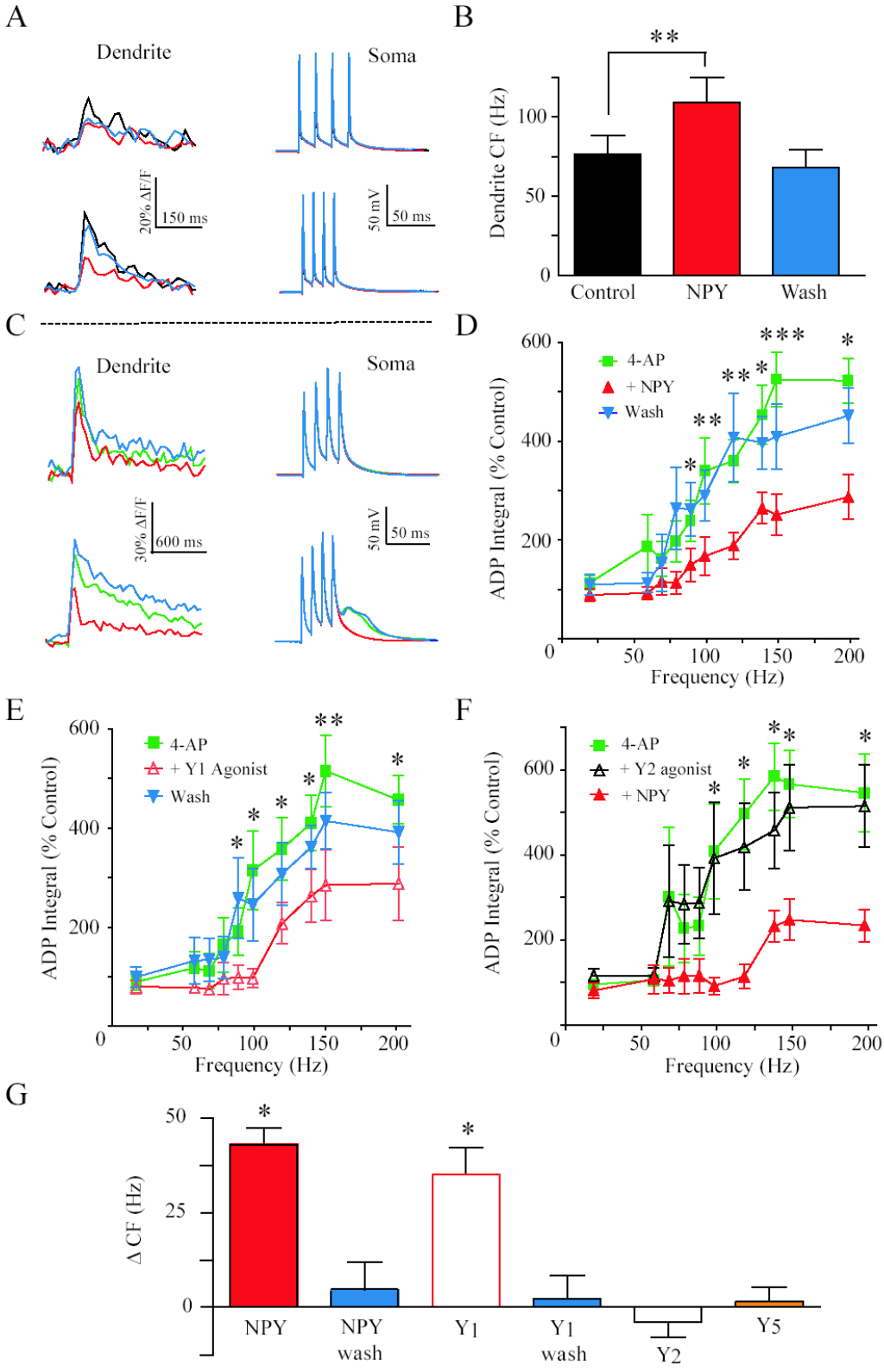
A
Dendrite
Soma
20% ΔF/F
150 ms
50 mV
50 ms
B
**
Dendrite CF (Hz)
100
50
0
Control
NPY
Wash
C
Dendrite
Soma
30% ΔF/F
600 ms
50 mV
50 ms
D
4-AP
+ NPY
Wash
ADP Integral (% Control)
600
400
200
0
50
100
150
200
Frequency (Hz)
E
4-AP
+ Y1 Agonist
Wash
ADP Integral (% Control)
Frequency (Hz)
F
4-AP
+ Y2 agonist
+ NPY
ADP Integral (% Control)
Frequency (Hz)
G
Δ CF (Hz)
50
25
0
NPY
NPY wash
Y1
Y1 wash
Y2
Y5

Y5 (Michel et al., 1998). Previous work suggested the presence of at least Y1 and Y2 receptors on DGCs (McQuiston et al, 1996). To determine which receptor subtype(s) mediate the NPY effect, we applied receptor-preferring agonists at 1 μM: F^7P^{34} [NPY] (for Y1), $ahx^{5\text{-}24}$[NPY] (for Y2), and [hPP^{1-17}, Ala^{31}, Aib^{32}]hNPY (AlaAibNPY, for Y5; El Bahh et al., 2005). The Y1 agonist significantly, and reversibly, reduced the magnitude of the ADP for frequencies between 90 and 200 Hz (Fig. 2.8E), much like the effect of NPY. When the Y2 agonist was applied there was no effect on the ADP response at any frequency studied (Fig. 2.8F). In 4 experiments, after first applying the Y2 agonist without effect on the ADP, we then applied NPY and observed an inhibition of ADP magnitude, consistent with the effect of NPY observed earlier, indicating that the cells were indeed sensitive to NPY (Fig. 2.8F). Similarly, application of the Y5 agonist had no effect on the ADP magnitude across all frequencies tested (not illustrated). In these experiments, NPY shifted the mean CF from 86 ± 5 Hz, to 128 ± 8 Hz (Fig. 2.8G; n=8; $P<0.01$) and washed out completely in 6 of 8 neurons (Fig. 2.8G). The Y1 agonist increased the average CF from 96 ± 5 to 131 ± 9 Hz (Fig. 2.8G; n=10; $P <0.001$), not significantly different from the shift caused by NPY ($P>0.36$). Neither the Y2 agonist (control: 95 ± 7 Hz, $ahx^{5\text{-}24}$: 91 ± 8 Hz; n=9; $P>0.71$), or the Y5 agonist (Control: 85 ± 10 Hz, AlaAib: 86 ± 10 Hz; n=6; $P > 0.94$) caused significant changes in CF (Fig. 2.8G). These data suggest that the NPY-mediated decrease in ADP amplitude and CF change results only from activation of the Y1R.

Modulation of Dendritic Ca^{2+} Electrogenesis by Dopamine

Although the ADP in DGCs is normally prevented from expression by dendritic K^+ channels, it is still strongly inhibited by Y1R activation. We therefore hypothesized that other neuromodulators might result in the unmasking of the ADP. Since D1 receptor activation shifted the frequency-dependent synaptic response, we tested the hypothesis

that activation of D1Rs would also unmask and/or potentiate CFs in rat DGCs. In some neurons tested in the absence of 4-AP, the D1R agonist SKF 81297 (10 μM) increased the integral of the ADP and unmasked a clear CF (Fig. 2.9A); this increase was subsequently inhibited by application of Cd^{2+} plus Ni^{2+} in all DGCs tested (Fig. 2.9A; both 50 μM; n=3). In other DGCs, SKF 81297 increased the ADP across all frequencies without inducing a clear CF. Fig. 2.9B shows the two distinct responses to SKF 81297 application: some DGCs demonstrated a CF (above; n=5), and other DGCs had no CF but showed a significantly increased ADP (below; n=9). Some DGCs tested in the presence of a low concentration of 4-AP (10 μM) did not have a CF, but application of SKF 81297 (10 μM) unmasked a robust CF, which reversed on washout of SKF 81297 (Fig. 2.9C,D). In neurons in which 4-AP (100 μM) unmasked a clear CF, SKF 81297 reversibly increased the magnitude of the ADP and decreased the CF (Fig. 2.9E,F). After the complete washout of SKF 81297 in 3 neurons, we applied NPY and observed an increase in the CF (Fig. 2.9F), showing that CFs can be shifted in both directions in the same DGC.

Because D1Rs have been shown to be positively coupled to adenylyl cyclase (Lisman and Grace, 2005), we applied the membrane-permeant cAMP analog, dibutyrl-cAMP (db-cAMP; 10 μM) in the presence of 4-AP (100 μM) and observed a CF change not significantly different from that seen with SKF 81297 (Fig. 2.9F; -23 ± 6 Hz, n=6, P = 0.974; unpaired t-test). Finally, we examined the interactions between Y1Rs and D1Rs. In 4/4 neurons with a clear CF in 4-AP (100 μM), simultaneous application of both NPY and SKF 81297 caused a significant rightward shift in CF, much like the effect of NPY alone (Fig. 2.9F). Next, to test whether NPY could suppress the increased excitability caused by dopamine, we unmasked a CF with SKF 81297 in DGCs that did not have a CF in the presence of low 4-AP (10 μM), then applied NPY in the presence of the D1R agonist. In 8 of 16 DGCs tested under these conditions, NPY significantly reduced the

Figure 2.9. D1R Agonist Increases Excitability of Dentate Granule Cell Dendrites. (A) Trains of somatic APs at 60, 110, and 120 Hz in normal saline (control, no 4-AP), after application of D1R agonist SKF 81297 (10 μM), and after Cd^{2+} plus Ni^{2+} application (each 50 μM) in the presence of SKF 81297. (B) SKF 81297 application in normal saline produced two distinct effects: The appearance of a CF (above; mean: 110 ± 13; n=5). *P<0.05, 40-70 Hz recordings compared to 100 Hz all in the presence of SKF, (paired t-test). The increase of the ADP across all frequencies (below; n=9). *P<0.05, control recording compared to SKF, (paired t-test).(C) Some DGCs did not show a CF in the presence of 10 μM 4-AP alone. However, application of SKF 81297 (10 μM) results in the reversible unmasking of a clear CF. (D) Integrals normalized to CF induced by SKF 81297 in DGCs did not show a CF with low 4-AP (10 μM) in the bath (n=4). Washout was in the presence of 4-AP. *P<0.05, 4-AP compared to + SKF (CF), (paired t-test). (E) Integrals normalized to CF induced by 4-AP. Application of SKF 81297 significantly increases the integral to the left of the CF (n=7). *P<0.05, 4-AP compared to + SKF, (paired t-test). (F**)** After 4-AP (10 or 100 μM) unmasks a CF, SKF 81297 reversibly decreases the CF by 23 ± 4 Hz (n=10) and washes out in the presence of 4-AP (n=6). NPY (1 μM) subsequently caused an increase in CF of 32 ± 6 Hz (n=3). The membrane-permeant cAMP analogue, dibutyrl-cAMP (10 μM) decreases the CF (23 ± 6 Hz; n=6) as did SKF 81297. When NPY (1 μM) and SKF 81297 (10 μM) were co-applied, a rightward CF change results (mean: 28 ± 7 Hz; n=4). *P<0.05, difference from 0, (one sample t test). (G) Integrals normalized to CF induced by SKF 81297 (10 μM) in DGCs that did not show a CF with low 4-AP (10 μM) in the bath. The addition of NPY (1 μM) in the presence of 4-AP and SKF decreases the integral (n=8). **P<0.01, ***P<0.001, 4-AP compared to + SKF (CF), (paired t-test). †P <0.05 ††P<0.01, + SKF (CF) compared to + NPY, (paired t-test).

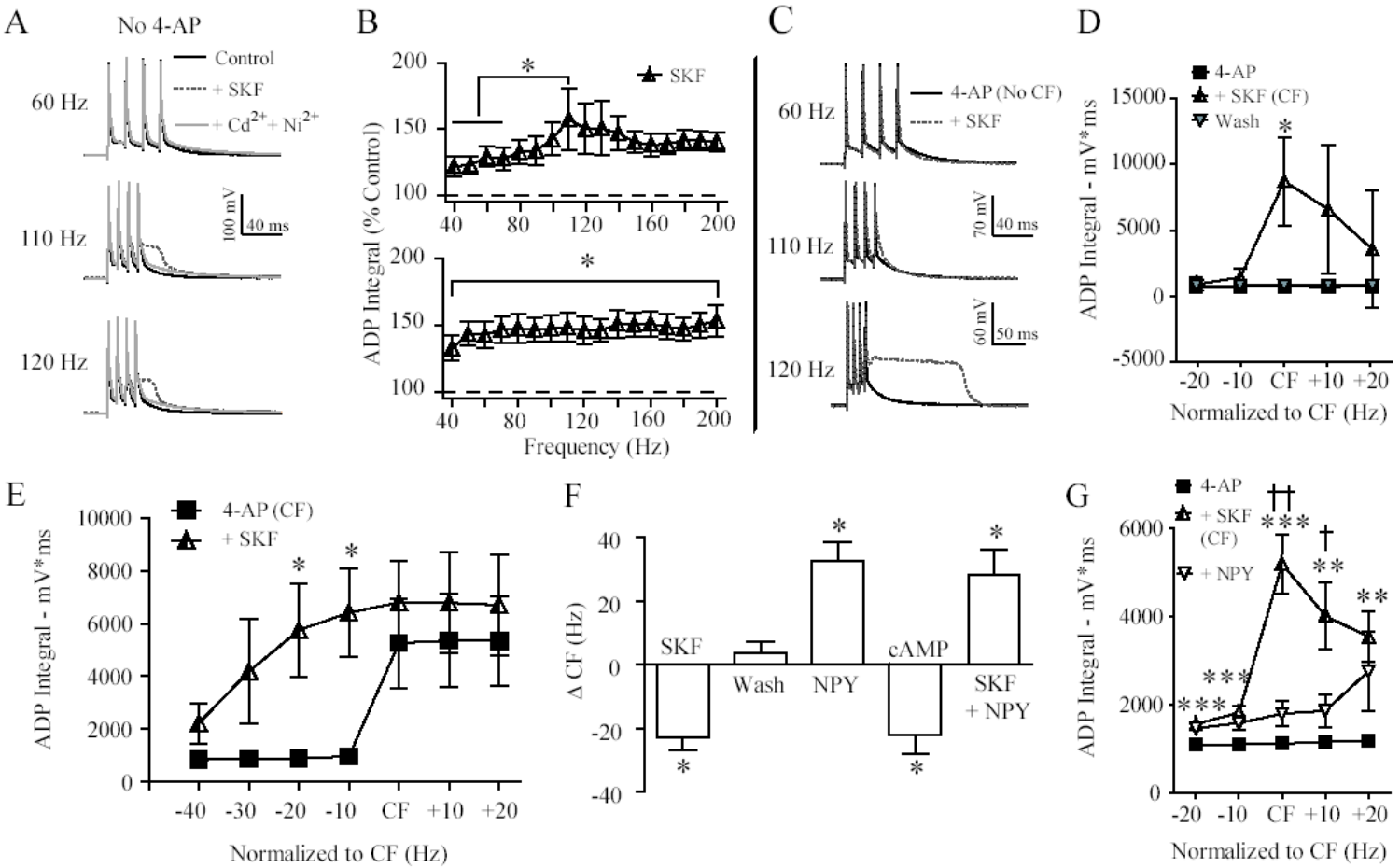
A
No 4-AP
Control
+ SKF
+ Cd2+ + Ni2+
60 Hz
110 Hz
120 Hz
100 mV
40 ms
B
SKF
ADP Integral (% Control)
Frequency (Hz)
C
4-AP (No CF)
+ SKF
60 Hz
110 Hz
120 Hz
70 mV
40 ms
60 mV
50 ms
D
4-AP
+ SKF (CF)
Wash
ADP Integral - mV*ms
Normalized to CF (Hz)
E
4-AP (CF)
+ SKF
ADP Integral - mV*ms
Normalized to CF (Hz)
F
Δ CF (Hz)
SKF
Wash
NPY
cAMP
SKF + NPY
G
4-AP
+ SKF (CF)
+ NPY
ADP Integral - mV*ms
Normalized to CF (Hz)

ADP magnitude at the CF, and 10 Hz above the CF (Fig. 2.9G).

To try to determine whether the D1 agonist is specifically inhibiting 4-AP sensitive K^+ channels, we measured the increase in the voltage-time integral of the ADP in the absence or presence of the D1 agonist in the absence of 4-AP or the presence of 3 different concentrations of 4-AP (10, 100 and 300 μM). Fig. 2.10A,B indicates the percent of the ADP in the presence of the D1 agonist that can be attributed to the D1 agonist's action. The D1 agonist causes a small but significant increase by itself in the absence of 4-AP, while it accounts for very close to 100% of the increase in the presence of both 10 and 100 μM 4-AP. Interestingly, at 300 μM 4-AP, the D1 agonist has no effect on the ADP. It also important to note that the above experiments with co-application of 4-AP and the D1 agonist were performed in the presence of APV (50 μM), and thus, the effects of the D1 agonist occur with NMDA receptors blocked. While these experiments are not conclusive, it does suggest that the effects of 4-AP and the D1 agonist do occlude one another. These findings are at least consistent with the hypothesis that the primary effect of the D1 agonist is postsynaptic and may result from an interaction with an A-type K^+ channel.

Facilitation of Long-Term Potentiation Induction by a D1 Agonist

Because the excitability of dendrites has been linked with plasticity of synaptic responses (Martin et al., 2000; Kampa et al., 2006), we postulated that the activation of D1Rs might facilitate plastic changes to DGC inputs. Previous studies have shown that the induction of LTP in immature DGCs can occur after pairing a burst of EPSPs with single APs, repeated at theta frequencies. This response is likely due to AP-enhanced, postsynaptic Ca^{2+} entry (Schmidt-Heiber et al., 2004). Since D1R activation typically increased the responsiveness to a 100 Hz train of bAPs, we tested whether a D1R agonist

Figure 2.10. 4-AP Occlusion of D1R Action.

(A) Trains of somatic APs from 50-150 Hz evoked large ADPs in the presence of a high concentration of 4-AP (300 μM). The application of D1 agonist (SKF 81297) did not change the ADP integral (n=6). (B) The percentage of the ADP integral was calculated by dividing the ADP integral in the presence of D1 agonist (SKF 81297) by the ADP integral in the concentrations of 4-AP just before D1 agonist application (0 mM was divided by control values). 0 mM 4-AP (n=6), 10 μM 4-AP (n=4), 100 μM 4-AP (n=8), 300 μM 4-AP (n=6). **P<0.01, ***P<.001 (one sample t-test, difference from 100).

A

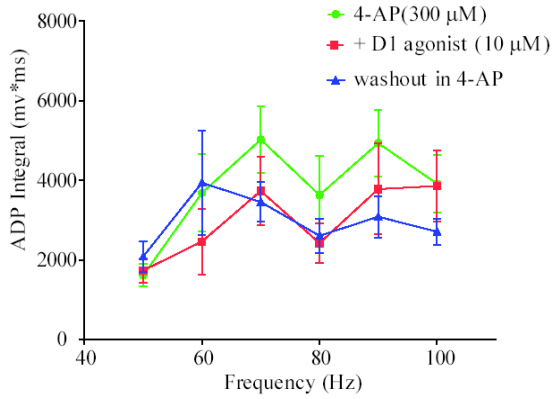
4-AP(300 µM)
+ D1 agonist (10 µM)
washout in 4-AP
ADP Integral (mv*ms)
8000
6000
4000
2000
0
40
60
80
100
Frequency (Hz)

B

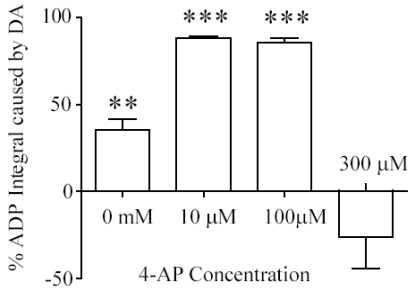
% ADP Integral caused by DA
100
50
0
-50
**
***
***
300 µM
0 mM
10 µM
100µM
4-AP Concentration

could permit LTP induction in DGCs with a theta-burst pairing protocol (TBP; Fig. 2.11A,B) at an intensity that alone was ineffective. Presynaptic stimuli were delivered focally via a saline-filled patch pipette placed in the medial perforant path (MPP), which conveys mainly spatial information (Fig. 2.11A; Ferbinteanu et al., 1999) and which innervates the middle dendritic segment mostly affected by the 4-AP sensitive K^+ channels. DGCs in the innermost GCL (IR: 523 ± 52 MΩ, n=11), were chosen because of their relatively elevated excitability (cf. Fig. 2.2). Under control conditions (i.e., in the absence of 4-AP or any synaptic blockers) we observed a small, but not significant, depression of synaptic amplitude 1 min after TBP_1 (75 ± 10% of control; n=7, P=0.0863) that returned to control values ten minutes later (110 ± 13% of control; n=7, P=0.4850). Following the addition of SKF 81297, a repetition of the identical TBP (TBP_2) resulted in a significantly larger ADP during the TBP_2 protocol (Fig. 2.11B-D), consistent with our previous findings (cf. Fig. 2.9). Ten minutes after pairing, we observed a robust enhancement of the EPSP amplitude in all DGCs tested (Fig. 2.11E; 162 ± 19% of control; n=7, P<0.0161). EPSP amplitude remained stably elevated at least 30 mins later (Fig. 2.11E, 142 ± 18% of control; n=7; P<0.0361). In similar experiments, the application of NPY (1 μM) on inner GCL neurons (456 ± 67 MΩ, n=11), caused neither enhancement nor depression of EPSP amplitude monitored up to 40 mins after TBP_2 (105 ± 10% of control; n=11, P=0.7036) indicating that NPY does not facilitate LTP induction (Fig. 2.11F), nor does it modulate perforant path neurotransmitter release under the present conditions (Klapstein and Colmers, 1993). Furthermore, LTP could not be induced either by repetition of TBP protocols or by application of the dopamine agonist alone (Fig. 2.11G,H). Finally, we tested whether blockade of postsynaptic VDCCs with NPY (Klapstein and Colmers, 1993), which had no effect on the TBP protocol (Fig. 2.11F), could inhibit dopamine-mediated LTP induction. The TBP protocol applied in

Figure 2.11. D1R Agonist Alters the Threshold for Long-Term Potentiation Induction.

(A) Representative stimulation and recording configuration of a neurobiotin filled DGC used to evoke medial perforant pathway (MPP) EPSPs recorded at the soma. (B) Sample trace during the TBP protocol involving the pairing of a burst of MPP evoked EPSPs and bAPs at 100 Hz, for 80 trials at theta (5 Hz). The ADP is increased after a subsequent TBP in the presence of bath applied D1 agonist (SKF 81297; 10 μM) in the same DGC from the inner GCL. (C) The ADP integral was calculated after the onset of the 5^{th} AP until return to baseline as previously described. Average ADP integral after TBP and TBP + D1 agonist (SKF 81297; 10 μM; n=7; *P<0.05, paired t test). (D) EPSPs recorded in control conditions, after TBP_1, and after TBP_2 in the presence of SKF 81297 (10 μM). (E) Theta-burst pairing at 100 Hz did not evoke LTP under control conditions (first ➤). However, with the application of SKF 81297 (10 μM) TBP (second ➤) results in long lasting potentiation (n=7). *P<0.05, difference from 100, (one sample t test). (F) The application of NPY (1 μM) had no effect on the EPSP after TBP (n=11). (G) After two subthreshold TBP protocols a third TBP in the presence of D1 receptor activation (SKF 81297; 10 μM) results in a long-lasting and significant increase in EPSP amplitude (n=3). All DGCs were from the inner GCL. *P<0.05, **P<0.01 (one sample t-test, difference from 100). (H) The D1 agonist was applied alone, with no TBP protocols and did not produce and change in the EPSP amplitude (n=5). (I) NPY1 agonist F^7P^{34} (1 μM) was bath applied with D1 agonist SKF 81297 (10 μM) for 5 mins before the TBP protocol (arrow). There was no change in EPSP amplitude 20 minutes after TBP. With subsequent application of SKF 81297 (10 μM), the TBP induces LTP (n=5). *P<0.05, (one sample t-test, difference from 100).

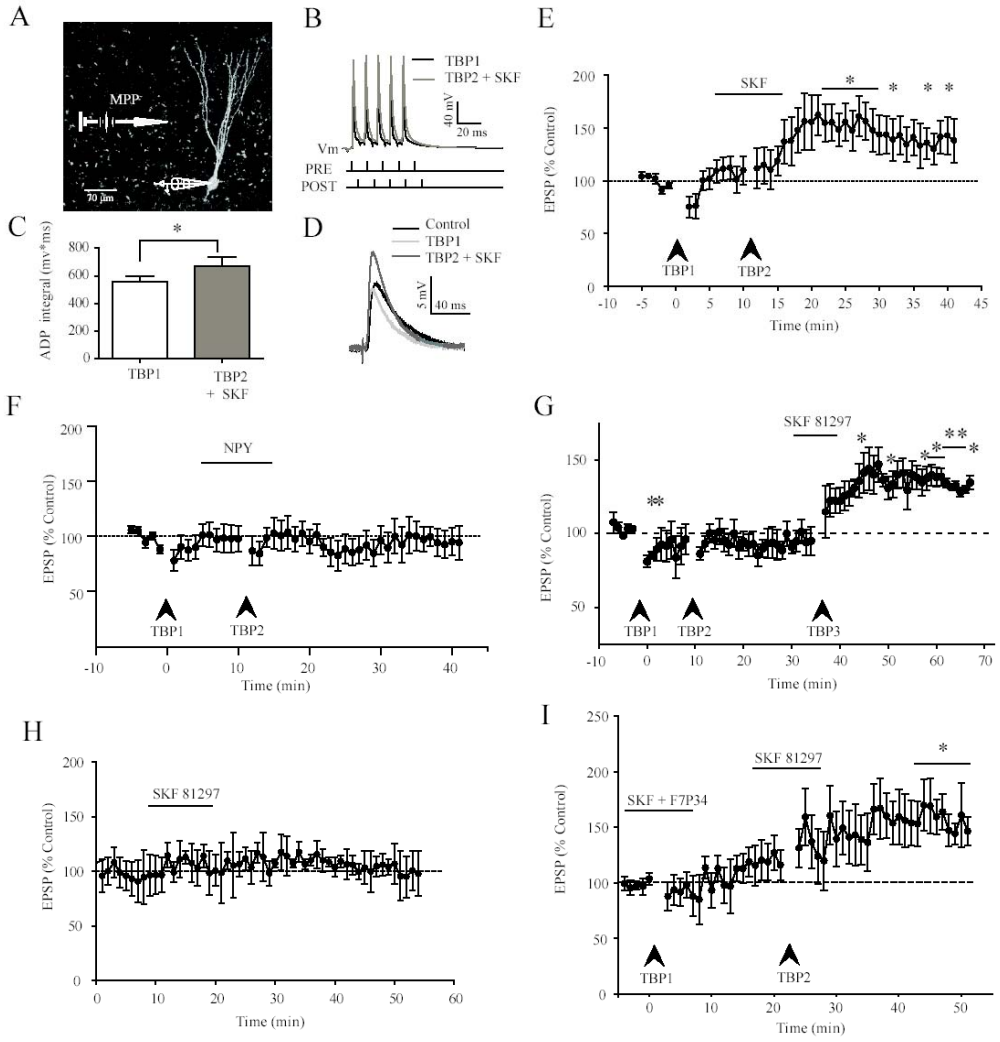
A
MPP
70 µm
B
TBP1
TBP2 + SKF
40 mV
20 ms
Vm
PRE
POST
C
ADP integral (mv*ms)
TBP1
TBP2
+ SKF
D
Control
TBP1
TBP2 + SKF
5 mV
40 ms
E
SKF
EPSP (% Control)
TBP1
TBP2
Time (min)
F
NPY
EPSP (% Control)
TBP1
TBP2
Time (min)
G
SKF 81297
EPSP (% Control)
TBP1
TBP2
TBP3
Time (min)
H
SKF 81297
EPSP (% Control)
Time (min)
I
SKF 81297
SKF + F7P34
EPSP (% Control)
TBP1
TBP2
Time (min)

the presence both of NPY and SKF 81297 resulted in no change in EPSP amplitude (Fig. 2.11I). Following washout of both compounds, we administered a second TBP in the presence of the D1 agonist alone. This resulted in robust LTP (Fig. 2.11I). Therefore, D1-receptor-mediated LTP induction in DGCs requires the untrammeled participation of postsynaptic VDCCs.

Human Dentate Granule Cells Respond to Y1R and D1R Activation

In parallel experiments, we performed whole-cell recordings from human DGCs in slices prepared from hippocampal biopsy specimens removed en-bloc from nine female and one male patient with medically-intractable, temporal lobe epilepsy (TLE; Fig. 2.12A). The average RMP of human DGCs was -68.5 ± 1.2 mV (n=19), significantly more depolarized than rat DGCs (Table 1), but similar to earlier reports of human DGCs (Dietrich et al., 1999). In these experiments, we studied dendritic properties using only somatic current clamp recordings. As in rat, human DGCs exhibited no significant somatic ADPs in control saline, and the application of 4-AP unmasked robust ADPs (Fig. 2.12B). The properties of the CF in human DGCs were qualitatively and quantitatively similar to those seen in rat. Specifically, the CF in human DGCs recorded in the presence of 100 μM 4-AP (111 ± 5 Hz; n=19) was not different from the CF of DGCs from any region of the GCL in male or female rats (Table 1). As in the rat, 50 μM Cd^{2+}completely abolished the ADP in all human neurons tested (4 of 4; Fig. 2.12C).

We next examined NPY's actions on the ADP in human DGCs in the presence of 100 μM 4-AP. Fig. 2.12C shows the ADP integral for 20-150 Hz, and, inset, the superimposed membrane potential traces of a human DGC recorded at 150 Hz under several conditions. In the presence of 4-AP, the application of 1 μM NPY caused a robust, washout-reversible change in the CF in human DGCs (23 ± 12 Hz; 6 of 7 DGCs; $P<0.05$), although this was significantly smaller than that observed in rats (42 ± 4 Hz;

Figure 2.12. D1R and Y1R Modulation of Human Dentate Granule Cells.
(A) Neurobiotin-filled image of a human DGC. Example of the density of dendritic spines (inset). Scale bar, 50 μm. Inset scale bar, 20 μm. (B) Trains of square pulse current injections at the soma at 60, 70, and 80 Hz in human DGC in the presence of 4-AP (100 μM). (C) The integral of the 4th action potential in the train recorded in control (□), then in the presence of 4-AP (100 μM; ■). Subsequently, NPY (1 μM; ▲) was applied. Following wash in 4-AP (▼), Cd^{2+} (50 μM; □). Inset - voltage traces after 150 Hz stimulation under the above conditions. (D) NPY causes a significant, reversible CF change when applied to human DGCs (n=6) similar to that seen in the rat. *P<0.05, difference from 0, (one sample t test). (E) Theta-burst pairing (TBP) at 100 Hz did not evoke LTP under control conditions (first ➤). However, with the application of SKF 81297 (10 μM) TBP (second ➤) results in long lasting potentiation (n=5). *P<0.05, **P<0.01 difference from 100, (one sample t test).

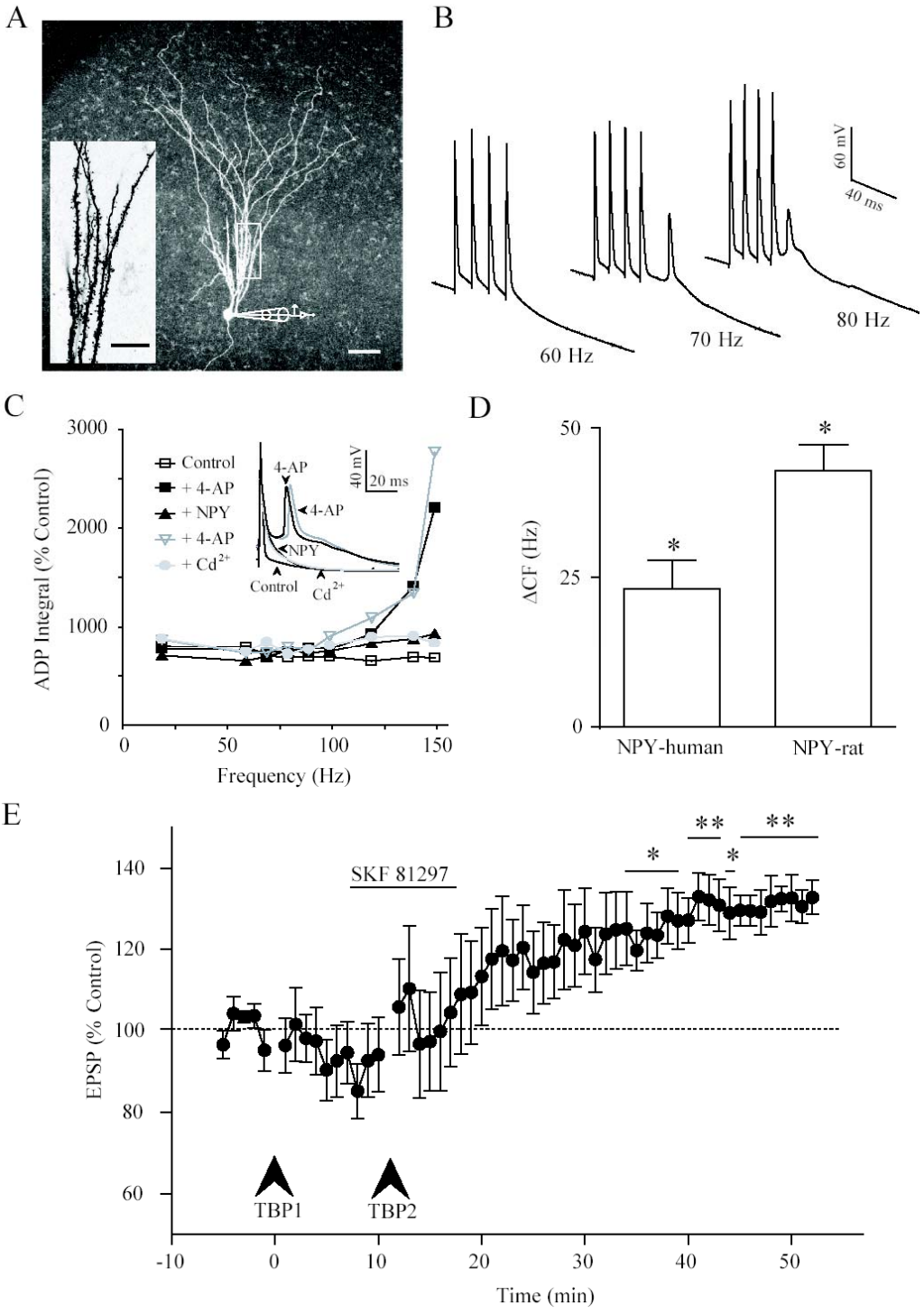
A
B
60 mV
40 ms
60 Hz
70 Hz
80 Hz
C
ADP Integral (% Control)
Frequency (Hz)
Control
+ 4-AP
+ NPY
+ 4-AP
+ Cd2+
4-AP
40 mV
20 ms
4-AP
NPY
Control
Cd2+
D
ΔCF (Hz)
NPY-human
NPY-rat
E
EPSP (% Control)
Time (min)
SKF 81297
TBP1
TBP2

Table 1. Comparison of Dentate Granule Cell Properties in Male and Female Rats and Female Humans.

Resting membrane potential (RMP), input resistance (IR), and critical frequency (CF) were quantified from male and female rat DGCs and female human DGCs. Data presented as mean ± standard error (s.e.)

	MALE RAT (n=138)		FEMALE RAT (n=16)		HUMAN FEMALE (n=18)	
	Mean	s.e.	**Mean**	s.e.	**Mean**	s.e.
RMP (mV)	-74.1	0.3	-74.7	1.2	-68.8	1.2
IR (MΩ)	316.9	12.6	297.3	29.2	283.9	28.8
CF (Hz)	109	3	97	7	111	5

Fig. 2.12D; P=0.010 vs. rat). Thus, NPY modulates bAP-induced CFs in both human and rat DGCs.

Finally, to test the hypothesis that this D1R response could also affect synaptic plasticity in human DGC, we performed TBP experiments on human DGCs in the absence and presence of the D1R agonist, focally stimulating the MPP as in the rat. Subthreshold TBP was without long-term effect, but the same protocol repeated in the same cells in the presence of 10 μM SKF 81297, resulted in a significant and sustained LTP of the synaptic response in 5 human DGCs (Fig. 2.12E).

DISCUSSION

Dentate granule cells are considered the "gatekeepers" of the hippocampal formation (Heinemann et al., 1992; Bartesaghi et al., 1995). Here we report that DGCs both from rats and from human epilepsy patients have the capacity to express frequency-dependent, backpropagation-activated Ca^{2+} responses, which are normally repressed by K^+ currents, but can be unmasked by low to moderate concentrations of 4-AP. Under physiological conditions, this dendritic Ca^{2+} electrogenesis serves to amplify high-frequency synaptic inputs, and it can be modulated in opposite directions by receptors for NPY and dopamine. In rat DGCs, dendritic Ca^{2+} electrogenesis is mediated by several types of VDCCs. Finally, D1R activation can predispose individual rat and human granule cells to the induction of LTP.

Regenerative potentials seen here in DGC dendrites are similar in their properties and frequency-dependence to those previously reported in neocortical L5 and L2/3 pyramidal neurons (Larkum et al., 1999b; Williams and Stuart, 2000; Waters et al., 2003; Larkum et al., 2007). Dendritic backpropagation and local Ca^{2+} electrogenesis are largely determined by factors including the types and densities of dendritic Na^+, K^+, and Ca^{2+} channels, and dendritic cable properties including diameter, length, and branching (Waters et al., 2005). Interestingly, despite differences in size, morphology and dendritic properties, the mean somatic CFs unmasked by 4-AP in DGCs are similar to those observed in L5, and L2/3 pyramidal neurons (109 Hz, 100 Hz and 128 Hz, for DGC, L5 and L2/3 pyramidal cells, respectively; Larkum et al., 2007), and were similar to those seen in distal DGC dendrites in the absence of 4-AP. As in L5 pyramidal neurons (Larkum et al., 1999b), the CF in DGCs depended critically on distal VDCCs, although the somato-dendritic coupling in DGCs was far more strongly regulated by 4-AP-sensitive K^+ channels as in CA1 pyramidal neurons (Golding et al., 1999; Metz et al.,

2007). Somato-dendritic coupling increases in DGCs when proximal dendritic K^+ channels are inhibited as we have shown with 4-AP and D1R agonists, and probably other neuromodulators coupled positively to adenylate cyclase. Whether the actions of dopamine or cAMP result from a reduction in 4-AP-sensitive K^+ currents, and enhancement of Ca^{2+} influx through phosphorylated VDCCs, or a combination of both actions, remains uncertain despite a number of approaches to address it. In any case, enhanced somato-dendritic coupling will permit bAPs to produce greater depolarization of distal dendrites, and when bAPs are above a CF, dendritic Ca^{2+} electrogenesis reciprocally depolarizes the soma, resulting in prolonged somatic ADPs.

Neuromodulation of dendritic excitability is a key aspect of synaptic integration (Sjöström et al., 2008). Although McQuiston et al., (1996) demonstrated that Y1Rs inhibit N-type VDCCs in DGCs, the interpretation of these results for the normal biology of the dentate gyrus was unclear. Here we have shown that NPY, by inhibiting distal Ca^{2+} influx via Y1Rs, can shift the CF of dendritic electrogenesis in DGCs at both low and high levels of somato-dendritic coupling in the rat. Also in the dentate gyrus, NPY can enhance G-protein regulated inwardly rectifying K^+ conductances (G_{IRK}) on hilar interneurons via the Y1-receptor (Paredes et al., 2003). Therefore, NPY application may enhance excitability in the dentate through an inhibition of GABAergic cells that project back to the molecular layer. However, we can rule out this possibility in our experiments for two reasons; because they were performed in the presence of $GABA_A$ antagonist, picrotoxin; and we observed an NPY-mediated decrease, not increase, in dendritic excitability. As an aside, because we applied NPY itself in our experiments with human DGCs, and did not examine the specific receptor subtypes involved, it is possible that Y2 or Y5 receptors may contribute to the modulation of the CF by NPY in humans. Most mossy fibers synapse onto dentate hilar interneurons, with a only a small percentage actually activating mossy cells and CA3 pyramids (Acsady et al., 1998). Therefore, the

mossy fiber pathway may overall mediate a net inhibition, with only a specific subset of CA3 pyramidal neurons being activated (Henze et al., 2000) Since many interneurons in the hilus express NPY (Kneisler et al., 1995), elevated mossy fiber activity is likely to enhance NPY release. Thus, in the dentate gyrus, NPY may function to dampen high levels of network activity by acting in a negative feedback manner to suppress dendritic excitability. It is intriguing to speculate that the relative levels of inhibition invoked by MF connectivity may serve to reduce background activity, making the MF input to CA3 greater by contrast.

The VTA fibers innervating the hippocampus participate in a novelty-detection system that promotes LTP and learning (Davis et al., 2004; Lisman and Grace, 2005; Sierra-Mercado et al., 2008). During exploratory behaviours, when gamma-frequencies have been observed in the dentate gyrus and DGCs fire at high rates (Bragin et al., 1995; Buzsaki, 1989; Csicsvari et al., 2003; Jung and McNaughton 1993, Leutgeb et al., 2007), the salience of a stimulus is likely to be signaled by release of dopamine from VTA projections to the molecular layer of the dentate gyrus (Gasbarri et al., 1994). Consistent with this, in mice in which NMDA receptors have been selectively knocked out in mesolimbic dopamine neurons, conditioned place preference to reward for cocaine and food is impaired (Zweifel et al, 2009, and R. Palmiter, personal communication), suggesting a loss of reward-primed spatial memory formation. Messenger RNA for D1R is expressed in DGCs, and receptor binding for D1Rs is dense on DGC dendrites (Mansour et al., 1992). Our results indicate that in the dentate gyrus, activation of D1Rs can enhance somato-dendritic coupling, increase the magnitude of the ADP, and alter DGC tuning to lower frequencies, all of which would promote elevations in dendritic $[Ca^{2+}]_i$ and thus, potentially, synaptic plasticity. Here, activation of D1Rs was also sufficient to convert previously sub-threshold trains of paired pre- and postsynaptic activity into robust, long-lasting synaptic potentiation, consistent with reports of

dopamine-mediated LTP induction in CA1 (Huang and Kandel, 1995; Li et al., 2003; Chen et al., 2007). Little is known about the downstream actions of dopamine receptors in the dentate gyrus (Leranth and Hajszan, 2007); however, in pyramidal neurons of hippocampal area CA1, dopamine can modulate dendritic excitability through downregulation of dendritic 4-AP-sensitive K^+ channels by activation of protein kinase A (PKA) or protein kinase C (PKC; Hoffman et al., 1998). D1/D5 receptor activation can also increase excitability via the above mechanism (Hoffman et al., 1999). Here, in some DGCs, D1R activation alone resulted in the unmasking of a CF (Fig. 2.9A,B), comparable to the effect of 4-AP (100 μM). However, even with 100 μM 4-AP present, we also observed a shift in the CF with SKF 81297 (Fig. 2.9F). While this concentration of 4-AP may leave some dendritic K^+ channels unblocked, this result could also arise from a D1R-mediated enhancement of dendritic VDCC activity, either via PKA activation, or directly (Kisilevsky et al., 2008). Ultimately, postsynaptic D1Rs might interact with synaptic inputs to promote branch-specific somato-dendritic coupling (Losonczy et al., 2008). Taken together, the results suggest that dopamine acting at D1Rs, can act as a novelty, or reward signal that increases the dendritic excitability DGCs and could thereby escorting important sensory based information past the inhibitory 'gate' of the dentate gyrus.

Our present findings demonstrate that most distal DGC dendrites, like those of many other neurons, are tuned to respond in a nonlinear fashion to high-frequency gamma activity. Whether this dendritic signal actually influences the DGC soma will depend on the complex interplay of dendritic voltage-dependent and receptor-mediated channels. Our results support the concept that dopaminergic afferents from the VTA can modulate long-term synaptic plasticity (Tran et al., 2008), a proxy for hippocampal memory formation (Morris et al., 2003; Whitlock et al. 2006). We have shown that, during bursting behaviour, DGC dendrites can support frequency-dependent activity that

is under regulation by endogenous neuromodulators, such as dopamine and NPY. D1R activation can likely increase dendritic excitability, either by reducing 4-AP sensitive K^+ channel activity, enhancing activity of postsynaptic VDCCs or both. The resultant increase in dendritic Ca^{2+} influx can facilitate plasticity when there is concurrent input from the MPP. Human DGCs and their inputs exhibit the same mechanism. It is thus likely that during exploration, when place cells fire a burst of APs for a labile representation, a concurrent novelty signal provided by VTA dopamine inputs can initiate plasticity and form a reward-based contextual memory (Zweifel et al, 2009). The local actions of NPY, arising from neurons downstream of the DGCs would tend to provide temporal limits to this process.

REFERENCES

Alger, B.E. and Teyler, T.J. (1976). Long-term and short-term plasticity in the CA1, CA3, and dentate regions of the rat hippocampal slice. Brain Res. *110*, 463-80.

Alexander, S.P.H., Mathie, A., Peters, J.A. (2008). Guide to Receptors and Channels (GRAC), 3rd edn. Br J Pharmacol *153* (Suppl. 2): S1–S209.

Andrásfalvy, B.K., Makara, J.K., Johnston, D. and Magee, J.C. (2008). Altered synaptic and non-synaptic properties of CA1 pyramidal neurons in Kv4.2 KO mice. J Physiol. *586*, 3881-92.

Bartesaghi, R., Gessi, T., and Migliore, M. (1995). Input-output relations in the entorhinal-hippocampal-entorhinal loop: entorhinal cortex and dentate gyrus. Hippocampus. *5*, 440-51.

Bartfai, T., Iverfeldt, K., Fisone, G. and Serfözö, P. (1998). Regulation of the release of coexisting neurotransmitters. Annu Rev Pharmacol Toxicol. *28*, 285-310.

Bliss, T.V. and Lømø , T. (1973). Long-lasting potentiation of synaptic transmission in the dentate area of the anaesthetized rabbit following stimulation of the perforant path. J Physiol. *232*, 331-356.

Brenner, R., Chen, Q.H., Vilaythong, A., Toney, G.M., Noebels, J.L., and Aldrich R.W. (2005). BK channel beta4 subunit reduces dentate gyrus excitability and protects against temporal lobe seizures. Nat Neurosci. *8*, 1752-1759.

Bragin, A. Jandó, G., Nádasdy, Z., Hetke, J., Wise, K., and Buzsáki, G. (1995). Gamma (40-100 Hz) oscillation in the hippocampus of the behaving rat. J Neurosci. *15*, 47-60.

Buzsáki, G. (1989). Two-stage model of memory trace formation: a role for "noisy" brain states. Neuroscience *31*, 551-70.

Csicsvari, J., Jamieson, B., Wise, K.D. and Buzsáki, G. (2003) Mechanisms of gamma oscillations in the hippocampus of the behaving rat. Neuron *37*, 311-322.

Davis, C.D., Jones, F.L. and Derrick, B.E. (2004). Novel environments enhance the induction and maintenance of long-term potentiation in the dentate gyrus. J Neurosci. *24*, 6497-506.

Dietrich, D., Clusmann, H., Kral, T., Steinhäuser, C., Blümcke, I., Heinemann, U., Schramm, J. (1999). Two electrophysiologically distinct types of granule cells in epileptic human hippocampus. Neuroscience *90*, 1197-1206.

Dumont, Y., Jacques, D., Bouchard, P. and Quirion, R. (1998). Species differences in the expression and distribution of the neuropeptide Y Y1, Y2, Y4, and Y5 receptors in rodents, guinea pig, and primates brains. J Comp Neurol. *402*, 372-384.

El Bahh, B., Balosso, S., Hamilton, T., Herzog, H., Beck-Sickinger, A.G., Sperk, G., Gehlert, D.R., Vezzani, A., Colmers, W.F. (2005). The anti-epileptic actions of neuropeptide Y in the hippocampus are mediated by Y and not Y receptors. Eur J Neurosci. *22*, 1417-30.

Ferbinteanu, J., Holsinger, R.M., and McDonald, R.J. (1999). Lesions of the medial or lateral perforant path have different effects on hippocampal contributions to place learning and on fear conditioning to context. Behav Brain Res. *101*, 65-84.

Gasbarri, A., Verney, C., Innocenzi, R., Campana, E. and Pacitti, C. (1994). Mesolimbic dopaminergic neurons innervating the hippocampal formation in the rat: a combined retrograde tracing and immunohistochemical study. Brain Res. *668*, 71-9.

Golding, N.L., Jung, H.Y., Mickus, T. and Spruston, N. (1999). Dendritic calcium spike initiation and repolarization are controlled by distinct potassium channel subtypes in CA1 pyramidal neurons. J Neurosci. *19*, 8789-8798.

Guo, H., Castro, P.A., Palmiter, R.D. and Baraban, S.C. (2002). Y5 receptors mediate neuropeptide Y actions at excitatory synapses in area CA3 of the mouse hippocampus. J Neurophysiol. *87*, 558-566.

Heinemann, U., Beck, H., Dreier, J.P., Ficker, E., Stabel, J., Zhang, C.L. (1992). The dentate gyrus as a regulated gate for the propagation of epileptiform activity. Epilepsy Res Suppl. *7*, 273-80.

Henze, D.A., Urban, N.N., and Barrionuevo, G. (2000). The multifarious hippocampal mossy fiber pathway: a review. Neuroscience *98*, 407-427.

Hoffman, D.A. and Johnston, D. (1998). Downregulation of transient K+ channels in dendrites of hippocampal CA1 pyramidal neurons by activation of PKA and PKC. J Neurosci. *18*, 3521-8.

Hoffman, D.A. and Johnston, D. (1999). Neuromodulation of dendritic action potentials. J Neurophysiol. *81*, 408-11.

Huang, Y.Y., and Kandel, E. R. (1995). D1/D5 receptor agonists induce a protein synthesis-dependent late potentiation in the CA1 region of the hippocampus. Proc Natl Acad Sci U S A *92*, 2446-2450.

Jones, O.T., Bernstein, G.M., Jones, E.J., Jugloff, D.G., Law, M., Wong, W., and Mills, L.R. (1997). N-Type calcium channels in the developing rat hippocampus: subunit, complex, and regional expression. J Neurosci. *17*, 6152-6164.

Jung, M.W. and McNaughton, B.L. (1993). Spatial selectivity of unit activity in the hippocampal granular layer. Hippocampus *3*, 165-182.

Kampa, B.M. and Stuart, G.J. (2006). Calcium spikes in basal dendrites of layer 5 pyramidal neurons during action potential bursts. J Neurosci. *26*, 7424-32.

Klapstein, G.J. and Colmers, W.F. (1993). On the sites of presynaptic inhibition by neuropeptide Y in rat hippocampus in vitro. Hippocampus *3*, 103-111.

Klapstein, G.J. and Colmers, W.F. (1997). Neuropeptide Y suppresses epileptiform activity in rat hippocampus in vitro. J Neurophysiol. *78*, 1651-61.

Kisilevsky, A.E. et al. (2008). D1 receptors physically interact with N-type calcium channels to regulate channel distribution and dendritic calcium entry. Neuron *58*, 557-70.

Köhler, C., Eriksson, L., Davies, S. and Chan-Palay, V. (1986). Neuropeptide Y innervation of the hippocampal region in the rat and monkey brain. J Comp Neurol. *244*, 384-400.

Kopp, J., Xu, Z.Q., Zhang, X., Pedrazzini, T., Herzog, H., Kresse, A., Wong, H., Walsh, J.H., and Hökfelt, T. (2002). Expression of the neuropeptide Y Y1 receptor in the CNS of rat and of wild-type and Y1 receptor knock-out mice. Focus on immunohistochemical localization. Neuroscience *111*, 443-532.

Kneisler, T.B. and Dingledine, R. (1995). Spontaneous and synaptic input from granule cells and the perforant path to dentate basket cells in the rat hippocampus. Hippocampus *5*, 151-164.

Kulla, A. and Manahan-Vaughan, D. (2000). Depotentiation in the dentate gyrus of freely moving rats is modulated by D1/D5 dopamine receptors. Cereb Cortex.*10*, 614-620.

Larkum, M.E., Zhu, J.J. and Sakmann, B. (1999a). A new cellular mechanism for coupling inputs arriving at different cortical layers. Nature *398*, 338-41.

Larkum, M.E., Kaiser, K.M. and Sakmann, B. (1999b). Calcium electrogenesis in distal apical dendrites of layer 5 pyramidal cells at a critical frequency of back-propagating action potentials. Proc Natl Acad Sci U S A *96*, 14600-14604.

Larkum, M.E., Waters, J., Sakmann, B. and Helmchen, F. (2007). Dendritic spikes in apical dendrites of neocortical layer 2/3 pyramidal neurons. J Neurosci. *27*, 8999-9008.

Leranth, C. and Hajszan, T. (2007). Extrinsic afferent systems to the dentate gyrus. In The Dentate gyrus: A Comprehensive Guide to Structure, Function, and Clinical Implications, H. Scharfman, ed. (Amsterdam, NL: Elsevier) pp. 63-84.

Leutgeb, J.K., Leutgeb, S., Moser, M.B., and Moser, E.I. (2007). Pattern separation in the dentate gyrus and CA3 of the hippocampus. Science *315*, 961-966.

Li, S., Cullen, W.K., Anwyl, R. and Rowan, M.J. (2003). Dopamine-dependent facilitation of LTP induction in hippocampal CA1 by exposure to spatial novelty. Nat Neurosci. *6*, 526-31.

Lisman, J.E. and Grace, A.A. (2005). The hippocampal-VTA loop: controlling the entry of information into long-term memory. Neuron *46*, 703-13.

Losonczy, A., Makara, J.K. and Magee, J.C. (2008). Compartmentalized dendritic plasticity and input feature storage in neurons. Nature *452*, 436-41.

Mansour, A., Meador-Woodruff, J.H., Zhou, Q., Civelli, O., Akil, H., and Watson, S.J. (1992). A comparison of D1 receptor binding and mRNA in rat brain using receptor autoradiographic and in situ hybridization techniques. Neuroscience *46*, 959-971.

Martin, S.J., Grimwood, P.D., and Morris, R.G. (2000). Synaptic plasticity and memory: an evaluation of the hypothesis. Annu Rev Neurosci *23*, 649-711.

McQuiston, A.R., Petrozzino, J.J., Connor, J.A. and Colmers, W.F. (1996). Neuropeptide Y1 receptors inhibit N-type calcium currents and reduce transient calcium increases in rat dentate granule cells. J Neurosci. *16*,1422-1429.

Michel, M.C., Beck-Sickinger, A., Cox, H., Doods, H.N., Herzog, H., Larhammar, D., Quirion, R., Schwartz, T., and Westfall, T. (1998). XVI. International Union of Pharmacology recommendations for the nomenclature of neuropeptide Y, peptide YY, and pancreatic polypeptide receptors. Pharmacol Rev. *50*,143-50.

Metz, A.E., Spruston, N. and Martina, M. (2007). Dendritic D-type potassium currents inhibit the spike afterdepolarization in rat hippocampal CA1 pyramidal neurons.J Physiol. *581*, 175-187.

Morris, R.G., Moser, E.I., Riedel, G., Martin, S.J., Sandin, J., Day, M., and O'Carroll, C. (2003). Elements of a neurobiological theory of the hippocampus: the role of activity-dependent synaptic plasticity in memory. Philos Trans R Soc Lond B Biol Sci *358*, 773-786.

O'Sullivan, G.J. et al. (2008). Dopamine D(1) vs D(5) receptor-dependent induction of seizures in relation to DARPP-32, ERK1/2 and GluR1-AMPA signalling. Neuropharmacology *54*,1051-1061.

Piatti V.C., Espósito, M.S., Schinder, A.F.(2006). The timing of neuronal development in adult hippocampal neurogenesis. Neuroscientist. *12*:463-468

Ruschenschmidt, C., Chen, J., Becker, A., Riazanski, V., and Beck, H. (2006). Functional properties and oxidative modulation of A-type K currents in hippocampal granule cells of control and chronically epileptic rats. Eur J Neurosci *23*, 675-685.

Scharfman, H.E. and Schwartzkroin, P.A. (1990). Responses of cells of the rat fascia dentata to prolonged stimulation of the perforant path: sensitivity of hilar cells and changes in granule cell excitability. Neuroscience *35*, 491-504.

Schmidt-Hieber, C., Jonas, P. and Bischofberger, J. (2004). Enhanced synaptic plasticity in newly generated granule cells of the adult hippocampus. Nature *429*, 184–187.

Serodio, P., and Rudy, B. (1998). Differential expression of Kv4 K+ channel subunits mediating subthreshold transient K+ (A-type) currents in rat brain. J Neurophysiol *79*, 1081-1091.

Sierra-Mercado, D., Dieguez, D. Jr. and Barea-Rodriguez, E.J. (2008). Brief novelty exposure facilitates dentate gyrus LTP in aged rats. Hippocampus *18*, 835-43.

Smith, D.M., and Mizumori, S.J. (2006). Hippocampal place cells, context, and episodic memory. Hippocampus *16*, 716-729.

Sperk, G., Hamilton, T. and Colmers, W.F. (2007). Neuropeptide Y in the dentate gyrus. In The Dentate gyrus: A Comprehensive Guide to Structure, Function, and Clinical Implications, H. Scharfman, ed. (Amsterdam, NL: Elsevier) pp. 285-297.

Staley, K.J. and Mody, I. (1992). Shunting of excitatory input to dentate gyrus granule cells by a depolarizing GABAA receptor-mediated postsynaptic conductance. J Neurophysiol. *68*, 197-212.

Stuart, G., Spruston, N., Sakmann, B. and Häusser, M. (1997). Action potential initiation and backpropagation in neurons of the mammalian CNS. Trends Neurosci. *20*, 125-131.

Stuart, G.J., Häusser, M. (2001). Dendritic coincidence detection of EPSPs and action potentials. Nat Neurosci. *4*:63-71.

Sjöström, P.J., Rancz, E.A., Roth, A. and Häusser, M. (2008). Dendritic excitability and synaptic plasticity. Physiol Rev. *88*, 769-840.

Tippens, A.L., Pare, J.F., Langwieser, N., Moosmang, S., Milner, T.A., Smith, Y., and Lee. A. (2008) Ultrastructural evidence for pre- and postsynaptic localization of Cav1.2 L-type Ca2+ channels in the rat hippocampus. J Comp Neurol. *506*, 569-583.

Tran, A.H., Uwano, T., Kimura, T., Hori, E., Katsuki, M., Nishijo, H., and Ono, T. (2008). Dopamine D1 receptor modulates hippocampal representation plasticity to spatial novelty. J Neurosci *28*, 13390-13400.

Vetter, P., Roth, A. and Häusser, M. (2001). Propagation of action potentials in dendrites depends on dendritic morphology. J Neurophysiol. *85*, 926-937.

Waters, J., Larkum, M., Sakmann, B., and Helmchen, F. (2003) Supralinear Ca2+ influx into dendritic tufts of layer 2/3 neocortical pyramidal neurons in vitro and in vivo. J. Neurosci. 23, 8558-8567.

Waters, J., Schaefer, A. and Sakmann, B. (2005). Backpropagating action potentials in neurones: measurement, mechanisms and potential functions. Prog Biophys Mol Biol. *87*, 145-170.

Whitlock, J.R., Heynen, A.J., Shuler, M.G., and Bear, M.F. (2006). Learning induces long-term potentiation in the hippocampus. Science *313*, 1093-1097.

Williams, S.R. and Stuart, G.J. (2000) Backpropagation of physiological spike trains in neocortical pyramidal neurons: Implications for temporal coding in dendrites. J. Neurosci. 20, 8238-8246.

Zweifel, L.S., Parker, J.G., Lobb, C.J., Rainwater, A., Wall, V.Z., Fadok, J.P., Darvas, M., Kim, M.J., Mizumori, S.J., Paladini, C.A.*, et al.* (2009). Disruption of NMDAR-dependent burst firing by dopamine neurons provides selective assessment of phasic dopamine-dependent behavior. Proc Natl Acad Sci U S A *106*, 7281-7288.

CHAPTER 3

Neuropeptide Y Inhibits Frequency-Dependent Ca^{2+} Electrogenesis in Layer 5 Pyramidal Neurons

INTRODUCTION

Many areas of the neocortex including the primary sensory cortices are able to integrate and store information, a process thought to involve changes in the strength of synaptic connections between neurons (Heynen and Bear, 2001; Gilbert et al., 2001). Because of the elaborate dendritic structure that spans all cortical layers and is compartmentalized for distinct information processing, layer 5 (L5) pyramidal neurons of the neocortex appear to be key integrators of synaptic input (Larkum et al., 2001). The most distal aspect of a L5 pyramidal neuron's dendrite, the apical tuft, receives the majority of its input from distal cortical areas that mainly comprises feedback information (Douglas and Martin, 2004), and is important in associative learning and attention (Sjostrom and Hausser, 2006; Gilbert and Sigman, 2007). Most subthreshold input to the distal tuft of a L5 pyramidal cell rarely reaches the soma (Berger et al., 2001), and thus has little or no effect on AP generation. However, above the threshold for Ca^{2+} electrogenesis, Ca^{2+}-action potentials can be generated distally, which can have profound consequences for synaptic plasticity. Ca^{2+}-dependent APs can arise from the interaction of a somatic action potential (backpropagating action potential; bAP; Larkum et al., 1999a, Nevian et al., 2007) that propagates back into the dendritic tree which coincides appropriately with local excitatory synaptic input, or alternatively, alone in response to trains of bAPs above a critical frequency (CF; Larkum et al., 1999b). Distal Ca^{2+}-APs are required for long term synaptic changes (Golding et al., 2002), but can also propagate to the soma and result in bursts of action potentials (APs; Schiller et al., 1997; Larkum et al., 1999a; Stuart and Hausser, 2001). Therefore, the excitability of the apical dendritic region can have a powerful effect on the processing of input.

Previous studies have shown that the exogenous compounds ketamine/xylazine, urethane, and pentobarbital (Potez and Larkum, 2008), and endogenous GABA (Perez-Garci et al., 2006) can modulate the CF in neocortical pyramidal neurons. However, in

order to attempt an understanding of the physiological function of L5 pyramidal neurons (Larkum et al., 1999a; Larkum et al., 2004) the modulation of information processing by other endogenous signals must be examined. Synaptic integration in the distal dendrites of cortical pyramidal neurons is likely to be regulated via other chemical messengers such as neuropeptides that have major neuromodulatory roles elsewhere in the brain, and are preferentially released with high-frequency oscillations (Hokfelt, 1991) that are common in the neocortical network (Sirota et al., 2008).

There is an abundance of Neuropeptide Y (NPY) in the cerebral cortex, where it is synthesized and stored by neurons in all lamina (Hendry et al., 1984), predominantly in nonpyramidal GABAergic interneurons (Hendry et al., 1984; Kohler et al., 1987). Interestingly, a poplulation of NPY-expressing neurons is found in neocortical layer 1-2 with horizontally-oriented projections (Hendry, et al., 1984), and are thus positioned to provide input to the distal apical dendritic region of many L5 pyramidal neurons. Furthermore, receptor autoradiography, *in situ* hybridization, and immunohistochemical studies indicate that Y1 receptors are mainly concentrated in layers I-III in the adult rat (Larsen et al., 1993, 1995; Dumont et al., 1996; Leroux, 2002) and localized to fibers and processes (Kopp et al., 2002). The relatively few physiological studies of NPY actions in the cortex have shown it to have presynaptic actions on inputs to L5 pyramidal cells resulting in either a long-lasting increase in GABAergic synaptic transmission, a decrease in AMPA receptor mediated excitatory transmission, or both (Bacci et al., 2002). Despite the abundant evidence of NPY receptors being located postsynaptically on dendrites of L5 pyramidal neurons, their physiological significance has yet to be determined. Recently, we have observed that activation of the Y1 receptor can modulate the CF in dentate granule cells (DGCs) of the hippocampus via inhibition of voltage-dependent Ca^{2+} channels (VDCCs; McQuiston et al., 1996a; Hamilton et al., submitted). Interestingly, the distribution of Y1 receptors on dendrites of DGCs is similar to the high

density of these receptors also found distally in L5 pyramidal neurons (Kopp et al., 2002).

Here we examined the effect of NPY and Y1 receptor activation on Ca^{2+} electrogenesis in L5 pyramidal neurons induced by trains of bAPs of different frequency, using simultaneous whole-cell recordings from dendrites and somata, or whole-cell somatic recordings, with or without simultaneous Ca^{2+}-imaging in the dendrite. Furthermore, we studied the effect of NPY on the supralinear response caused by the temporal pairing of a bAP and an EPSP. We found that NPY has an inhibitory effect on Ca^{2+}-dependent regenerative potentials in distal apical dendrites, thus indicating an important role for NPY in the processing of higher cortical information.

METHODS

Slice Preparation

Young adult (P25-35) Wistar or Sprague Dawley rats were decapitated and the whole brain was removed and immersed in cold (0-4 ºC) aCSF containing (in mM): NaCl 125, KCl 2.5, NaH_2PO_4 1.25, $NaHCO_3$ 25, MgCl 1, glucose 25, $CaCl_2$ 2, pH 7.4, saturated with 95% O_2, 5% CO_2 (carbogen). Parasagittal slices (300 μm) of the somatosensory cortex were cut with a Vibratome and maintained in carbogenated aCSF at 37 ºC for 15 minutes, and then brought to room temperature (24 °C) until experimentation. L5 pyramidal neurons were chosen after visual identification of an intact distal apical dendrite with the use of infrared differential interference contrast (IR-DIC) or oblique illumination (Perez-Garci et al., 2006).

Electrophysiology

Dual and single whole-cell current clamp experiments were performed with aCSF (33-34 ºC) constantly perfused over the slice in a recording chamber at the focus of a fixed-stage microscope (Perez-Garci et al., 2006). In some experiments, recording pipettes (soma: 5-10 MΩ; dendrite: 15-20 MΩ) were pulled from thick-walled borosilicate glass (1511-M, Freidrick and Dimmock, Millville, NJ), while in other experiments they were pulled from thin-walled borosilicate tubing (5-6 MΩ, TW 150F – WPI, Sarasota, FL). Pipettes were filled with a solution containing (in mM): K-gluconate 105, HEPES 10, KCl 30, $MgCl_2$ 2, MgATP 2, Na_2ATP 2, GTP 0.3, and 0.2% biocytin or neurobiotin, pH 7.3. In some experiments, the pipette solution also contained Alexa 594 (10 μM; Invitrogen, Carlsbad CA) to enable the visualization of the dendritic tree, and/or Oregon Green BAPTA 1 (OGB-1; 100 μM; Invitrogen) for Ca^{2+} imaging. Dendritic and somatic recordings were made with Axoclamp-2B amplifiers (Axon Instruments, Foster

City, CA, USA) or Dagan BVC-700 amplifiers (Dagan Corp., Minneapolis MN). Trains of APs were evoked with 1 ms depolarizing square pulses of 1-5 nA current injections at the somatic pipette at frequencies from 20-200 Hz. In pairing experiments, dendritic current injection was in the shape of a double exponential as previously described (Larkum et al., 1999a) and evoked 1 ms after the start of somatic current injection.

Ca^{2+} Imaging

Intracellular Ca^{2+} imaging experiments began with the loading of L5 pyramids with OGB-1 (100 μM) and Alexa 594 (10 μM) for approximately 45 mins via a somatic pipette. Fluorescence was measured with a 512 X 512 back-illuminated frame transfer CCD camera (PXL or Micromax, Roper, Tucson, AZ). Images were binned at 2 X 2 or 4 X 4 and acquired at frame rates of ~ 40 Hz.

Immunohistochemistry

After slowly removing the pipette from the neuron, slices were carefully removed from the recording chamber, fixed in 4% paraformaldehyde for at least 48 hrs, then washed in a potassium phosphate buffer solution (KPBS) containing KH_2PO_4 (3.57 mM), K_2HPO_4 (anhydrous; 16.43 mM), and NaCl (15.4 mM), then dehydrated in 25% sucrose for 48-72 hrs. Slices were then incubated in SA conjugated Alexa 555 (Molecular Probes), 2% normal goat serum (Rockland), and 0.3% triton X-100 (Sigma St. Louis, MO) for 2 hrs. After washout with KPBS slices were mounted on slides with Prolong Gold antifade reagent (Invitrogen) and imaged with an upright confocal microscope.

Drugs

Unless otherwise indicated, all compounds were applied via the bath. Human NPY (NPY) was purchased from Peptidec Technologies (Pierrefonds, Quebec). The

receptor preferring agonist F^7P^{34}[NPY] was made by solid-state synthesis as described previously (El Bahh et al., 2005). The Y1 antagonist, BIBO 3304 ((R)-N-[[4-(aminocarbonylaminomethyl)-phenyl]methyl]-N2-(diphen ylacetyl)-argininamide trifluoroacetate) was a gift of Dr. H Doods, Boehringer Ingelheim. Because NPY can require a prolonged time to wash out, BIBO 3304 was used in some experiments after an NPY application to shorten the wash-out time. For localized application, NPY (1 μM) and Alexa 594 (1 μM), were dissolved in aCSF and loaded into a borosilicate glass puffer pipette. The pipette was moved into position (distally, or at the soma) under visual guidance and control recordings were taken before drug application commenced. Pressure ejection of the fluorescent NPY-containing solution was observed periodically for the duration of the 5 min application.

Statistical Analysis

Analysis of the CF was performed as previously described (Larkum et al., 1999b). Briefly, to calculate the CF at the soma we measured the amplitude at a single time point after the last AP evoked at the cell body for all frequencies tested (20-200 Hz; Fig. 3.1). This is referred to as the ADP amplitude, which provides similar results as the use of the ADP integral in CF calculation (time-voltage integral; Potez and Larkum, 2008). To calculate the dendritic CF we measured the time-voltage integral of all 4 depolarizations above the resting potential (Fig. 3.1), which is a more sensitive measure than using the amplitude because dendritic depolarizations broaden as they reach the CF (Larkum et al., 1999b). The somatic ADP amplitude, dendritic integral, or peak Ca^{2+} transient (in imaging experiments) were plotted against frequency and a sigmoidal curve was generated. The CF was defined as the frequency at half-maximal amplitude of this curve (Fig. 3.1).

Figure 3.1. Calculation of the Critical Frequency.

Shown is a representative recording configuration for dual whole-cell recording experiments. For each frequency sweep either the amplitude of the somatic ADP (vertical red line), or dendritic integral (hatched area under the curve) were plotted as a function of frequency (below). The 'critical frequcency' (CF) was calculated as 50 % of the rise of the sigmoidal curve fit to each data set (blue arrow).

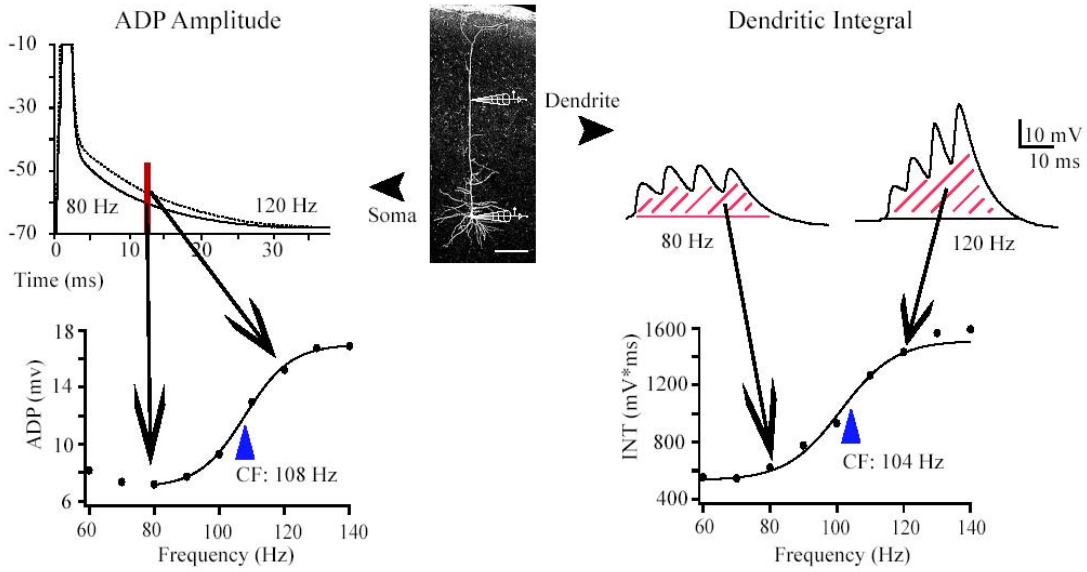
ADP Amplitude
-10
-30
-50
-70
80 Hz
120 Hz
0
10
20
30
Time (ms)
18
14
10
6
ADP (mv)
CF: 108 Hz
60
80
100
120
140
Frequency (Hz)
Soma
Dendrite
Dendritic Integral
10 mV
10 ms
80 Hz
120 Hz
1600
1200
800
400
INT (mV*ms)
CF: 104 Hz
60
80
100
120
140
Frequency (Hz)

All data presented are as mean ± s.e.m unless otherwise indicated, with "n" being the number of neurons analyzed. For comparisons of group values, Student's t-tests were used with alpha values of 0.05. One-sample t-tests were used to compare means with the hypothetical value of 0 or 100. We used multiple t-tests and not an ANOVA because of the small sample sizes and because we were *a priori* interested in particular comparisons and did not conduct all possible pairwise comparisons.

RESULTS

NPY Increases the Critical Frequency

To study the effects of NPY on Ca^{2+} electrogenesis, in the first series of experiments, we simultaneously recorded membrane potential from pipettes placed at the soma and distal (>500 μm from the soma) apical dendrite of L5 cells and used a protocol that evoked a train of 4 somatic APs at frequencies from 20-200 Hz (Fig. 3.2A,B; Larkum et al, 1999; Larkum et al., 2007; Potez and Larkum, 2008). Under control conditions, we observed a supralinear increase in dendritic potential responses above a CF (see Methods). Supralinear activity was observed reliably in each neuron examined, as previously described (Larkum et al., 1999b; Fig. 3.2B). At the same frequency as a regenerative response was observed at the dendritic electrode, somatic recordings also demonstrated a jump in the ADP amplitude, consistent with earlier reports that distal regenerative activity can propagate forward, and result in nonlinear behavior at the soma at the same (critical) frequency (Larkum et al., 1999a; Larkum et al., 1999b; Larkum et al., 2001; Perez-Garci et al., 2006; Fig. 3.2B). In paired dendritic and somatic recordings, the somatic CF was not significantly different from the CF recorded at the distal dendrite (Soma: 117 ± 8 Hz, Dendrite: 113 ± 7 Hz; P=0.2248, n=6). To study whether NPY affected this frequency-dependent regenerative activity, we first applied NPY (1 μM) via the bath and repeated the above frequency sweeps protocol. At the soma, NPY increased the CF by 13 ± 4 Hz (P<0.017, n=6); this reversed upon washout in the presence of Y1 receptor selective antagonist BIBO 3304 (1 μM; CF shift, vs control: -1 ± 5 Hz; n=6; Fig. 3.2C,E,G). Similar results were observed in the simultaneous dendritic recordings. NPY increased the dendritically recorded CF by 14 ± 3 Hz (P< 0.0045, n=6), which again reversed upon washout in the presence of BIBO 3304 (CF shift, compared to control: -1 ±

Figure 3.2. NPY Increases the Critical Frequency.

(A) A neurobiotin filled L5 pyramidal neuron with representative dendritic (> 500 μm from the soma) and somatic whole-cell electrodes. Scale bar: 200 μm. (B) Critical frequencies were evoked with trains of 4 somatic APs (1 ms square pulses of 1-5 nA current injections at the soma). Shown is the afterdepolarization (ADP) of the 4^{th} action potential at the soma. Inset is the dendritic response recorded simultaneously from the distal dendrite. Above a CF (100 & 110 Hz, dotted lines) supralinear responses were seen at the soma and dendrite. (C-D) Compared to control responses (black) bath application of NPY (1 μM, red) and subsequent wash in Y1 antagonist, BIBO 3304 (1 μM, blue) had little effect on trains below the CF at the dendrite (70 Hz). Above the CF (100 Hz) NPY decreases the 3^{rd} and 4^{th} dendritic depolarizations, this reverses in the presence of BIBO 3304. (E) Somatic ADP amplitudes were plotted against frequency (60-140 Hz, shown here), and sigmoidal fits were calculated. The critical frequencies were determined as the half-maximal rise of the sigmoidal curve (arrows). NPY (CF-123 Hz, red) increases the CF compared to control (CF-108 Hz, black), which reverses in the presence of BIBO 3304 (CF-105 Hz, blue). (F) The time-voltage integral (INT) for simultaneous dendritic recordings as in E, were plotted against frequency and sigmoidal fits were calculated. NPY (CF-121 Hz, red) increases the CF compared to control (CF-104 Hz, black), which reverses in the presence of BIBO 3304 (CF-100 Hz, blue). (G-H) The average shifts in CF relative to control were calculated at the soma and dendrite after NPY application (n=6, red), washout in BIBO 3304 (n=6, blue), and after a subsequent application of NPY, still in the presence of BIBO 3304 (n=3). (I-J) The average shifts in CF relative to control were calculated at the soma and dendrite after Y1 agonist application (F^7P^{34}[NPY], 1 μM; n=3). * $P<0.05$, (one-sample t-test).

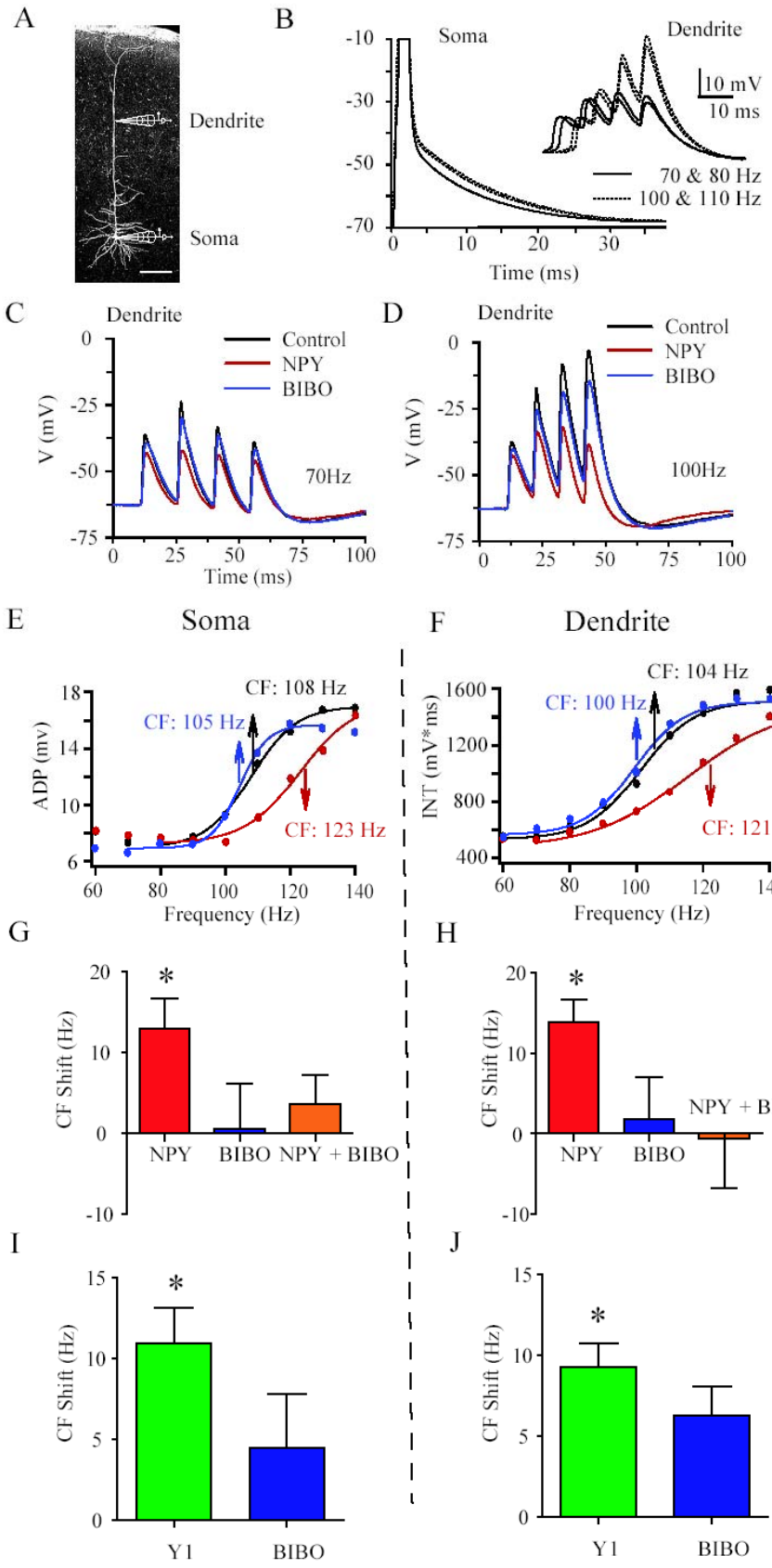
A
Dendrite
Soma
B
Soma
Dendrite
10 mV
10 ms
70 & 80 Hz
100 & 110 Hz
Time (ms)
C
Dendrite
Control
NPY
BIBO
70Hz
V (mV)
Time (ms)
D
Dendrite
Control
NPY
BIBO
100Hz
V (mV)
E
Soma
CF: 108 Hz
CF: 105 Hz
CF: 123 Hz
ADP (mv)
Frequency (Hz)
F
Dendrite
CF: 104 Hz
CF: 100 Hz
CF: 121 Hz
INT (mV*ms)
Frequency (Hz)
G
CF Shift (Hz)
NPY
BIBO
NPY + BIBO
H
CF Shift (Hz)
NPY
BIBO
NPY + BIBO
I
CF Shift (Hz)
Y1
BIBO
J
CF Shift (Hz)
Y1
BIBO

5 Hz; P=0.759, n=6; Fig. 3.2D,F,H). The CF shift caused by NPY at the dendrite was not significantly different from the CF shift caused by NPY at the soma (P= 0.5214, n=6). NPY also decreased the amplitude of the somatic ADP at the original CF (-36.4 ± 11.7 % of control; P<0.0359, n=5) that reversed with washout in BIBO 3304 (-7.6 ± 21.3 % of control; P=0.7433, n=5). At the dendrite, NPY decreased the time-voltage integral at the original CF by 30.3 ± 4.0 % of control (P<0.0006, n=6); this response returned to 5.3 ± 8.2 % of control (P=0.5495, n=6) with washout in BIBO 3304.

Y1 Receptor Mediates the Increase in Critical Frequency

To determine the NPY receptor subtype (s) responsible for the CF shift we bath applied the potent Y1-specific antagonist BIBO 3304 (1 μM), and then applied NPY (1 μM) in neurons that had already shown a response to NPY that reversed upon washout. Under these conditions there was no significant change in CF at the dendrite (CF shift: -1 ± 6 Hz; P= 0.9373, n=3; Fig. 3.2G,H) or at the soma (CF shift: 4 ± 4 Hz; P= 0.4179, n=3; Fig. 3.2G,H).

To verify that the action of NPY is mediated by Y1 receptor activation we performed an additional set of experiments with dual whole-cell recordings, as above, and applied the Y1-receptor preferring agonist F^7P^{34} [NPY]. As expected, bath application of the Y1 agonist reversibly shifted the CF at both the soma (11 ± 2 Hz; P< 0.0379, n=3) and at the distal dendrite (9 ± 2 Hz; P< 0.0251, n=3; Fig. 3.2I,J). These data are consistent with the hypothesis that the Y1 receptor mediates NPY's activity in these L5 neurons.

NPY Does Not Act at Presynaptic Sites on Layer 5 Pyramidal Cells

To test the possibility that NPY may be acting either via the inhibition of glutamatergic input, an increase in GABAergic neurotransmission, or both (Bacci et al.,

2002), we blocked both excitatory and inhibitory neurotransmission by bath application of kynurenic acid (1 mM) and picrotoxin (100 μM), respectively. In these experiments we measured only the somatic ADP, as it has previously been shown to be a reliable indicator of distal dendritic activity in L5 pyramidal neurons (Perez-Garci et al., 2006). Across all frequencies tested (20 – 200 Hz) there was no effect of the synaptic blockers on the ADP or the CF relative to control recordings (data not shown). Interestingly, the blockade of ionotropic synaptic responses did not affect the ability of NPY to reversibly inhibit the ADP and increase the CF in 7 pyramidal neurons (Fig. 3.3A,B). The CF shift caused by NPY was 18 ± 5 Hz ($P<0.0119$, n=7). This was not significantly different from the NPY-induced CF shift recorded from neurons in the absence of the synaptic blockers (No Syn Blk - CF shift: 13 ± 4 Hz; $P=0.0751$). These results indicate that NPY's effect on dendritic electrogenesis is not mediated by actions on synaptic inputs.

NPY Acts Via Distal, But Not Somatic Receptors

Previous studies have shown a very high density of postsynaptic Y1 receptors in distal dendrites of L5 pyramidal neurons (Kopp et al., 2002). In other areas of the brain, such as the dentate gyrus of the hippocampus, Y1 receptors are also located postsynaptically, where they inhibit voltage-dependent Ca^{2+} channels (McQuiston et al., 1996a; Hamilton et al., submitted). Together with our observation of an NPY-mediated CF shift in both the soma and distal dendrite, we hypothesize that Y1 receptors in distal dendrites are responsible for this effect. To test this, we filled pyramidal neurons with Alexa 594 (10 μM) and OGB-1 (100 μM) via somatic whole-cell recordings in order to record simultaneous Ca^{2+} transients and somatic V_m. Using the same frequency sweep protocol as above, we were able to simultaneously record the frequency dependence of distal dendritic Ca^{2+} transients, along with ADP responses recorded electrically at the

Figure 3.3. NPY Inhibits the Critical Frequency in the Presence of Synaptic Blockade.

After bath application of kynurenic acid (KYN, 1 mM) and picrotoxin (PTX, 100 μM) for at least 20 mins, the subsequent application of NPY (1 μM) still in the presence of PTX and KYN was still able to reversibly inhibit the CF recorded at the soma. (A) Above the CF (80 Hz) NPY (dotted line) decreases the ADP relative to PTX + KYN (solid line). (B) NPY significantly and reversibly increases the average CF (n=7). *P<0.05, **P<0.01, (paired t-test).

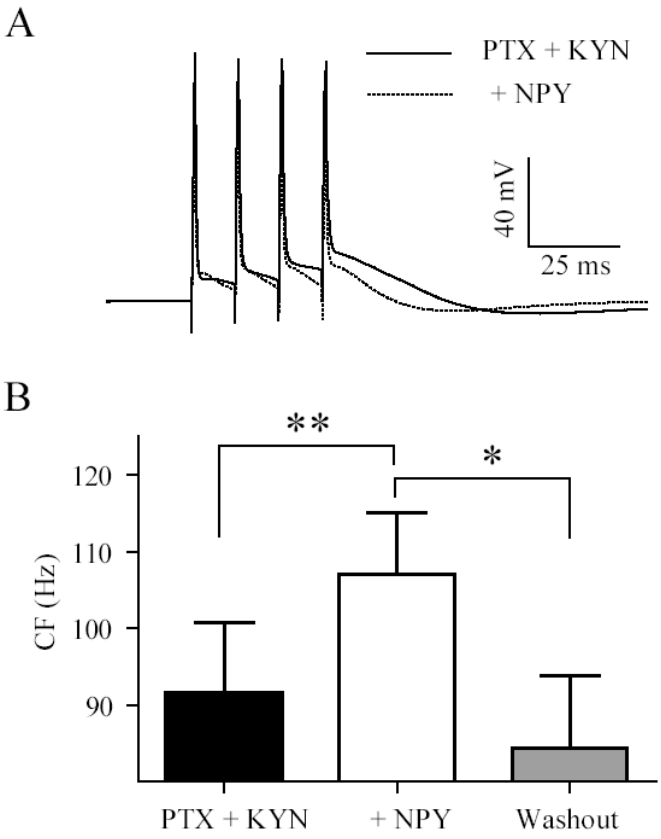
A
PTX + KYN
+ NPY
40 mV
25 ms
B
**
*
120
110
100
90
CF (Hz)
PTX + KYN
+ NPY
Washout

soma (Larkum et al., 1999b). A pipette containing a solution of NPY (1 μM) and Alexa 594 (1 μM; Fig. 3.4A) was used for focal peptide application. Frequency sweeps under control conditions (pipette in position, but no puffing) evoked stable CFs recorded both at the soma and at the dendrite. Prior to focal application of NPY to the dendrite, the mean CF recorded via Ca^{2+} transients in the distal dendrite was 93 ±10 Hz, and the CF recorded at the soma via the ADP was 91 ± 9 Hz; not significantly different from that seen in the dendrite (P=0.2389, n=6). Local application of NPY onto the distal dendrite (between the first distal branch point and the end of the tuft) resulted in a significant CF shift of 11 ± 1 Hz (P<0.004, n=6) measured via the somatic ADP, and 9.3 ± 2 Hz (P< 0.0004, n=6) measured via distal Ca^{2+} transients (Fig. 3.4). This response reversed shortly after application ceased. Distal NPY application also significantly decreased the peak Ca^{2+} transient at the control CF by 18 ± 4 % (P< 0.015, n=6) which returned to a 4.6 ± 8.8 % decrease compared to control (P=0.6288, n=6) with washout. The ADP amplitude at the soma was also significantly decreased (by 36.8 % ± 8.6 compared to control CF; P<0.0078, n=6) and returned to an increase of 2.9 ± 8.9 % compared to control (P=0.7553, n=6) after washout.

Next, after a washout of NPY and recovery of the CF, we moved the applicator pipette to near the soma. Critical frequencies returned to values not significantly different from the start of the experiment (soma-CF: P=0.9664, n=6; dendrite-CF: P=1.000, n=6). By contrast with the responses above, NPY application to the soma had significant effects on neither the distal dendritic CF, nor the somatic CF (Fig. 3.4C; n=4), nor the peak Ca^{2+} transient (Ctl: 106.7 ± 22.2 a.u., NPY: 92.0 ± 16.6 a.u.; P<0.3316, n=4), nor the ADP amplitude (Ctl: 6.2 ± 2 mV, NPY: 8.7 ± 3.9 mV; P<0.3418, n=4). Since the locus of somatic application was also on at least the proximal basal dendrites, we can presume that NPY does not act there to alter the CF. These data indicate that NPY acts at distal dendritic, but not somatic sites to affect dendritic Ca^{2+} electrogenesis.

Figure 3.4. NPY Acts at the Distal Dendrite and not at the Soma.

(A) L5 pyramidal neurons were filled with fluorescent Ca^{2+} dye, OGB-1 (100 μM), and Alexa 594 (10 μM) via a somatic patch pipette. Shown is a distal application of NPY via a puffer pipette filled with NPY (1 μM), Alexa 594 (1 μM), and aCSF. The box is representative of the region of distal Ca^{2+} imaging. The arrow represents the direction of flow of the perfusion. (B) The ADP amplitude at the soma and simultaneous peak Ca^{2+} currents in the distal dendrite were recorded before and after a distal application of NPY, and the CFs were calculated (left panels). Inset is representative Ca^{2+} transients. In the same neuron, after a washout of NPY, the pipette was moved to the soma and NPY was applied there (right panels). (C) The CFs, calculated via the somatic ADP (black) and distal dendritc peak Ca^{2+} currents (grey) were shifted only when NPY was applied to the distal dendrite (NPY Distal, n=6). The effect of the distal NPY puff washed out (Wash Distal; n=6). Subsequent application of NPY at the soma (NPY soma) had no effect on the somatic ADP and distal dendritc Ca^{2+} CF (n=4). * $P<0.05$, difference from 0, (one-sample t-test).

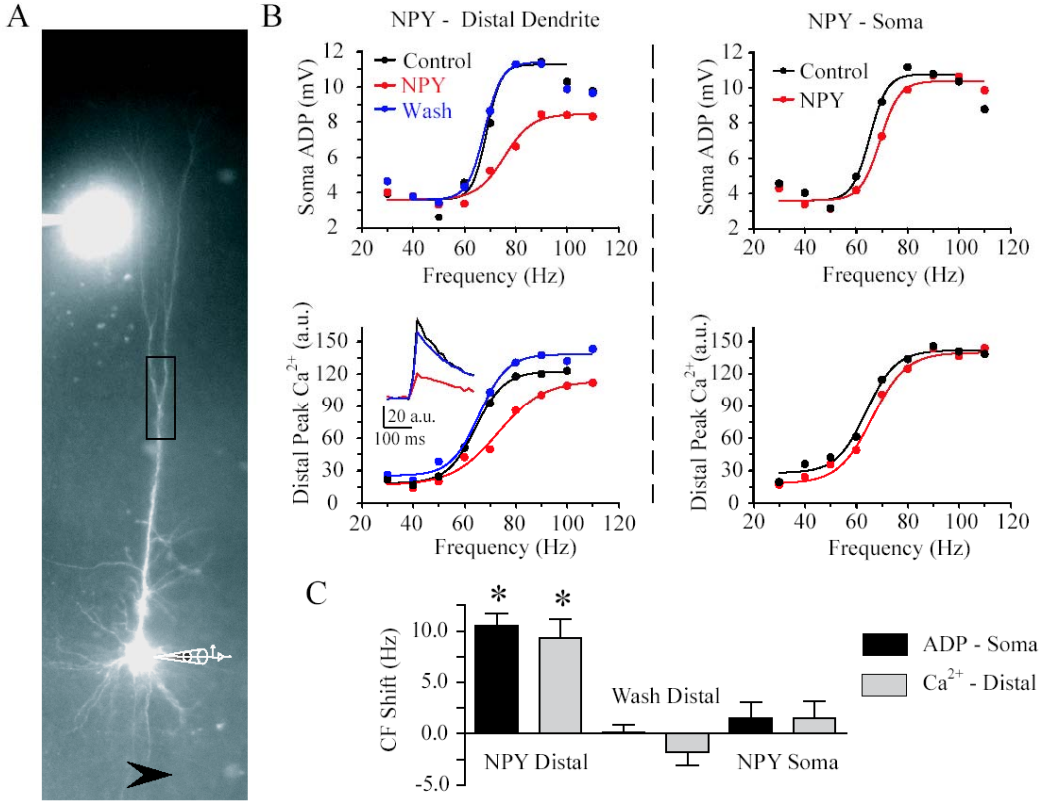
A
B
NPY - Distal Dendrite
NPY - Soma
Control
NPY
Wash
Soma ADP (mV)
Frequency (Hz)
Distal Peak Ca2+ (a.u.)
20 a.u.
100 ms
C
CF Shift (Hz)
ADP - Soma
Ca2+ - Distal
Wash Distal
NPY Distal
NPY Soma

Dendro-Somatic Coupling is Inhibited by NPY

The temporal pairing of an EPSP and a bAP can have significant effects on synaptic strength (Larkum et al., 1999a). When a single EPSP is appropriately timed with a single bAP, the result is a supralinear dendritic response that is dependent on a combination of Na^+, K^+, (Stuart and Hausser, 2001) and distal dendritic Ca^{2+} influx (Koester and Sakmann, 1998). The amplitude of the dendritic EPSP is also critical for the induction of a dendritic Ca^{2+} spike (Stuart and Hausser, 2001). Based on our findings of an NPY-mediated increase in the CF, we hypothesized that the threshold for a supralinear response would increase with the application of NPY. With simultaneous recordings of the soma and distal apical dendrite, we simulated an EPSP with injection of a current waveform at the dendritic electrode, and simultaneously evoked a somatic AP. This combination has been shown to produce a maximal response in L5 pyramidal neurons when the timing of the 2 stimuli is nearly simultaneous (Larkum et al., 1999a). We progressively increased the amplitude of the dendritic current waveform in 100 pA increments, and observed a robust increase in dendritic potential, coincident with an additional (or in some cases multiple) AP(s) at the soma (Fig. 3.5A, black trace). We considered the 'pairing threshold,' to be the amount of dendritic current injection that first caused a stable supralinear dendritic response. For example, in Fig. 3.5A,ii. the pairing threshold occurred with the injection of 1.3 nA of dendritic current. To test whether NPY could modulate the pairing threshold, we bath-applied NPY (1 μM) and repeated the experiment. NPY had no effect on the the dendritic or somatic responses below the pairing threshold. However, NPY increased the amount of dendritic current required to reach the pairing threshold. In 4 neurons, NPY significantly reduced the integral at, and above the control pairing threshold in dendritic recordings (Fig. 3.5A,B). On average in the presence of NPY the dendritic current injected needed to increase 225 ± 63 pA to reach the pairing threshold (n=4). This modulation of the pairing threshold by

Figure 3.5. NPY Inhibits the Pairing Threshold for an EPSP and a bAP.

(A) Dual somatic and distal dendritic (> 500 μm from soma) recordings were performed. Somatic APs were generated at the soma with a square-wave injection (4 nA, 1 ms) and paired (Δt = 5ms) with a subthreshold distal EPSP at the dendritic electrode. Recordings were made at the dendrite (left column) and soma (right column) similar to the recording configuration in Fig. 3.1. Subthreshold pairings (D_{inj}: dendrite: 1.2 nA, S_{inj}: soma 4 nA) produced no regenerative activity in the dendrite (i.). By increasing D_{inj} in 100 pA steps Ca^{2+}-spikes were observed at, and above, a pairing threshold (ii.; D_{inj}: 1.3 nA) and result in an additional AP at the soma (ii.-iv., black traces). Bath application of NPY (1 μM) had no effect on sub-threshold pairing (i.), but inhibited the supralinear activity above the pairing threshold, and the additional spike at the soma (ii. and iii.). (B) The integral of the dendritic recording was normalized to the pairing threshold before (Control, black) and after NPY application (red; n=4). *P<0.05, control vs. NPY, (paired t-test). (C) Same as in B., but for simultaneous recordings of somatic integral (n=4). *P<0.05, control vs. NPY, (paired t-test).

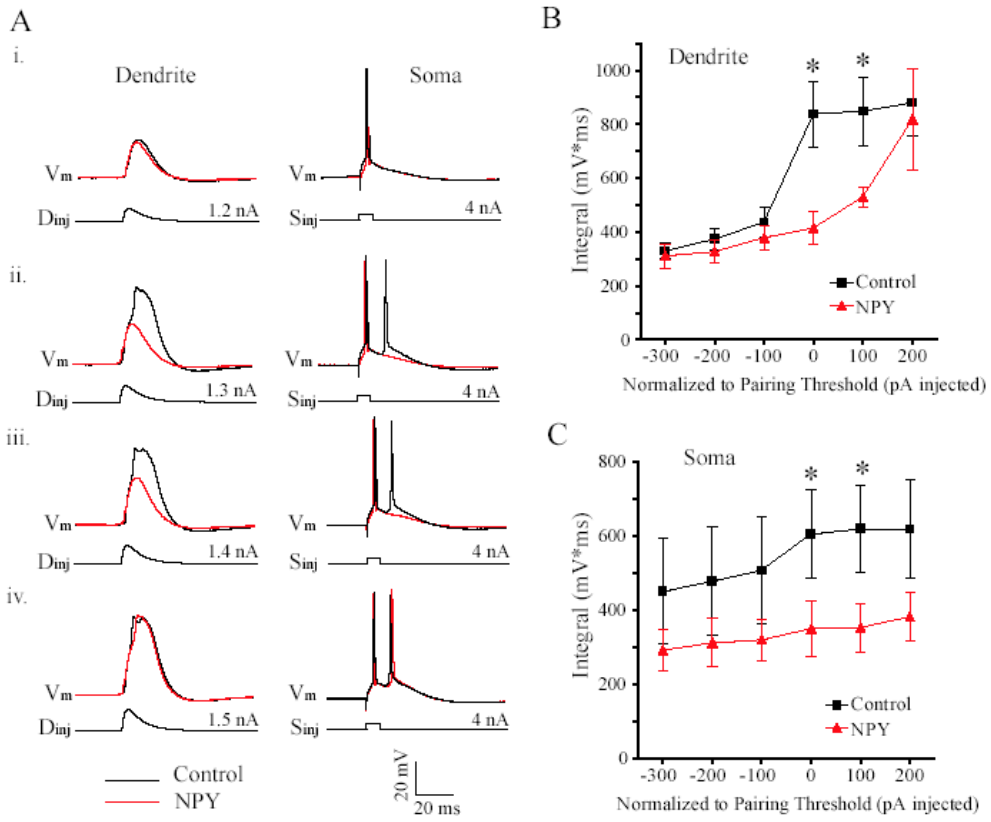
A
i.
Dendrite
Soma
Vm
Dinj
1.2 nA
Sinj
4 nA
ii.
1.3 nA
iii.
1.4 nA
iv.
1.5 nA
Control
NPY
20 mV
20 ms
B
Dendrite
Integral (mV*ms)
Control
NPY
Normalized to Pairing Threshold (pA injected)
C
Soma

NPY also resulted in the lack of a second somatic AP at, and above, the pairing threshold (Fig. 3.5A,C). The modulation of Ca^{2+}–dependent regenerative activity is consistent with NPY increasing the CF, likely through the inhibition of VDCCs.

DISCUSSION

In this study we investigated the effect of NPY on regenerative Ca^{2+} currents in dendrites of neocortical L5 pyramidal neurons. Consistent with earlier reports, we found that the distal apical dendrite can generate regenerative events both above a CF of backpropagating action potentials, and with near-simultaneous pre- and postsynaptic activity (Koester and Sakmann, 1998; Larkum et al., 1999a; Larkum et al., 1999b). With locally applied NPY we have shown that this regenerative activity is inhibited by activation of Y1 receptors located on the distal apical dendrite, and not at the soma.

Action potentials were recorded with simultaneous whole-cell recordings at the distal dendrite and soma of individual L5 pyramidal neurons of the somatosensory cortex. We were able to reliably evoke regenerative dendritic potentials with brief trains of backpropagating somatic APs at or above a critical (intratrain) frequency, as described previously (Larkum et al., 1999a; Larkum et al., 1999b). The CFs measured at the soma were identical with those recorded simultaneously at the distal dendrite, either with a pipette or with Ca^{2+} imaging. This is consistent with previous reports indicating that Ca^{2+} spikes generated in distal apical dendrites of L5 cells can propagate to the soma (Larkum et al., 2001; Larkum et al., 2004).

It is well established that L5 pyramidal neurons have 3 functional compartments that are located at the soma and basal dendrites, oblique dendrites, and distal apical dendrite (Larkum et al., 2001). The somatic region and tufted distal apical region are each capable of generating Na^{+}- and Ca^{2+}-Na^{+}-APs, respectively, while the oblique dendrites can mediate the communication between the two regions (Larkum et al., 2001). Since there is a concentration of Y1 receptors on the dendrites of L5 pyramidal neurons (Kopp et al., 2002), we hypothesized that these postsynaptic receptors would decrease Ca^{2+}-influx, resulting in an increased CF, similar to the actions of Y1 receptors in the dentate gyrus (Hamilton et al., submitted). Recent work suggests that the most

electrically active, NPY-expressing neurons are those that reside in layer 1 (Karagiannis et al., 2009), where the most distal parts of the L5 dendrites also extend. In our first experiments we found that NPY increased the CF in both somatic and dendritic recordings and this was mediated by an Y1 receptor. Next, we therefore sought to determine which region(s) NPY targeted to increase the neuronal CF. In an attempt to answer this question we applied NPY locally to the distal dendrite, then to the soma-basal dendritic regions in the same neurons. NPY significantly increased the CF when applied distally, and not at the soma, consistent with a dense distribution of Y1 receptors on the distal apical dendrite (Kopp et al., 2002). The effect of the puff was less marked than with bath application of NPY, quite possibly because the NPY puff was localized and may not have activated as many dendritic receptors as did bath application (see Fig. 3.4A). Because of the relatively small volume of the soma, we can be confident that the area of NPY application sufficiently covered the soma and the most proximal basal dendrites.

It has been shown previously that NPY can induce a delayed inhibition of GABAergic synaptic transmission on to L5 pyramidal neurons (Bacci et al., 2002). In those experiments, NPY increased the amplitude of evoked inhibitory postsynaptic currents (IPSC) and the frequency of depolarization (20 mM KCl) -induced miniature IPSCs on to L5 pyramidal neurons (Bacci et al., 2002). Indeed, an increase in $GABA_A$ and $GABA_{B1b}$ receptor activation will also inhibit dendritic Ca^{2+} spikes in L5 pyramidal neurons (Larkum et al., 1999b; Perez-Garci et al., 2006). However, the NPY-mediated effect seen here did not persist long after washout and was not as long lasting as that observed by Bacci and colleagues (2002). Instead, we observed an inhibition of regenerative activity during NPY application that washed out after about 10 minutes (Fig. 3.4). Furthermore, the effect of NPY was not changed by blockade of $GABA_A$ receptors with picrotoxin (Fig. 3.4). It is thus unlikely that the effect of NPY on the CF and pairing

threshold were by an increase in interneuronal GABA release. Instead, we have found a novel postsynaptic action of NPY in L5 pyramidal neurons. Elsewhere in the brain, NPY has been shown to increase a G-protein-activated inwardly-rectifying K^+ conductance (G_{IRK}; Rhim et al., 1997; Sun and Miller, 1999; Acuna-Goycolea et al., 2005; Chee and Colmers, unpublished observations) and block a hyperpolarization-activated cation conductance (I_h; Giesbrecht and Colmers, unpublished observations); both actions could potentially hyperpolarize the membrane and inhibit Ca^{2+} spikes (Berger et al., 2001). The absence of any change in the membrane potential, even at the dendritic electrode, during or after NPY application suggests that it is unlikely that a dendritic G_{IRK} or I_h mediates the actions of NPY. A candidate mechanism is the inhibition of VDCCs. An NPY-mediated inhibition of N-Type VDCCs has been observed in the hippocampus, at both pre- and postsynaptic sites (Qian et al., 1997; McQuiston et al., 1996a, 1996b). Our findings are consistent with Y1-mediated frequency-dependent inhibition of distal VDCCs observed in DGCs of the hippocampus (Hamilton et al., submitted).

Top-down information is carried to layer 1 of the cortex (Cauller, 1995; Douglas and Martin, 2004), while bottom-up thalamic input synapses on to layer 4 stellate excitatory interneurons that innervate a wide region of L5 pyramidal cells (Cauller, 1995; Bannister, 2005). Near simultaneous stimulation of both of these inputs can result in supralinear dendritic responses that are sufficient to generate bursts of somatic APs (Larkum et al., 1999a). Here we have shown that the release of NPY on to the distal apical dendrite can inhibit Ca^{2+} spikes and decrease its sensitivity to near simultaneous pre- and postsynaptic input. This action of NPY is positioned to have a dramatic inhibitory effect on the integration of top-down and bottom-up input. Taken together, the vast distribution in superficial cortical layers and the compartment-specific action on L5 pyramidal neurons makes NPY a candidate neuromodulator to have a profound influence on higher-order cortical processes such as learning, memory, and attention.

REFERENCES

Acuna-Goycolea, C., Tamamaki, N., Yanagawa, Y., Obata, K., and van den Pol, A.N. (2005). Mechanisms of neuropeptide Y, peptide YY, and pancreatic polypeptide inhibition of identified green fluorescent protein-expressing GABA neurons in the hypothalamic neuroendocrine arcuate nucleus. J Neurosci *25*, 7406-7419.

Bacci, A., Huguenard, J.R., and Prince, D.A. (2002). Differential modulation of synaptic transmission by neuropeptide Y in rat neocortical neurons. Proc Natl Acad Sci U S A *99*, 17125-17130.

Bannister, A.P. (2005). Inter- and intra-laminar connections of pyramidal cells in the neocortex. Neurosci Res *53*, 95-103.

Birtoli, B., and Ulrich, D. (2004). Firing mode-dependent synaptic plasticity in rat neocortical pyramidal neurons. J Neurosci *24*, 4935-4940.

Cauller, L. (1995). Layer I of primary sensory neocortex: where top-down converges upon bottom-up. Behav Brain Res *71*, 163-170.

Cooper, D.C. (2002). The significance of action potential bursting in the brain reward circuit. Neurochem Int *41*, 333-340.

Douglas, R.J., and Martin, K.A. (2004). Neuronal circuits of the neocortex. Annu Rev Neurosci *27*, 419-451.

Dumont, Y., Fournier, A., St-Pierre, S., and Quirion, R. (1996). Autoradiographic distribution of [125I]Leu31,Pro34]PYY and [125I]PYY3-36 binding sites in the rat brain evaluated with two newly developed Y1 and Y2 receptor radioligands. Synapse *22*, 139-158.

El Bahh, B., Balosso, S., Hamilton, T., Herzog, H., Beck-Sickinger, A.G., Sperk, G., Gehlert, D.R., Vezzani, A., and Colmers, W.F. (2005). The anti-epileptic actions of neuropeptide Y in the hippocampus are mediated by Y and not Y receptors. Eur J Neurosci *22*, 1417-1430.

Gaspar, P., Berger, B., Lesur, A., Borsotti, J.P., and Febvret, A. (1987). Somatostatin 28 and neuropeptide Y innervation in the septal area and related cortical and subcortical structures of the human brain. Distribution, relationships and evidence for differential coexistence. Neuroscience *22*, 49-73.

Gilbert, C.D., Sigman, M., and Crist, R.E. (2001). The neural basis of perceptual learning. Neuron *31*, 681-697.

Gilbert, C.D., and Sigman, M. (2007). Brain states: top-down influences in sensory processing. Neuron *54*, 677-696.

Golding, N.L., Staff, N.P., and Spruston, N. (2002). Dendritic spikes as a mechanism for cooperative long-term potentiation. Nature *418*, 326-331.

Hamilton, T.J., Wheatley, B.M, Sinclair, D.B., Bachmann, M., Larkum, M.E., and Colmers, W.F. (submitted). Dopamine modulates synaptic plasticity in dendrites of rat and human dentate granule cells. Science.

Hendry, S.H., Jones, E.G., and Emson, P.C. (1984). Morphology, distribution, and synaptic relations of somatostatin- and neuropeptide Y-immunoreactive neurons in rat and monkey neocortex. J Neurosci *4*, 2497-2517.

Heynen, A.J., and Bear, M.F. (2001). Long-term potentiation of thalamocortical transmission in the adult visual cortex in vivo. J Neurosci *21*, 9801-9813.

Kampa, B.M., Letzkus, J.J., and Stuart, G.J. (2006). Requirement of dendritic calcium spikes for induction of spike-timing-dependent synaptic plasticity. J Physiol *574*, 283-290.

Karagiannis, A., Gallopin, T., David, C., Battaglia, D., Geoffroy, H., Rossier, J., Hillman, E.M., Staiger, J.F., and Cauli, B. (2009). Classification of NPY-expressing neocortical interneurons. J Neurosci *29*, 3642-3659.

Koester, H.J., and Sakmann, B. (1998). Calcium dynamics in single spines during coincident pre- and postsynaptic activity depend on relative timing of back-propagating action potentials and subthreshold excitatory postsynaptic potentials. Proc Natl Acad Sci U S A *95*, 9596-9601.

Kohler, C., Schultzberg, M., and Radesater, A.C. (1987). Distribution of neuropeptide Y receptors in the rat hippocampal region. Neurosci Lett *75*, 141-146.

Kopp, J., Xu, Z.Q., Zhang, X., Pedrazzini, T., Herzog, H., Kresse, A., Wong, H., Walsh, J.H., and Hokfelt, T. (2002). Expression of the neuropeptide Y Y1 receptor in the CNS of rat and of wild-type and Y1 receptor knock-out mice. Focus on immunohistochemical localization. Neuroscience *111*, 443-532.

Larkum, M.E., Kaiser, K.M., and Sakmann, B. (1999a). Calcium electrogenesis in distal apical dendrites of layer 5 pyramidal cells at a critical frequency of back-propagating action potentials. Proc Natl Acad Sci U S A *96*, 14600-14604.

Larkum, M.E., Zhu, J.J., and Sakmann, B. (1999b). A new cellular mechanism for coupling inputs arriving at different cortical layers. Nature *398*, 338-341.

Larkum, M.E., Zhu, J.J., and Sakmann, B. (2001). Dendritic mechanisms underlying the coupling of the dendritic with the axonal action potential initiation zone of adult rat layer 5 pyramidal neurons. J Physiol *533*, 447-466.

Larkum, M.E., Watanabe, S., Nakamura, T., Lasser-Ross, N., and Ross, W.N. (2003). Synaptically activated Ca2+ waves in layer 2/3 and layer 5 rat neocortical pyramidal neurons. J Physiol *549*, 471-488.

Larkum, M.E., Senn, W., and Luscher, H.R. (2004). Top-down dendritic input increases the gain of layer 5 pyramidal neurons. Cereb Cortex *14*, 1059-1070.

Larkum, M.E., Waters, J., Sakmann, B., and Helmchen, F. (2007). Dendritic spikes in apical dendrites of neocortical layer 2/3 pyramidal neurons. J Neurosci *27*, 8999-9008.

Larsen, P.J., Sheikh, S.P., Jakobsen, C.R., Schwartz, T.W., and Mikkelsen, J.D. (1993). Regional distribution of putative NPY Y1 receptors and neurons expressing Y1 mRNA in forebrain areas of the rat central nervous system. Eur J Neurosci *5*, 1622-1637.

Larsen, P.J., Sheikh, S.P., and Mikkelsen, J.D. (1995). Neuropeptide Y Y1 receptors in the rat forebrain: autoradiographic demonstration of [125I][Leu31,Pro34]-NPY binding sites and neurons expressing Y1 receptor mRNA. J Recept Signal Transduct Res *15*, 457-472.

Leroux, P. (2002). Localization and characterization of NPY/PYY receptors in rat frontoparietal cortex during development. J Comp Neurol *442*, 35-47.

McQuiston, A.R., Petrozzino, J.J., Connor, J.A., and Colmers, W.F. (1996a). Neuropeptide Y1 receptors inhibit N-type calcium currents and reduce transient calcium increases in rat dentate granule cells. J Neurosci *16*, 1422-1429.

McQuiston, A.R., and Colmers, W.F. (1996b). Neuropeptide Y2 receptors inhibit the frequency of spontaneous but not miniature EPSCs in CA3 pyramidal cells of rat hippocampus. J Neurophysiol *76*, 3159-3168.

Nevian, T., Larkum, M.E., Polsky, A., and Schiller, J. (2007). Properties of basal dendrites of layer 5 pyramidal neurons: a direct patch-clamp recording study. Nat Neurosci *10*, 206-214.

O'Donohue, T.L., Chronwall, B.M., Pruss, R.M., Mezey, E., Kiss, J.Z., Eiden, L.E., Massari, V.J., Tessel, R.E., Pickel, V.M., DiMaggio, D.A., and et al. (1985). Neuropeptide Y and peptide YY neuronal and endocrine systems. Peptides *6*, 755-768.

Perez-Garci, E., Gassmann, M., Bettler, B., and Larkum, M.E. (2006). The GABAB1b isoform mediates long-lasting inhibition of dendritic Ca2+ spikes in layer 5 somatosensory pyramidal neurons. Neuron *50*, 603-616.

Potez, S., and Larkum, M.E. (2008). Effect of common anesthetics on dendritic properties in layer 5 neocortical pyramidal neurons. J Neurophysiol *99*, 1394-1407.

Qian, J., Colmers, W.F., and Saggau, P. (1997). Inhibition of synaptic transmission by neuropeptide Y in rat hippocampal area CA1: modulation of presynaptic Ca2+ entry. J Neurosci *17*, 8169-8177.

Remy, S., and Spruston, N. (2007). Dendritic spikes induce single-burst long-term potentiation. Proc Natl Acad Sci U S A *104*, 17192-17197.

Rhim, H., Kinney, G.A., Emmerson, P.J., and Miller, R.J. (1997). Regulation of neurotransmission in the arcuate nucleus of the rat by different neuropeptide Y receptors. J Neurosci *17*, 2980-2989.

Sirota, A., Montgomery, S., Fujisawa, S., Isomura, Y., Zugaro, M., and Buzsaki, G. (2008). Entrainment of neocortical neurons and gamma oscillations by the hippocampal theta rhythm. Neuron *60*, 683-697.

Sjostrom, P.J., and Hausser, M. (2006). A cooperative switch determines the sign of synaptic plasticity in distal dendrites of neocortical pyramidal neurons. Neuron *51*, 227-238.

Sperk, G., Hamilton, T., and Colmers, W.F. (2007). Neuropeptide Y in the dentate gyrus. Prog Brain Res *163*, 285-297.

Stuart, G., Spruston, N., Sakmann, B., and Hausser, M. (1997). Action potential initiation and backpropagation in neurons of the mammalian CNS. Trends Neurosci *20*, 125-131.

Stuart, G.J., and Hausser, M. (2001). Dendritic coincidence detection of EPSPs and action potentials. Nat Neurosci *4*, 63-71.

Sun, L., and Miller, R.J. (1999). Multiple neuropeptide Y receptors regulate K+ and Ca2+ channels in acutely isolated neurons from the rat arcuate nucleus. J Neurophysiol *81*, 1391-1403.

Wang, S.J. (2005). Activation of neuropeptide Y Y1 receptors inhibits glutamate release through reduction of voltage-dependent Ca2+ entry in the rat cerebral cortex nerve terminals: suppression of this inhibitory effect by the protein kinase C-dependent facilitatory pathway. Neuroscience *134*, 987-1000.

CHAPTER 4

General Discussion

In this thesis I have examined the modulation of dendritic excitability in DGCs and in L5 pyramidal neurons of the somatosensory cortex. This chapter will highlight the major findings and attempt to explain the role of NPY and dopamine in the hippocampus and in the neocortex.

Frequency-Dependent Dendritic Activity in Dentate Granule Cells

Dendrites are not passive structures. They are able to generate and transmit complex potentials orthodromically and antidromically under specific internal and external states (Stuart et al., 1997; Waters et al., 2005). In particular, regenerative potentials in distal dendrites of L5 pyramidal neurons and CA1 pyramidal neurons occur with sufficiently large influxes of Ca^{2+}, mainly through VDCCs (Larkum et al., 1999a, 1999b; Stuart and Hausser, 2001). The pairing of appropriately-timed EPSPs and bAPs, or high-frequency trains of bAPs, can sufficiently depolarize the distal dendrite above a threshold for dendritic Ca^{2+} spike generation. This threshold is unique for each neuron, and is characterized by passive and active properties such as density and types of dendritic Na^{+}, K^{+}, and Ca^{2+} channels, and cable properties including dendritic diameter, length, and branching (Waters et al., 2005). The dendritic structure of a DGC is very different from a tufted L5 pyramidal neuron, notably because DGCs have multiple apical dendrites and a higher branch order than a L5 pyramid with a single apical dendrite (Fig. 2.2 and Fig. 3.2). However, we have observed that DGCs can respond in a supralinear manner to high frequency trains of EPSPs and are capable of generating frequency-dependent distal Ca^{2+} currents much like those observed in L5 pyramids (Larkum et al., 1999b). When dendritic potassium conductances were blocked at least to some degree by 4-AP, we found that AP trains in granule cells around CFs of 70-140 Hz generated Ca^{2+} electrogenesis. Although the range of CFs is the same in the two cell types, the major

difference between DGCs and L5 pyramids is the level of soma-dendrite coupling. Under quiescent conditions in the hippocampal slice, we measured CFs in DGC distal dendrites with Ca^{2+} imaging and no 4-AP present, but the supralinear currents had no effect at the soma (Fig. 2.2). However, with the inhibition of 4-AP-sensitive K^+ channels, the dendrite and soma can become tightly coupled. By blocking what is likely an A-type, transient K^+ conductance (Fig. 2.4) in the dendrites, bAPs are more likely to be of greater amplitude in distal dendrites, and if distal Ca^{2+} spikes are generated, they are more likely to propagate orthodromically to the soma. Therefore, we have called the action of 4-AP the 'unmasking' of a somatic CF, which is functionally the equivalent to an increase in soma-dendrite coupling. We have shown that dendritic, T-, L-, and N- type VDCCs mediate the CF, consistent with findings from L2/3 and L5 pyramidal neurons (Larkum et al., 1999b; Larkum et al., 2007). Younger DGCs have a higher density of T-type VDCCs (Schmidt-Hieber et al., 2004), which may explain their lower CFs. However, a higher input resistance and more compact dendritic tree also likely contribute to this difference. P/Q- and R-type VDCCs are also present in DGCs (Sochivko et al., 2002) and may also play a role in Ca^{2+} electrogenesis in DGCs, but this has yet to be examined. Taken together, we have conclusively shown that dendrites of DGCs can respond in a supralinear manner to frequency-dependent activity.

Modulation of Dendritic Electrogenesis in Dentate Granule Cells

Recent studies on bAPs indicate that many intrinsic and extrinsic mechanisms have evolved to regulate dendritic excitability (Sjöström et al., 2008). Neuromodulation of dendritic excitability has been examined in the relatively accessible dendrites of L5 pyramidal neurons, but not in the dentate gyrus. In the dentate gyrus there are many candidate neuromodulators that could regulate distal dendritic information processing. Because dentate hilar interneurons, many of which express NPY, receive mossy fiber

inputs (Kneisler et al., 1995), elevated activity in the MF pathway will also enhance NPY release into the molecular layer. Furthermore, granule cell dendrites are innervated by a dense network of NPYergic terminals (Köhler et al., 1986), originating with hilar interneurons that overlap with very strong immunoreactivity for Y1 receptors (Kopp et al., 2002). In the dentate gyrus, dendritic Y1 receptors inhibit N-type VDCCs (McQuiston et al., 1996), in sharp contrast to the purely presynaptic actions of NPY mediated via Y2 receptors in hippocampal areas CA1 and CA3 (Klapstein and Colmers, 1997; El Bahh et al., 2005). Here we have shown that NPY, by inhibiting distal Ca^{2+} influx via Y1 (and not Y2 or Y5) receptors, can shift the CF in DGCs at both low and high levels of somato-dendritic coupling. Consistent with reports of NPY inhibiting N-type VDCCs (McQuiston et al., 1996), we found no significant difference between the CF shift caused by the antagonist of N-type VDCCs, ω-Conotoxin GVIA (31 ± 10 Hz), and NPY (33 ± 5 Hz). Through the blockade of distal VDCCs NPY may also have other significant functions because Ca^{2+} is an important second messenger. A rise in intracellular Ca^{2+} can also alter gene transcription, cellular migration, and dendritic neurotransmitter release (Elmslie, 2003). Therefore, the action of NPY may also have longer lasting consequences.

It has been well demonstrated that in CA1 and CA3, NPY can act as a potent anti-epileptic agent (El Bahh et al., 2005), and may do so even *in vivo* (Tu et al., 2005). In the dentate gyrus, NPY could provide negative feedback to DGCs, thereby acting as a low-pass filter to suppress elevated network activity. Though not a primary biological activity, this action could also decrease epileptic activity. However, as we have shown, the action of NPY is also very important in the modulation of synaptic plasticity (Fig. 2.11).

We also sought to determine whether endogenous compounds could act in opposition to NPY, and increase dendritic excitability. Dopamine was a likely candidate

because there is a dense distribution of D1 receptors on DGC dendrites (Mansour et al., 1992) and VTA afferents innervate the hippocampus and are thought to be involved in a novelty-detection system that promotes LTP and learning (Lisman and Grace, 2005; Davis et al, 2004; Sierra-Mercado et al., 2008). Application of the D1 agonist, SKF 81297 potentiated the response to trains of EPSPs in a frequency-dependent manner, and also enhanced somato-dendritic coupling observed via an increase in the size of the ADP, and lowering of the CF. Because there was no effect of either NPY or the D1 agonist on synaptic responses below the CF range of ~70 Hz, it appears most likely that the nonlinearity and its modulation derive from the activation of postsynaptic Y1 and D1 receptors, rather than of any presynaptic targets. A major mechanism behind a D1-mediated increase in excitability in the hippocampus and prefrontal cortex has been shown to be an inhibition of voltage gated K^+ channels via the PKA pathway (Hoffman et al., 1998; Dong and White, 2003). Consistent with this mechanism we observed that high concentrations of 4-AP (300 μM) seemed to occlude the effect of the D1 agonist, SKF 81297 (Fig. 2.10). However, the lack of a specifc A-type K^+ channel blocker, and the difficulty in obtaining dendritic whole-cell recordings in DGCs makes this a difficult question to answer. Experiments repeated in Kv 4.2, Kv 4.3, or Kv 1.4 knockout mice would certainly provide a starting point. Recent work also suggests a direct interaction of D1 receptors with N-type VDCCs (Kisilevsky et al., 2008). As we have shown, the CF is mediated by VDCC activity and not K^+ channels, and since SKF 81297 was still able to lower the CF in 4-AP (100 μM), the possibility exists that it may also potentiate Ca^{2+} currents. An enhancement of N-type currents by angiotensin II has been observed (Washburn and Ferguson, 2001), and P-type currents are also prone to potentiation by adenosine 2B receptors via the cAMP-PKA pathway (Mogul et al., 1993). Therefore, the D1 receptor mediated increase in dendritic excitability may result from a decrease in A-

type K^+ channel activity, a potentiation of one or more subtypes of VDCCs, or a combination of the two.

Since D1-receptors can up regulate cAMP, and db-cAMP application lowered the CF (Fig. 2.9), it can be hypothesized that other neuromodulators that activate the PKA pathway will have the same result. For example, vasoactive intestinal polypeptide (VIP) positive cells are found throughout the hippocampus (Kohler, 1983; Sloviter and Nilaver, 1987) where PAC-1, VPAC-1, and VPAC-2 receptors have also been identified (Joo et al., 2004). Recently, VIP as been shown to regulate NMDA currents in CA1 pyramidal neurons, which can lead to enhanced LTP (Yang et al., 2009). In our studies, we observed a VIP-mediated lowering of the CF (Appendix Figure 3) consistent with a role of the cAMP-PKA pathway in mediating excitability. Many other neuromodulators such as acetylcholine (Welsby et al., 2009), pituitary adenylate cyclase-activating polypeptide (PACAP; Vaudry et al., 1998), and noradrenaline (Oh et al., 2009) are candidates to increase dendritic excitability and potentiate plasticity via this pathway.

Long-Term Potentiation in the Dentate Gyrus

In the dentate gyrus we have shown that granule cell dendrites are attuned to high frequency information from either afferent input, or backpropagating action potentials. This is a somewhat expected finding since high frequency gamma oscillations (40-100 Hz) have been shown to occur in the perforant pathway input to the dentate gyrus (Bragin et al., 1995; Csicsvari et al., 2003), and DGCs *in vivo* are capable of firing high frequency bursts (Jung and McNaughton; Leutgeb et al., 2007), during exploratory behaviour. Therefore, to approximate the physiological conditions under which an animal may form a spatial memory, we paired trains of presynaptic MPP EPSPs and backpropagating action potentials at an upper gamma frequency (100 Hz). Interestingly, this pairing protocol was itself, ineffective, although similar protocols have been used to evoke LTP

elsewhere in the brain (Kampa et al., 2006). The lack of plasticity was unfortunate, but not surprising given anecdotal evidence from other investigators who have unsuccessfully attempted to study LTP in dentate gyrus *in vitro*. Furthermore, in our experiments involving trains of bAPs we never observed any frequency-dependent regenerative events at the soma unless we coupled the dendrite and soma with 4-AP or D1 agonist application. Therefore, we hypothesized that with an increase in dendritic excitability, regenerative Ca^{2+} currents would be a key component of synaptic plasticity. D1 agonist application and a repetition of the TBP protocol resulted in LTP observed in both rat and human DGCs that was not due D1 agonist application alone, or repeated TBP protocols. Since the Y1 agonist is known to act on N-type VDCCs in DGC (McQuiston et al., 1996), and it was able to block D1-induced LTP (Fig 2.11), we can conclude that Ca^{2+} influx through VDCCs is a necessary component of LTP induction by dopamine.

Since Bliss and Lømø's report of long lasting potentiation in rabbit dentate gyrus *in vivo* (1973), there has been a tremendous amount of research on LTP in animal model systems. It is important to note that the D1 agonist was able to induce LTP in human DGCs almost identically to our experiments in the rat.

Our results are consistent with behavioural observations that the hippocampus is necessary for drug-induced conditioned place preference (CPP). Recently, dorsal dentate gyrus lesions produced by injection of colchicine, which preferentially damages DGCs (Goldschmidt and Steward, 1980), have been shown to completely abolish cocaine-induced CPP, and context-conditioned fear (Hernandez-Rabaza, et al., 2008). Also, by impairing dopamine release from VTA afferents, some of which project to the hippocampus, the ability to perform cue-related spatial memory tasks such as the T-maze, Morris water maze, and CPP tasks is greatly impaired (Zweifel et al., 2009). Dopamine release from the VTA to the dentate gyrus seems to be a signal of salience to induce learning of contextual memories. Our studies indicate that NPY is positioned to limit this

type of learning, however, behavioural studies of this nature are lacking, and the conditions underlying the release of NPY from hilar interneurons are unknown.

NPY in the Somatosensory Cortex

Principal neurons of the somatosensory cortex integrate primary sensory information from the thalamus with top-down input from higher order cortical areas. This is governed, in part, by a compartmentalized dendritic structure and the presence of two zones that can generate regenerative depolarizing potentials (Yuste et al., 1994; Larkum et al., 2001). One of these areas is the relatively well-characterized somatic AP zone, capable of initiating Na^+-APs. The other AP zone lies in the distal apical dendrite where it can process synaptic input and cellular activity (bAPs), and ultimately generate Ca^{2+}-Na^+-APs that can have a profound effect on the output of the neuron (Larkum et al., 1999b; Larkum et al., 2005). Here, we have shown that the distal dendritic Ca^{2+}- Na^+-AP zone is prone to modulation by NPY1 receptors, whereas the somatic Na^+-AP zone is not. We also suggest the observed NPY-mediated decrease in Ca^{2+}-influx was not due to Y1 receptors on basal dendrites. We did not confirm that the locus of the NPY was sufficient to cover all distal basal dendrites, however, this region of a L5 pyramidal neuron is electrotonically separate from the distal apical dendrite (Nevian et al., 2007), and therefore unlikely to have any effect on distal Ca^{2+}-Na^+-APs. Our results are consistent with an action at the distal apical dendrite. NPY acts to de-couple the distal dendrite and the soma by inhibiting the distal Ca^{2+} spike while having no effect on somatic APs. Our studies indicate that NPY can disrupt the communication between the distal apical dendrite and soma, and therefore, could have a commanding influence on higher order cortical processes, such as learning and attention (Larkum et al., 2004).

Final Conclusions

NPY and dopamine can each have a profound effect on frequency-dependent dendritic excitability. We have shown that in DGCs and in L5 pyramidal neurons soma-dendrite coupling has a heavy influence on output (Larkum et al., 1999a; Andrásfalvy et al., 2008). Furthermore, the mechanisms that underlie dendritic regenerative activity are important regulators of plasticity and are prone to modulation. In an opposing manner, Y1R can decrease, and D1R activation can increase, regenerative dendritic activity in DGCs of the rat and human. During specific behaviours, such as exploration, NPY and dopamine likely play a major role in neocortical and hippocampal plasticity.

Future Directions

The observations in this thesis will contribute to the understanding of neuronal information processing. However, much remains to be discovered. I have shown that, by regulation of Ca^{2+} electrogenesis by G protein-coupled receptors such as Y1 and D1, activity of the dendrites of DGCs and L5 pyramidal neurons are prone to modulation, especially during high frequency input and during bursts of APs. Therefore, the specific behavioural circumstances that trigger the release of NPY and dopamine in the dentate gyrus and neocortex are of significant interest. Behavioural studies with simultaneous electrophysiological and neurochemical recordings (Johnson et al., 2008) could provide interesting insights into the external cues that trigger neuromodulator release in these brain areas.

Recent genetic manipulations have knocked out specific receptor subtypes in specific neuronal populations (e.g. Zweifel et al., 2008, 2009) and investigated the resulting behavioural alterations. This advancing technology is another exciting avenue for exploring the role of NPY and dopamine. For example, with a targeted knockout of

D1R in DGCs, based on the findings in this thesis, it would be hypothesized that reward-based contextual memories could not be formed.

This thesis has also led to some specific and exciting questions:

1. What subtype of voltage-dependent Ca^{2+} channels does NPY inhibit in layer 5 pyramdial neurons?
2. Does dopamine act to increase dendritic excitability through A-type K^+ channel receptor insertion (Kim et al., 2007), voltage-dependent Ca^{2+} channel modulation (Kisilevsky et al., 2008), or possibly via Na^+ channel modulation?
3. Is the D1R-induced long-term potentiation in the dentate gyrus dependent on NMDA receptors?
4. The D2 receptor typically acts in opposition to D1 receptor activation. D2 receptor activation also results in the decrease in cAMP activity via G_i. Therefore, will D2 receptor activation block LTP induction in the dentate gyrus, and will it inhibit D1R induced long-term potentiation?

REFERENCES

Andrasfalvy, B.K., Makara, J.K., Johnston, D., and Magee, J.C. (2008). Altered synaptic and non-synaptic properties of CA1 pyramidal neurons in Kv4.2 knockout mice. J Physiol *586*, 3881-3892.

Bliss, T.V., and Lomo, T. (1973). Long-lasting potentiation of synaptic transmission in the dentate area of the anaesthetized rabbit following stimulation of the perforant path. J Physiol *232*, 331-356.

Bragin, A., Jando, G., Nadasdy, Z., Hetke, J., Wise, K., and Buzsaki, G. (1995). Gamma (40-100 Hz) oscillation in the hippocampus of the behaving rat. J Neurosci *15*, 47-60.

Csicsvari, J., Jamieson, B., Wise, K.D., and Buzsaki, G. (2003). Mechanisms of gamma oscillations in the hippocampus of the behaving rat. Neuron *37*, 311-322.

Davis, C.D., Jones, F.L., and Derrick, B.E. (2004). Novel environments enhance the induction and maintenance of long-term potentiation in the dentate gyrus. J Neurosci *24*, 6497-6506.

Dong, Y., and White, F.J. (2003). Dopamine D1-class receptors selectively modulate a slowly inactivating potassium current in rat medial prefrontal cortex pyramidal neurons. J Neurosci *23*, 2686-2695.

Douglas, R.J., and Martin, K.A. (2004). Neuronal circuits of the neocortex. Annu Rev Neurosci *27*, 419-451.

El Bahh, B., Balosso, S., Hamilton, T., Herzog, H., Beck-Sickinger, A.G., Sperk, G., Gehlert, D.R., Vezzani, A., and Colmers, W.F. (2005). The anti-epileptic actions of neuropeptide Y in the hippocampus are mediated by Y and not Y receptors. Eur J Neurosci *22*, 1417-1430.

Elmslie, K.S. (2003). Neurotransmitter modulation of neuronal calcium channels. J Bioenerg Biomembr *35*, 477-489.

Goldschmidt, R.B., and Steward, O. (1980). Preferential neurotoxicity of colchicine for granule cells of the dentate gyrus of the adult rat. Proc Natl Acad Sci U S A *77*, 3047-3051.

Hernandez-Rabaza, V., Hontecillas-Prieto, L., Velazquez-Sanchez, C., Ferragud, A., Perez-Villaba, A., Arcusa, A., Barcia, J.A., Trejo, J.L., and Canales, J.J. (2008). The hippocampal dentate gyrus is essential for generating contextual memories of fear and drug-induced reward. Neurobiol Learn Mem *90*, 553-559.

Hoffman, D.A., and Johnston, D. (1998). Downregulation of transient K+ channels in dendrites of hippocampal CA1 pyramidal neurons by activation of PKA and PKC. J Neurosci *18*, 3521-3528.

Johnson, M.D., Franklin, R.K., Gibson, M.D., Brown, R.B., and Kipke, D.R. (2008). Implantable microelectrode arrays for simultaneous electrophysiological and neurochemical recordings. J Neurosci Methods *174*, 62-70.

Joo, K.M., Chung, Y.H., Kim, M.K., Nam, R.H., Lee, B.L., Lee, K.H., and Cha, C.I. (2004). Distribution of vasoactive intestinal peptide and pituitary adenylate cyclase-activating polypeptide receptors (VPAC1, VPAC2, and PAC1 receptor) in the rat brain. J Comp Neurol *476*, 388-413.

Jung, M.W., and McNaughton, B.L. (1993). Spatial selectivity of unit activity in the hippocampal granular layer. Hippocampus *3*, 165-182.

Kampa, B.M., Letzkus, J.J., and Stuart, G.J. (2006). Requirement of dendritic calcium spikes for induction of spike-timing-dependent synaptic plasticity. J Physiol *574*, 283-290.

Kim, J., Jung, S.C., Clemens, A.M., Petralia, R.S., and Hoffman, D.A. (2007). Regulation of dendritic excitability by activity-dependent trafficking of the A-type K+ channel subunit Kv4.2 in hippocampal neurons. Neuron *54*, 933-947.

Kisilevsky, A.E., Mulligan, S.J., Altier, C., Iftinca, M.C., Varela, D., Tai, C., Chen, L., Hameed, S., Hamid, J., Macvicar, B.A., and Zamponi, G.W. (2008). D1 receptors physically interact with N-type calcium channels to regulate channel distribution and dendritic calcium entry. Neuron *58*, 557-570.

Kisilevsky, A.E., and Zamponi, G.W. (2008). D2 dopamine receptors interact directly with N-type calcium channels and regulate channel surface expression levels. Channels (Austin) *2*, 269-277.

Klapstein, G.J., and Colmers, W.F. (1993). On the sites of presynaptic inhibition by neuropeptide Y in rat hippocampus in vitro. Hippocampus *3*, 103-111.

Kneisler, T.B., and Dingledine, R. (1995). Spontaneous and synaptic input from granule cells and the perforant path to dentate basket cells in the rat hippocampus. Hippocampus *5*, 151-164.

Kohler, C. (1983). A morphological analysis of vasoactive intestinal polypeptide (VIP)-like immunoreactive neurons in the area dentata of the rat brain. J Comp Neurol *221*, 247-262.

Kohler, C., Eriksson, L., Davies, S., and Chan-Palay, V. (1986). Neuropeptide Y innervation of the hippocampal region in the rat and monkey brain. J Comp Neurol *244*, 384-400.

Kopp, J., Xu, Z.Q., Zhang, X., Pedrazzini, T., Herzog, H., Kresse, A., Wong, H., Walsh, J.H., and Hokfelt, T. (2002). Expression of the neuropeptide Y Y1 receptor in the CNS of rat and of wild-type and Y1 receptor knock-out mice. Focus on immunohistochemical localization. Neuroscience *111*, 443-532.

Larkum, M.E., Kaiser, K.M., and Sakmann, B. (1999a). Calcium electrogenesis in distal apical dendrites of layer 5 pyramidal cells at a critical frequency of back-propagating action potentials. Proc Natl Acad Sci U S A *96*, 14600-14604.

Larkum, M.E., Waters, J., Sakmann, B., and Helmchen, F. (2007). Dendritic spikes in apical dendrites of neocortical layer 2/3 pyramidal neurons. J Neurosci *27*, 8999-9008.

Larkum, M.E., Zhu, J.J., and Sakmann, B. (1999b). A new cellular mechanism for coupling inputs arriving at different cortical layers. Nature *398*, 338-341.

Larkum, M.E., Zhu, J.J., and Sakmann, B. (2001). Dendritic mechanisms underlying the coupling of the dendritic with the axonal action potential initiation zone of adult rat layer 5 pyramidal neurons. J Physiol *533*, 447-466.

Leutgeb, J.K., Leutgeb, S., Moser, M.B., and Moser, E.I. (2007). Pattern separation in the dentate gyrus and CA3 of the hippocampus. Science *315*, 961-966.

Lisman, J.E., and Grace, A.A. (2005). The hippocampal-VTA loop: controlling the entry of information into long-term memory. Neuron *46*, 703-713.

Magee, J.C., and Carruth, M. (1999). Dendritic voltage-gated ion channels regulate the action potential firing mode of hippocampal CA1 pyramidal neurons. J Neurophysiol *82*, 1895-1901.

Mansour, A., Meador-Woodruff, J.H., Zhou, Q., Civelli, O., Akil, H., and Watson, S.J. (1992). A comparison of D1 receptor binding and mRNA in rat brain using receptor autoradiographic and in situ hybridization techniques. Neuroscience *46*, 959-971.

McQuiston, A.R., Petrozzino, J.J., Connor, J.A., and Colmers, W.F. (1996). Neuropeptide Y1 receptors inhibit N-type calcium currents and reduce transient calcium increases in rat dentate granule cells. J Neurosci *16*, 1422-1429.

Mogul, D.J., Adams, M.E., and Fox, A.P. (1993). Differential activation of adenosine receptors decreases N-type but potentiates P-type Ca2+ current in hippocampal CA3 neurons. Neuron *10*, 327-334.

Oh, M.M., McKay, B.M., Power, J.M., and Disterhoft, J.F. (2009). Learning-related postburst afterhyperpolarization reduction in CA1 pyramidal neurons is mediated by protein kinase A. Proc Natl Acad Sci U S A *106*, 1620-1625.

Schmidt-Hieber, C., Jonas, P., and Bischofberger, J. (2004). Enhanced synaptic plasticity in newly generated granule cells of the adult hippocampus. Nature *429*, 184-187.

Sierra-Mercado, D., Dieguez, D., Jr., and Barea-Rodriguez, E.J. (2008). Brief novelty exposure facilitates dentate gyrus LTP in aged rats. Hippocampus *18*, 835-843.

Sjostrom, P.J., Rancz, E.A., Roth, A., and Hausser, M. (2008). Dendritic excitability and synaptic plasticity. Physiol Rev *88*, 769-840.

Sloviter, R.S., and Nilaver, G. (1987). Immunocytochemical localization of GABA-, cholecystokinin-, vasoactive intestinal polypeptide-, and somatostatin-like immunoreactivity in the area dentata and hippocampus of the rat. J Comp Neurol *256*, 42-60.

Sochivko, D., Pereverzev, A., Smyth, N., Gissel, C., Schneider, T., and Beck, H. (2002). The Ca(V)2.3 Ca(2+) channel subunit contributes to R-type Ca(2+) currents in murine hippocampal and neocortical neurones. J Physiol *542*, 699-710.

Stuart, G., Spruston, N., Sakmann, B., and Hausser, M. (1997). Action potential initiation and backpropagation in neurons of the mammalian CNS. Trends Neurosci *20*, 125-131.

Stuart, G.J., and Hausser, M. (2001). Dendritic coincidence detection of EPSPs and action potentials. Nat Neurosci *4*, 63-71.

Tu, B., Timofeeva, O., Jiao, Y., and Nadler, J.V. (2005). Spontaneous release of neuropeptide Y tonically inhibits recurrent mossy fiber synaptic transmission in epileptic brain. J Neurosci *25*, 1718-1729.

Vaudry, D., Basille, M., Anouar, Y., Fournier, A., Vaudry, H., and Gonzalez, B.J. (1998). The neurotrophic activity of PACAP on rat cerebellar granule cells is associated with activation of the protein kinase A pathway and c-fos gene expression. Ann N Y Acad Sci *865*, 92-99.

Washburn, D.L., and Ferguson, A.V. (2001). Selective potentiation of N-type calcium channels by angiotensin II in rat subfornical organ neurones. J Physiol *536*, 667-675.

Waters, J., Schaefer, A., and Sakmann, B. (2005). Backpropagating action potentials in neurones: measurement, mechanisms and potential functions. Prog Biophys Mol Biol *87*, 145-170.

Welsby, P.J., Rowan, M.J., and Anwyl, R. (2009). Intracellular mechanisms underlying the nicotinic enhancement of LTP in the rat dentate gyrus. Eur J Neurosci *29*, 65-75.

Yang, K., Trepanier, C.H., Li, H., Beazely, M.A., Lerner, E.A., Jackson, M.F., and Macdonald, J.F. (2009). Vasoactive intestinal peptide acts via multiple signal pathways to regulate hippocampal NMDA receptors and synaptic transmission. Hippocampus.

Yuste, R., Gutnick, M.J., Saar, D., Delaney, K.R., and Tank, D.W. (1994). Ca2+ accumulations in dendrites of neocortical pyramidal neurons: an apical band and evidence for two functional compartments. Neuron *13*, 23-43.

Zilberter, Y., Harkany, T., and Holmgren, C.D. (2005). Dendritic release of retrograde messengers controls synaptic transmission in local neocortical networks. Neuroscientist *11*, 334-344.

Zweifel, L.S., Argilli, E., Bonci, A., and Palmiter, R.D. (2008). Role of NMDA receptors in dopamine neurons for plasticity and addictive behaviors. Neuron *59*, 486-496.

Zweifel, L.S., Parker, J.G., Lobb, C.J., Rainwater, A., Wall, V.Z., Fadok, J.P., Darvas, M., Kim, M.J., Mizumori, S.J., Paladini, C.A., *et al.* (2009). Disruption of NMDAR-dependent burst firing by dopamine neurons provides selective assessment of phasic dopamine-dependent behavior. Proc Natl Acad Sci U S A *106*, 7281-7288.

APPENDIX

Appendix Figure 1. 4-AP Induces Complex Spikes.

Complex spikes appear after 4-AP application (A.) Complex spikes were observed in DGCs with long current injections in the presence of 4-AP (50 of 56), but not in normal ACSF (0 of 121).

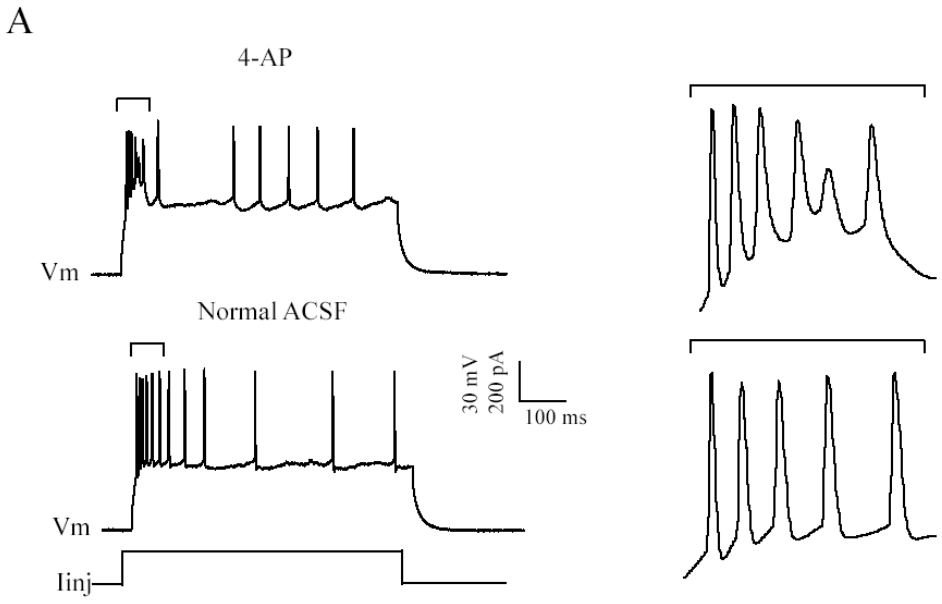
A
4-AP
Vm
Normal ACSF
30 mV
200 pA
100 ms
Vm
Iinj

Appendix Figure 2. Internal EGTA Concentration Affects Afterdepolarization Size and Critical Frequency.

All experiments were performed in the presence of 4-AP (100 μM) (A) Changes in CF and amplitude of the ADP with alteration of intracellular EGTA concentration (in mM): 10 (▲; n=16), 1 (◇; n=11), and 0 (●; n=10). ADP integral is significantly greater with 10 mM and 1 mM EGTA in the intracellular solution compared with 0 mM. Inset (i.) is a comparison of supracritical responses at 120 Hz with different intracellular EGTA concentrations as indicated. *P<0.05, **P<0.01, ***P<0.001, 10 mM compared to 0 mM (paired t-test). †P <0.05, 1 mM compared to 0 mM (paired t-test).

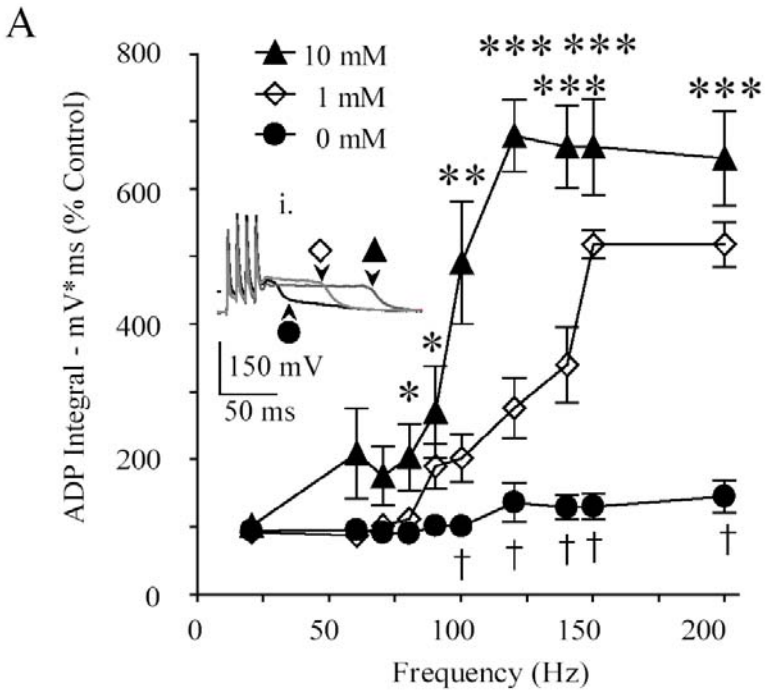
A
800
600
400
200
0
ADP Integral - mV*ms (% Control)
10 mM
1 mM
0 mM
i.
150 mV
50 ms
0
50
100
150
200
Frequency (Hz)

Appendix Figure 3. Vasoactive Intestinal Polypeptide Decreases the Critical Frequency.

(A) In the presence of 4-AP (100 μM) stable critical frequencies were recorded at the soma via the ADP in DGCs. Vasoactive intestinal polypeptide (VIP; 30 nM) was applied via the bath and resulted in a reversible shift in the CF. ($n = 4$; $^{**}P < 0.01$; One sample t-test).

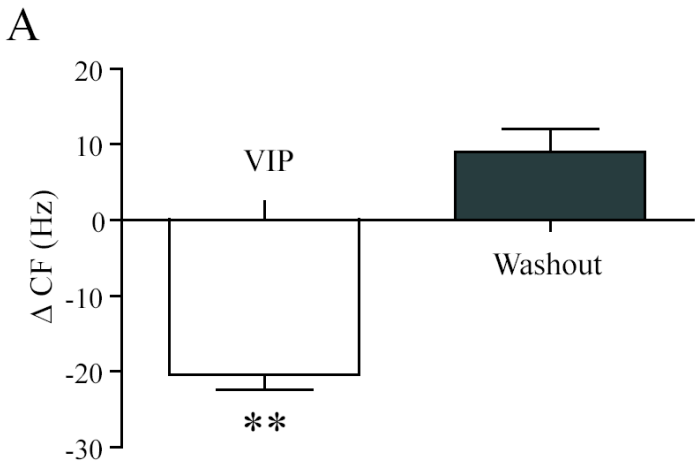
A
20
10
0
-10
-20
-30
Δ CF (Hz)
VIP
Washout
**